Методика атомно-силовои микроскопии пьезоотклика для исследования сегнетоэлектрических и сегнетоэластических структур

А. Л. Холкин, Университет г. Авейро, Португалия

Dept. of Ceramics and Glass Engineering
Center for Research in Ceramics and Composite Materials
University of Aveiro
Portugal

СПбГПУ, 24 июня 2011 года

Acknowledgments

- **Group members:** I. Bdikin, D. Kiselev, R. Pullar,V. Bystrov, D. Karpinsky, V. Khomchenko, A. Heredia, V. Shvartsman, R. Lopes, N. Panwar, F. Figueiras. E. Bosnet

- **EU rojects "Multiceral", "Nanomotion", "SIMMEC", "PodiTrodi"**

- **Portuguese projects:** PTDC/FIS/81442/2006, PTDC/CTM/73030/2006, PTDC/CTM/68614/2006

- **Collaborators:** S.V. Kalinin, A. Gruverman, A. Sternberg, K. Bormanis, B. Dkhil, J. Petzelt, N. Pertsev, E. Mishina, A. Sigov, S. Vakhrushev, I. Pronin, J. Banys, J. Scott, …

- **Companies:** NT-MDT Integrated solutions for NanoTechnology; Asylum Research The Technology Leader in Scanning Probe and Atomic Force Microscopy

ОГЛАВЛЕНИЕ

Why nanoscale ferroelectrics?


THE POSSIBILITIES ARE INFINITE FUJITSU

選択は自由。
でも実績ある次世代メモリは、
FRAMだけです。

FRAMは、富士通が世界で初めて量産化。
高速書き込み/長寿命/省電力のアドバンテージで、
OA機器など幅広い用途で導入が進んでいます。

High Speed
FRAM
Power-Saving
Random Access

Seeds for Needs. 富士通の電子デバイス
FRAMメモリLSI

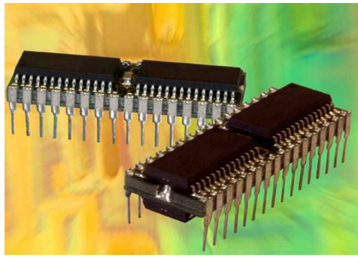

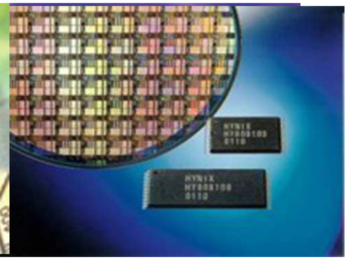

FeRAM - a dream semiconductor memory:

- **High-density (as DRAM)**
- **High-speed (as SRAM)**
- **Nonvolatile (as Flash)**

Over 30 million products using FRAM have already been shipped, including metering, RFID and smart-card devices (source: Ramtron, 2007).

Ferroelectric non-volatile memories

4 Mb FRAM cell, Samsung Electronics

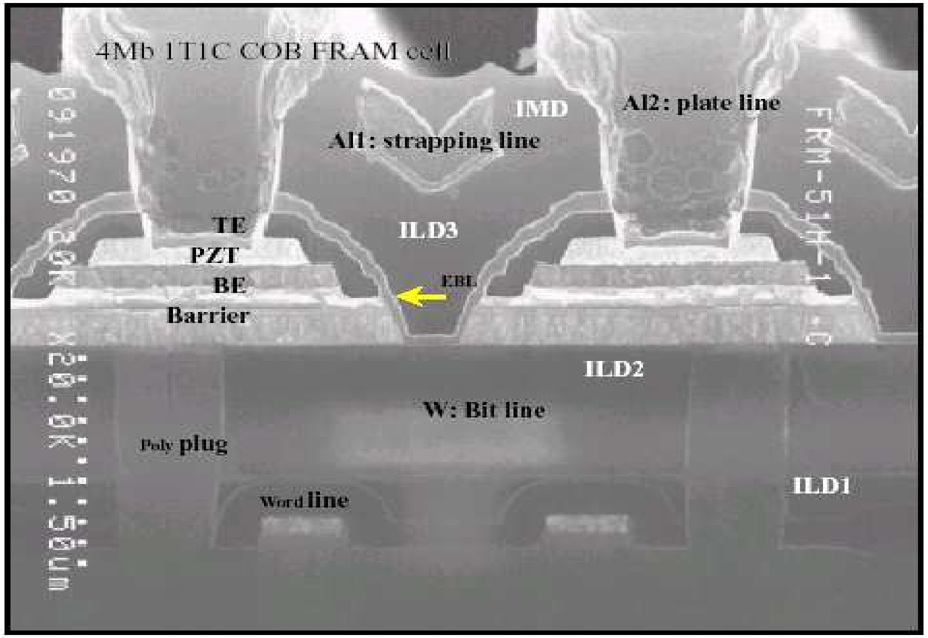

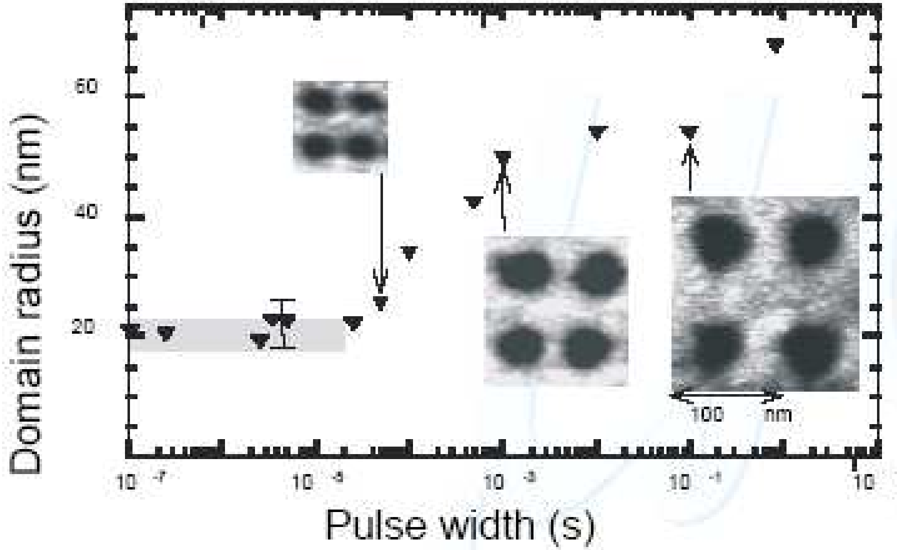

bit erasing

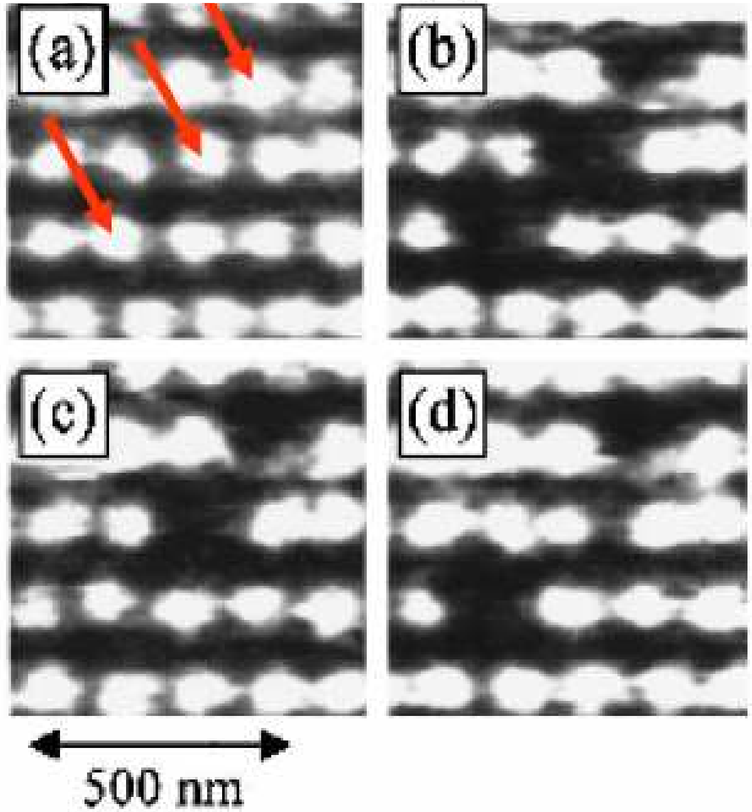

Writing and erasing ferroelectric domains

Paruch et al., APL (2001)

Minimum domain size ~5-10 nm → **6-50 Gb/cm²**

PiezoMEMS: cantilevers, nanoshells, nanotubes

Tube injector

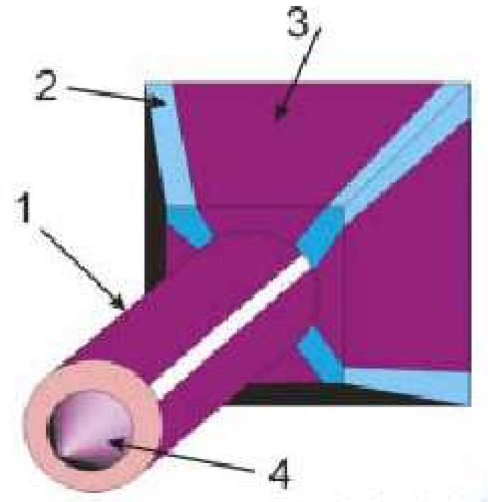

BIONIC EAR

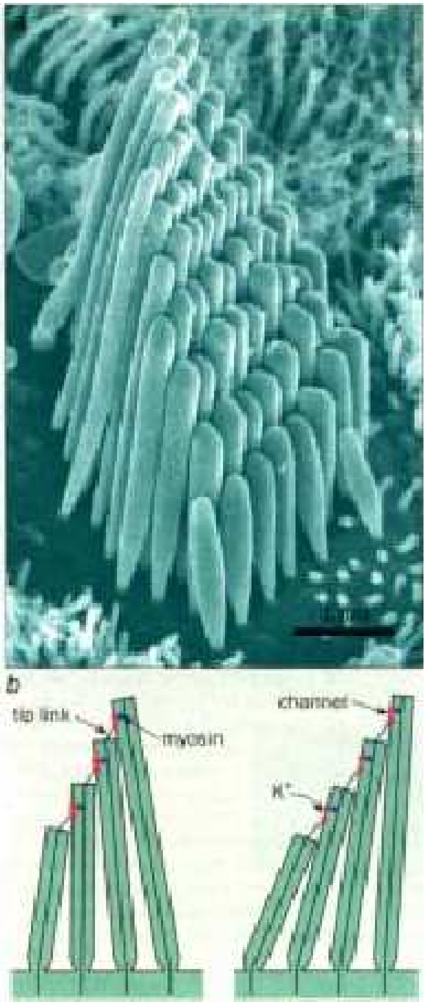

Cantilevers for mass detection

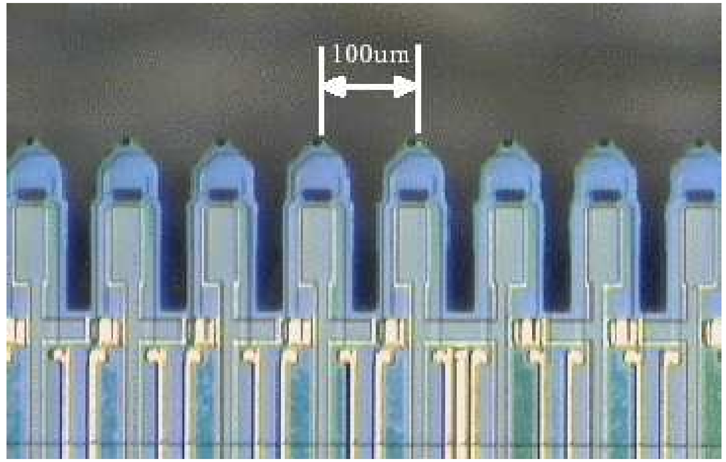

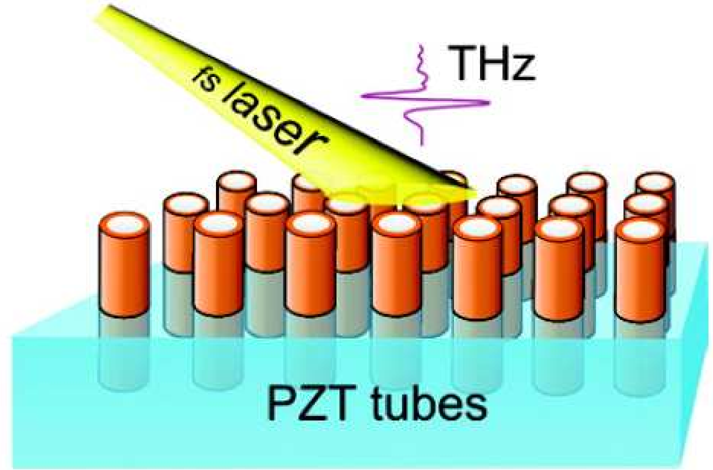

Nanogenerator

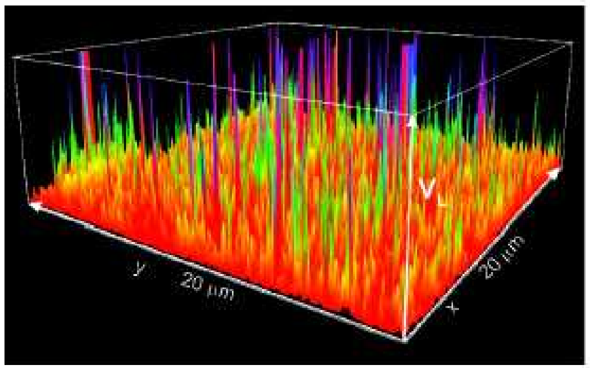

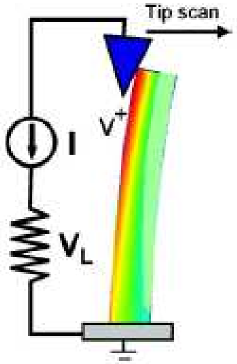

Questions to be answered

- Domain structure at the nm scale?
- Is material switchable at the nm dimension?
- What is the minimum domain or domain wall size?
- Ferroelectricity in ceramics: grain and grain boundary effects?
- Local polarization in systems with broken symmetry?
- Piezoelectricity and ferroelectricity in nanostructures?

Electromechanics: from mm to nm

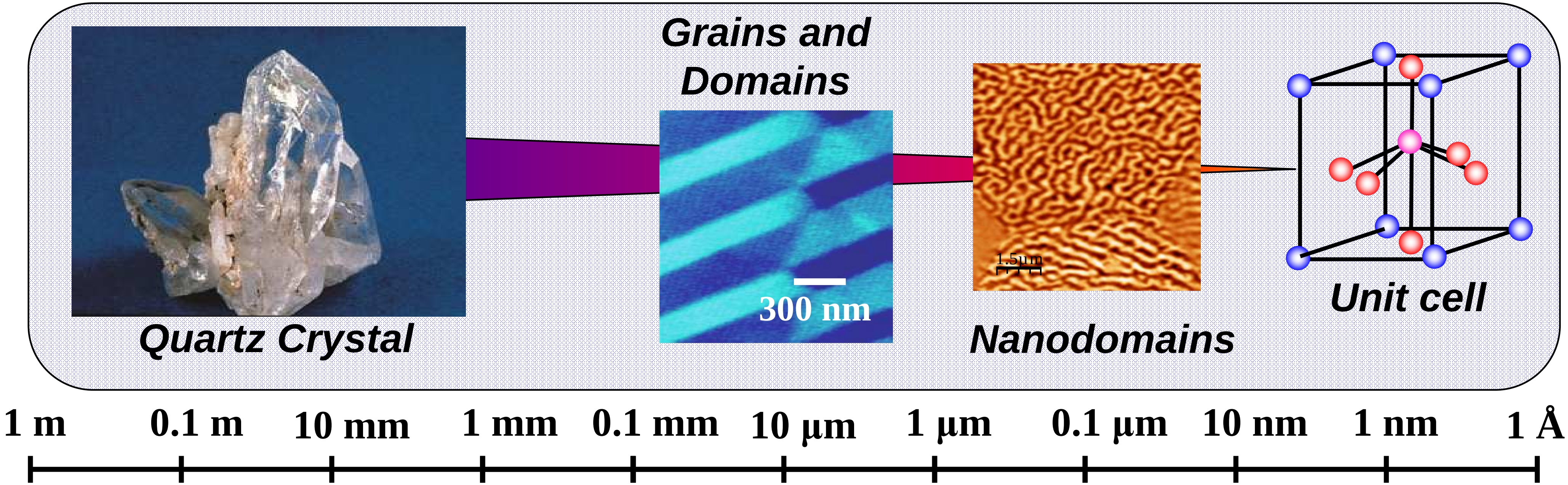

We need Scanning Probe Microscopy to image ELECTROMECHANICAL properties of ferroelectrics

$$S = QP^2(E) = Q[P_s + P_{ind}(E)]^2 = QP_s^2 + 2Q\varepsilon_o\varepsilon P_s E + QP_{ind}^2$$

Piezoresponse
at 1ω (1st harmonic)

$$S_{1\omega} = 2Q\varepsilon_o\varepsilon P_s E_o \sin(\omega t)$$

Piezoresponse Force Microscopy

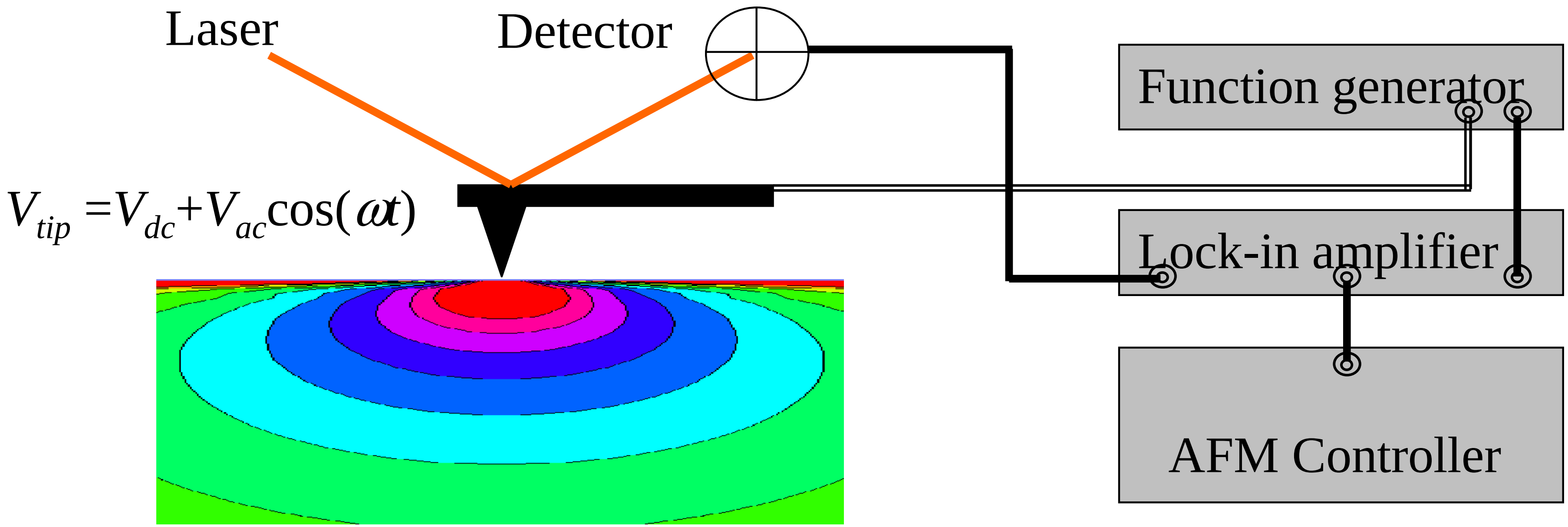

Application of AC bias to the tip

$$V_{tip} = V_{dc} + V_{ac}\cos(\omega t)$$

results in cantilever deflection

$$d = d_0 + A(\omega, V_{dc}, \ldots)V_{ac}\cos(\omega t + \varphi)$$

Phase: domain orientation

Magnitude: local piezoelectric properties

Constant bias: hysteresis loop, polarization switching

Piezoresponse in 3 dimensions

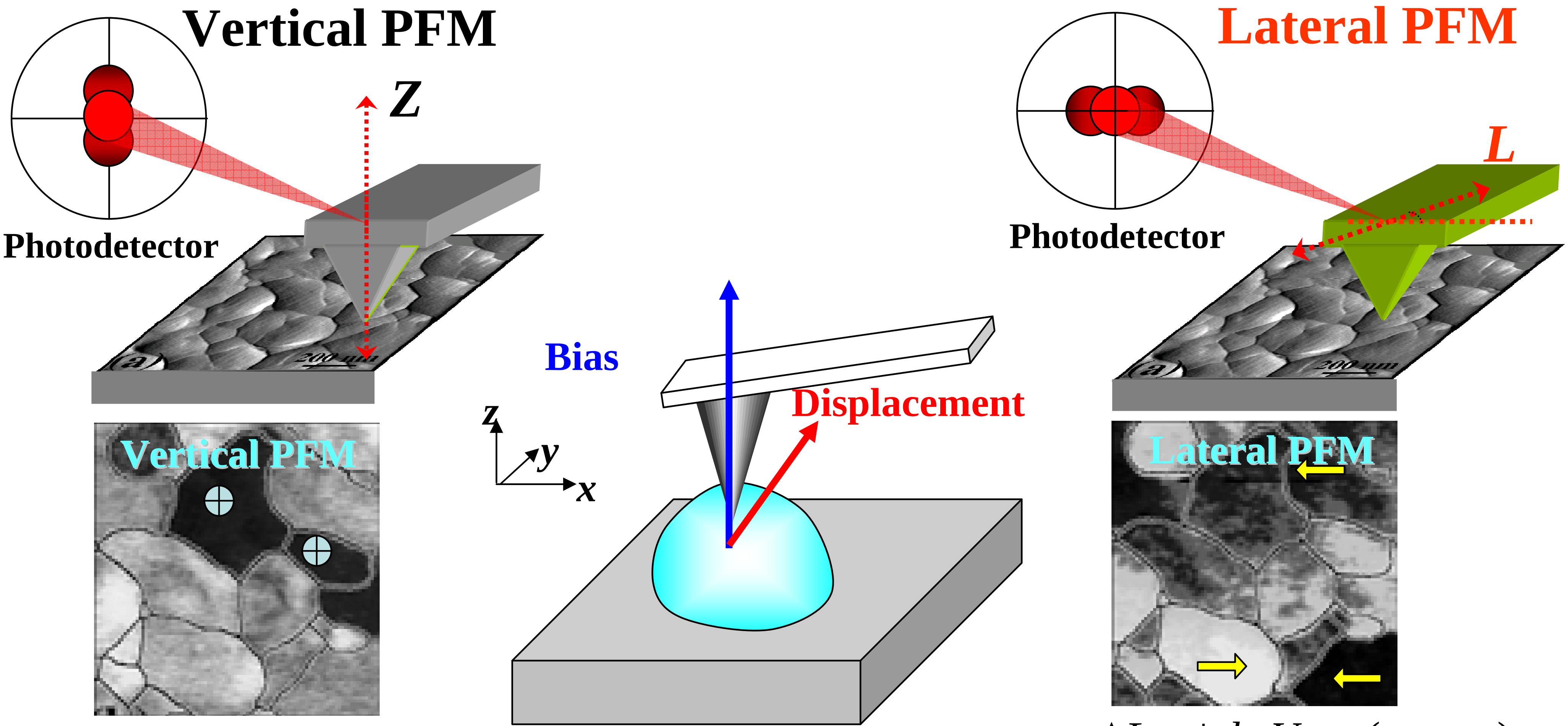

$\Delta Z = \pm d_{33} V \cos(wt + \varphi)$

$\Delta L = \pm d_{15} V \cos(wt + \varphi)$

PFM allows complete 3D reconstruction of polarization vector at the nanoscale level:

Vertical + Lateral PFM (*x*) + Lateral PFM (*y*) = 3D PFM

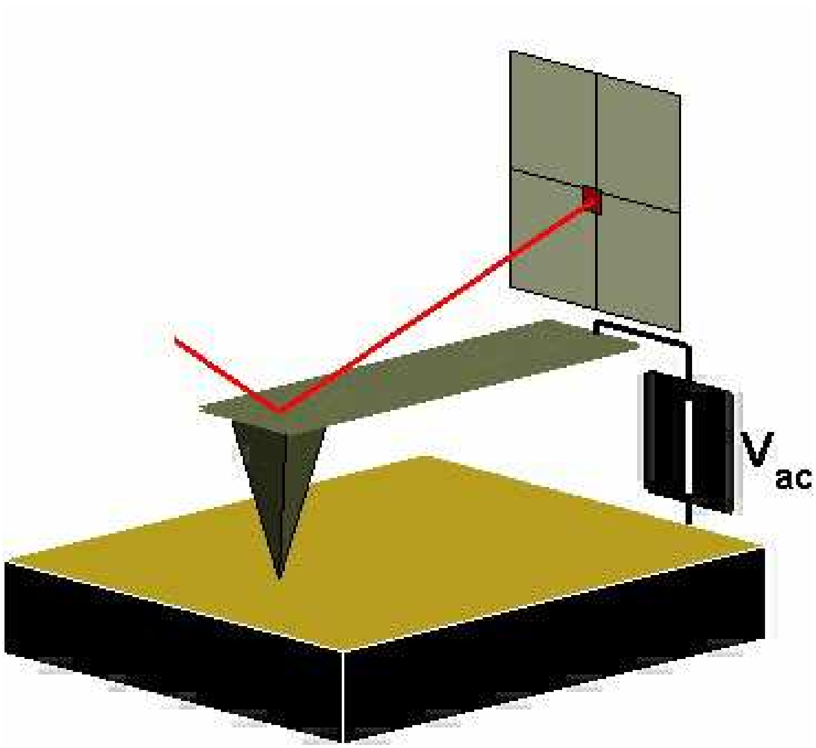
V_{ac}

How PFM is related to materials properties: tip-electrode interaction

Local Detection:

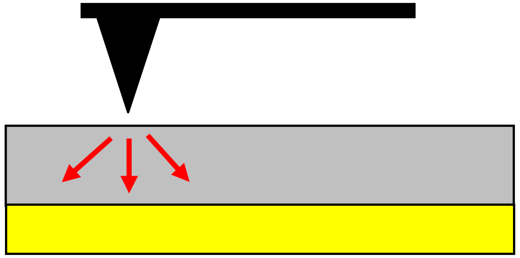

The bias is applied between tip and bottom electrode

Pro: 1. Resolution is higher
2. Writing is possible

Con: 1. Very sensitive to tip-surface contact
2. Difficult to interpret

Components of PFM contrast

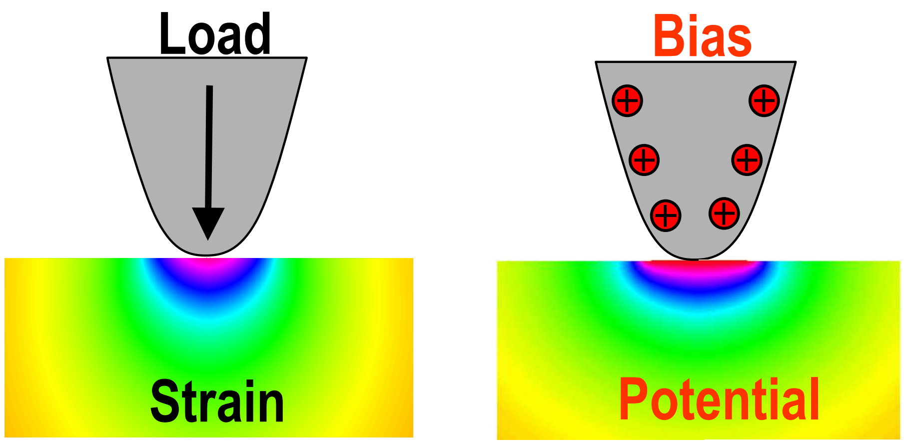

In piezoelectric materials, electrical and mechanical phenomena are coupled

1. **Tip-surface contact mechanics**
   - origins of PFM signal
2. Cantilever dynamics
   - Detection mechanism
3. Field structure in material
   - Resolution
   - Hysteresis measurements
   - Switching phenomena

In a local detection case, exact solution is available only for transversally isotropic materials. For general case, we conjecture that vPFM = d_{33}, x-LPFM = d_{34} and y-LPFM = d_{35}.

Piezoelectricity under dc field

$$d_{33}(E_{dc}) = 2Q\varepsilon_o\varepsilon(E_{dc})P(E_{dc})$$

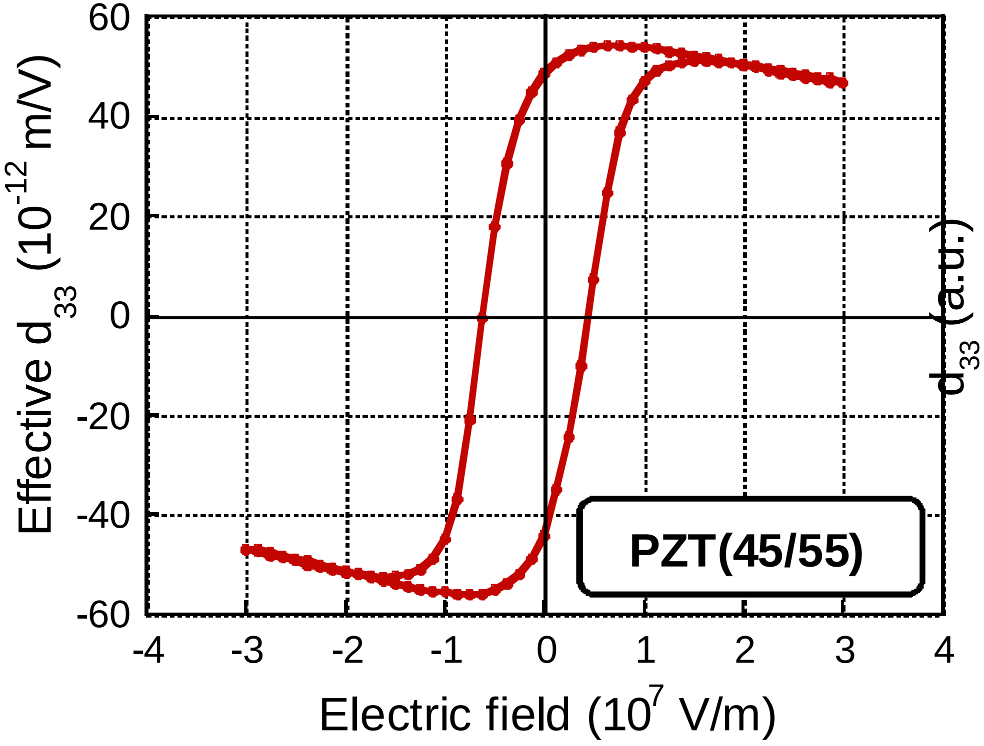

Kholkin et al, *Rev. Sci. Instr.* (1996)

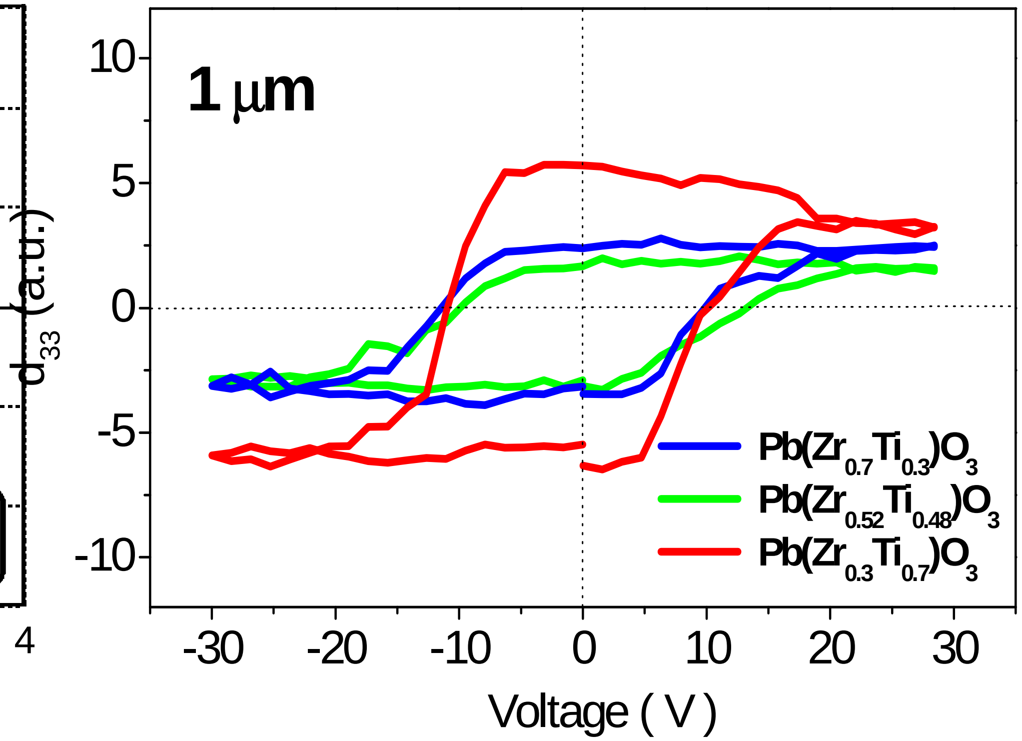

Kholkin et al, *J. Electroceram.* (2007)

Nanohysteresis by PFM

Voltage sweep in PFM

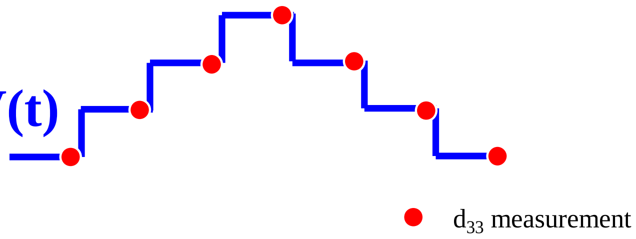

Step mode

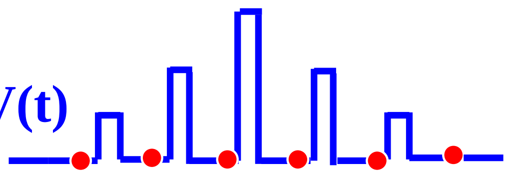

Pulse mode

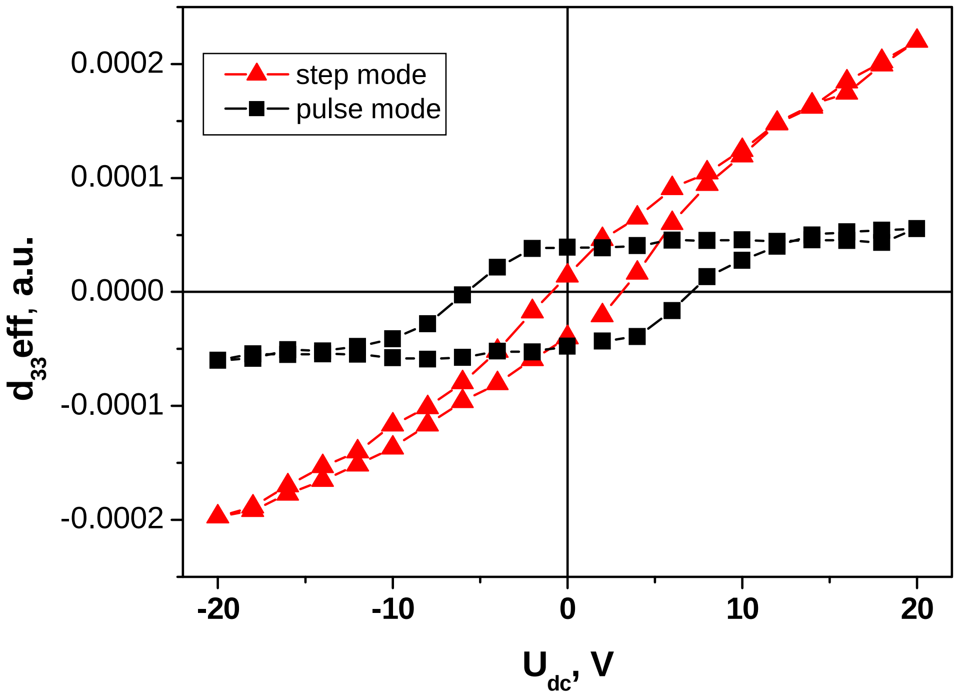

PZT film, 1 μm, courtesy INOSTEK

$$A\cos\varphi = -\underbrace{\frac{K}{k_{lever}}\frac{\partial C}{\partial z}(V_{dc}+V_k)}_{\text{Electrostatic term}} \pm d_{33}V_o$$

Hong et al., JAP (2001)

- **Electrostatic term distorts the shape of the hysteresis in step mode and adds artificial offset (if $V_k \neq 0$)**

Hysteresis via PFM

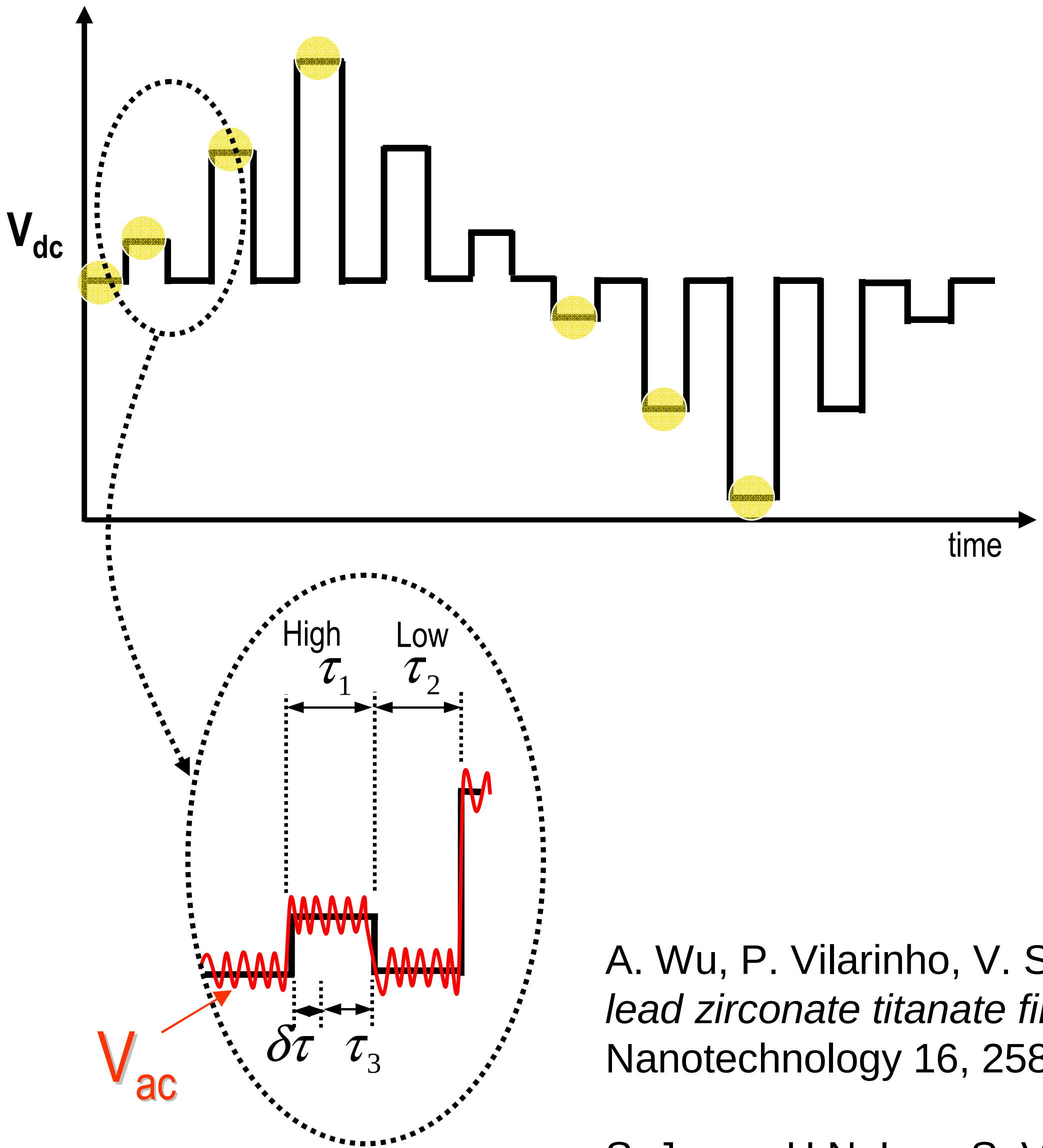

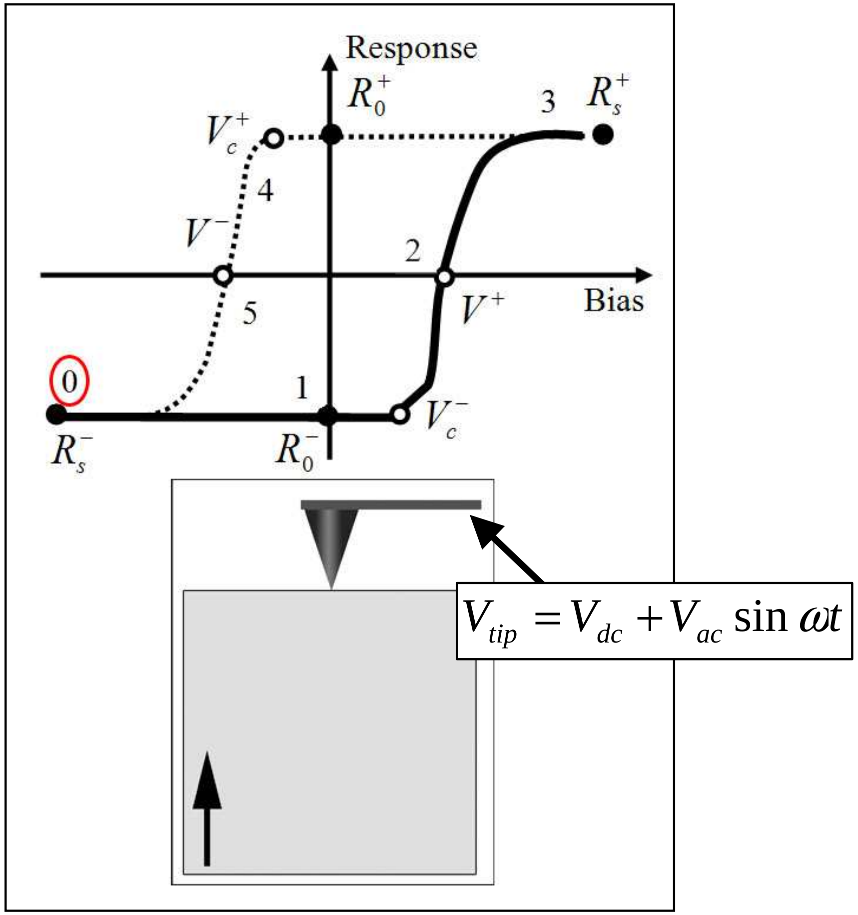

A. Wu, P. Vilarinho, V. Shvartsman, A. L. Kholkin, "*Domain populations in lead zirconate titanate films of different compositions via PFM*", Nanotechnology 16, 2587 (2005).

S. Jesse, H.N. Lee, S. V. Kalinin, *Quantitative Mapping of Switching Behavior in Piezoresponse Force Microscopy*, Rev. Sci. Instr. 77, 073702 (2006).

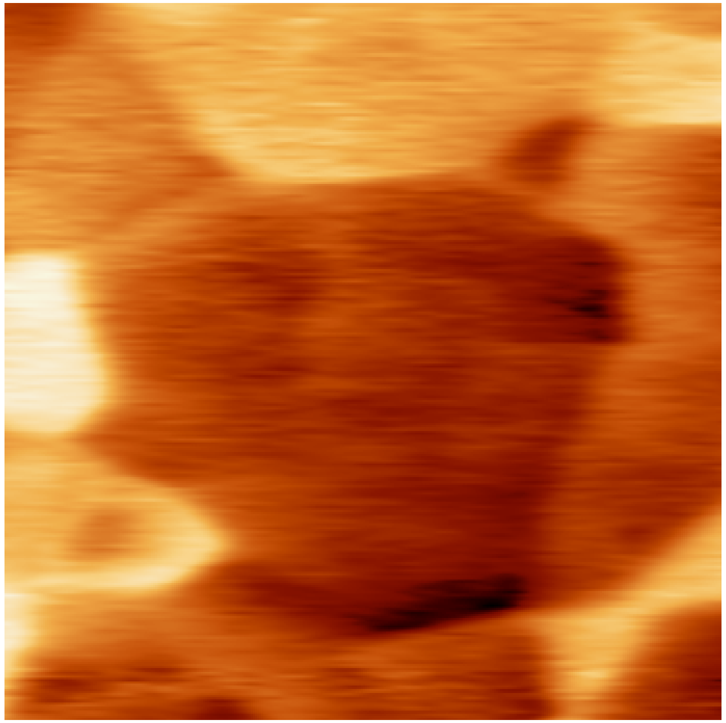

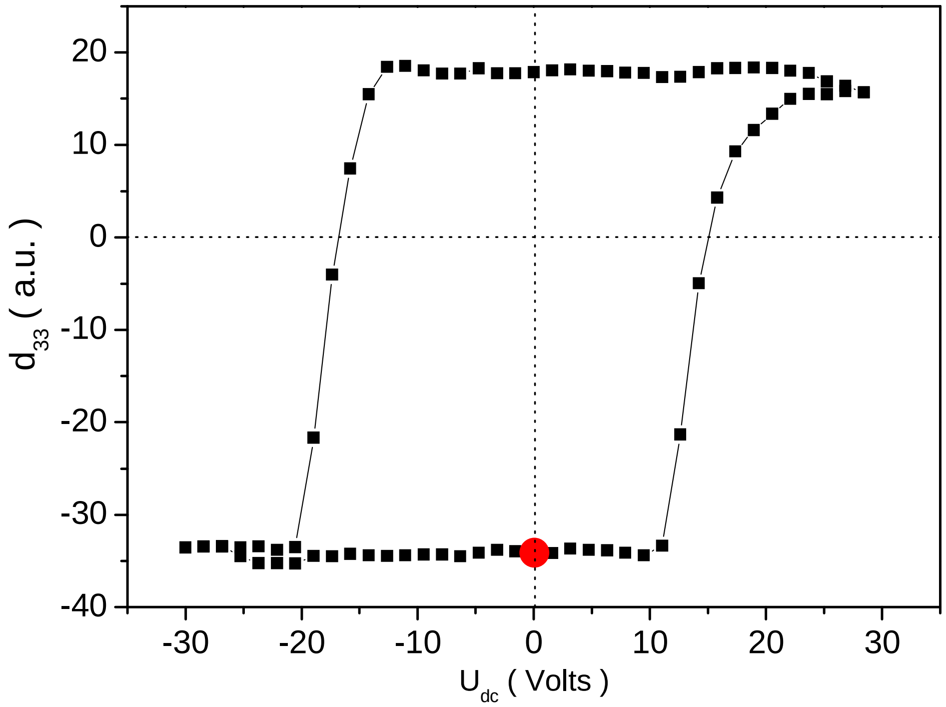

20
10
0
-10
-20
-30
-40
d_{33} (a.u.)
-30
-20
-10
0
10
20
30
U_{dc} (Volts)

Deconvolution of hysteresis by PFM

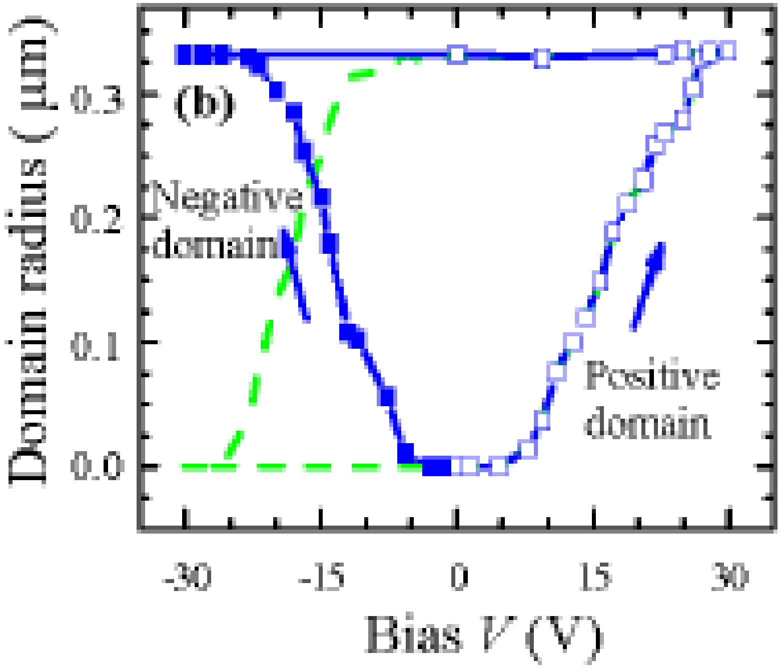

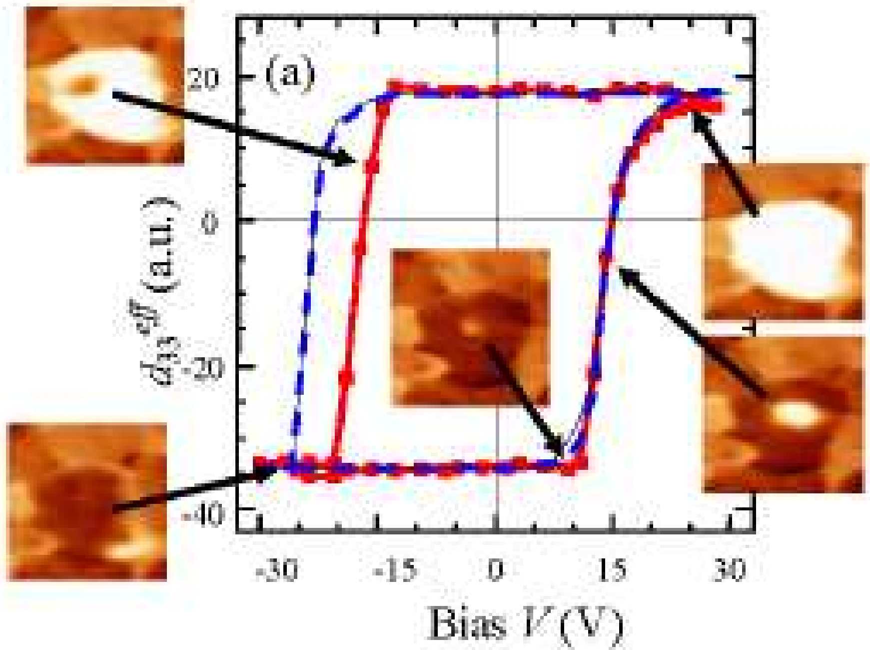

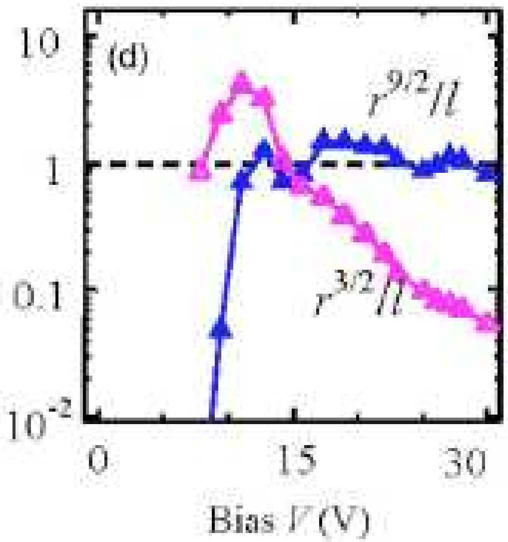

- r<<l leads to unphysically large tip size

- Prolate domains due to effective screening of depolarization filed

- Shift of domain center due to drift

I. K. Bdikin et al., *Appl. Phys. Lett.* 92, 182909 (2008).

“Barkhausen” jumps in hysteresis

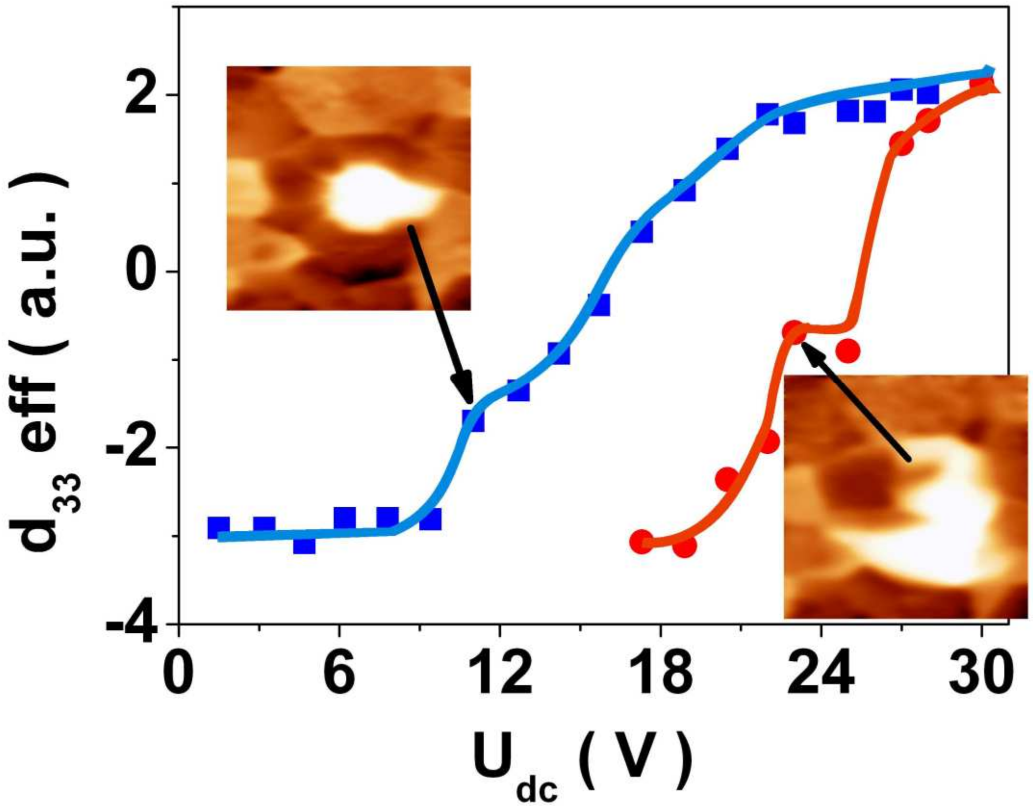

Using d_{33}(V) mapping notable kinks are observed that correspond to the jumps of domain walls
nanoscale Barkhausen effect

Bdikin et al, Appl. Phys. Lett. 92 (2008)

Domain dynamics via PFM: $BaTiO_3$

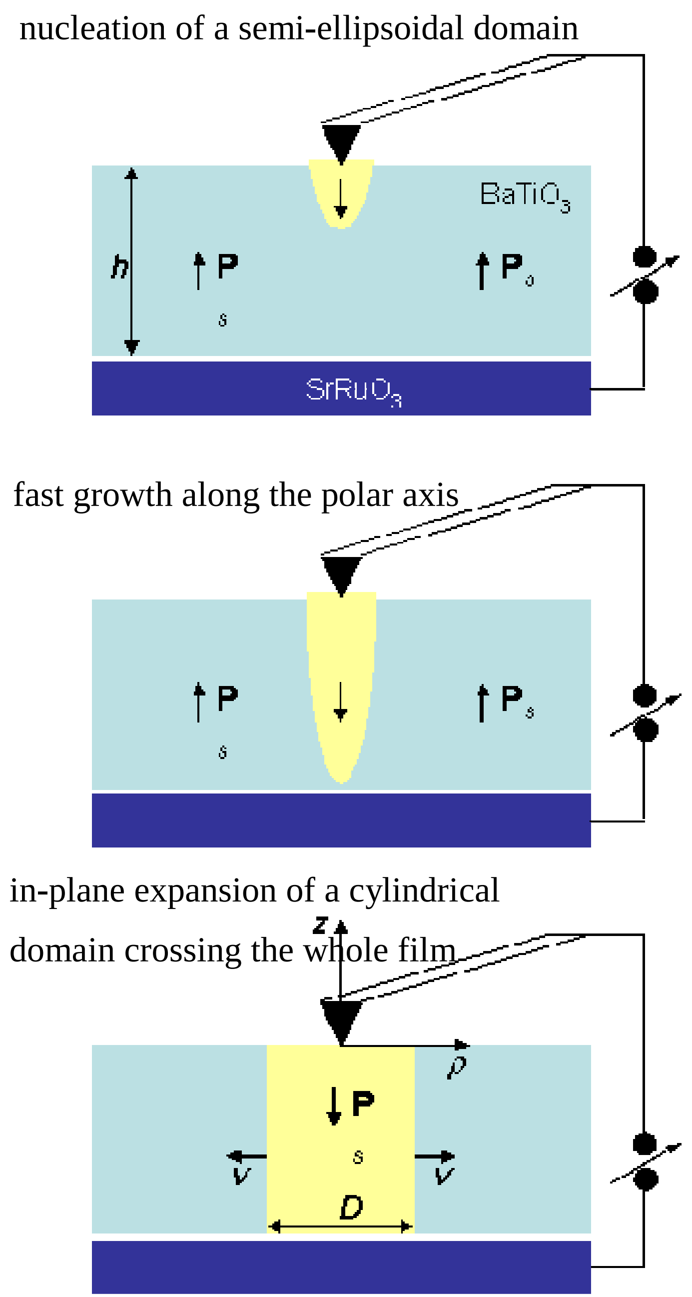

Formation and growth of a 180° domain

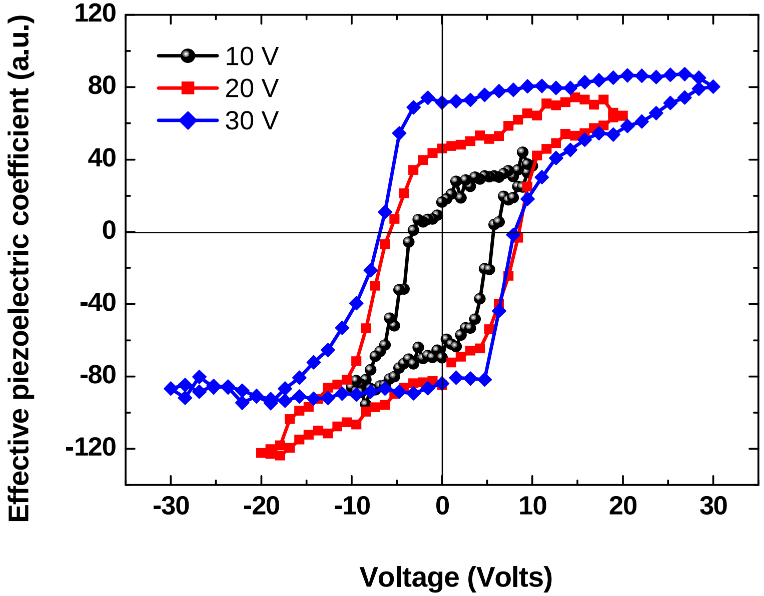

PFM hysteresis loops

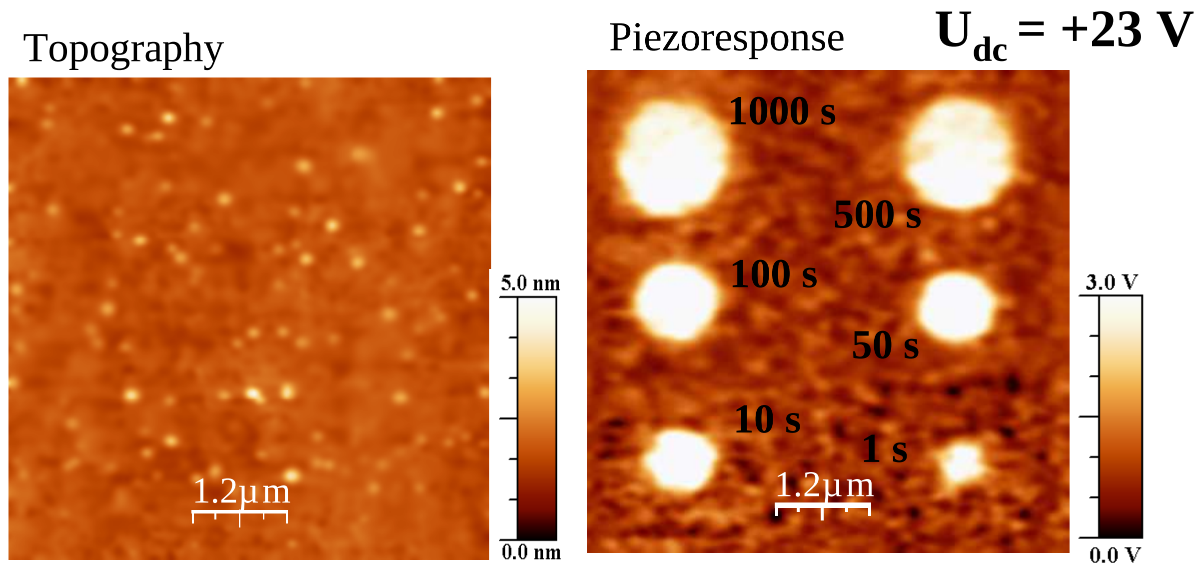

Topography and PFM images of the 60-nm-thick epitaxial $BaTiO_3$ film

Pertsev et al, Nanotechnology **19** (2008)

Domain size vs. voltage and pulse duration

Fitting of experimental data by the formula

$$D = c_1(\ln\tau + c_2)^2$$

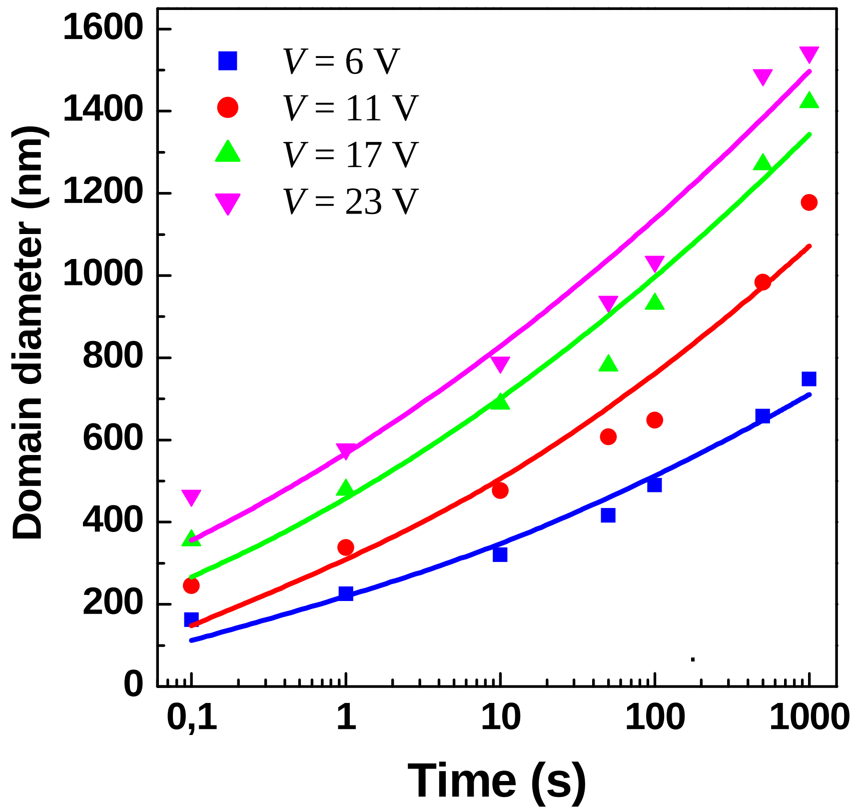

Fitting of experimental data by the formula

$$D = c_3 V(c_4 - \ln V)^2$$

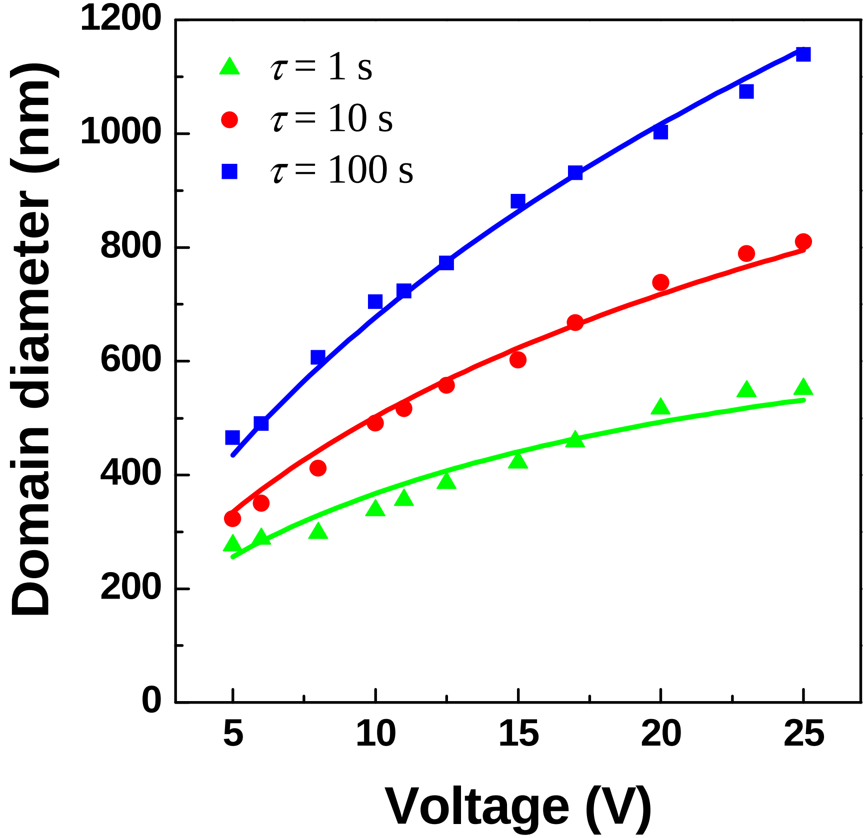

Proposed equation for the writing time and voltage of domain diameter D

$$D \approx KV\left\{\ln\left(\frac{\nu_\infty\tau}{kV}\right) - \ln\left[\ln\left(\frac{\nu_\infty\tau}{KV}\right) - 1\right]\right\}$$

Pertsev et al, Nanotechnology **19** (2008)

Proof of the creep model for $BaTiO_3$ (propagation of domain wall through random potential)

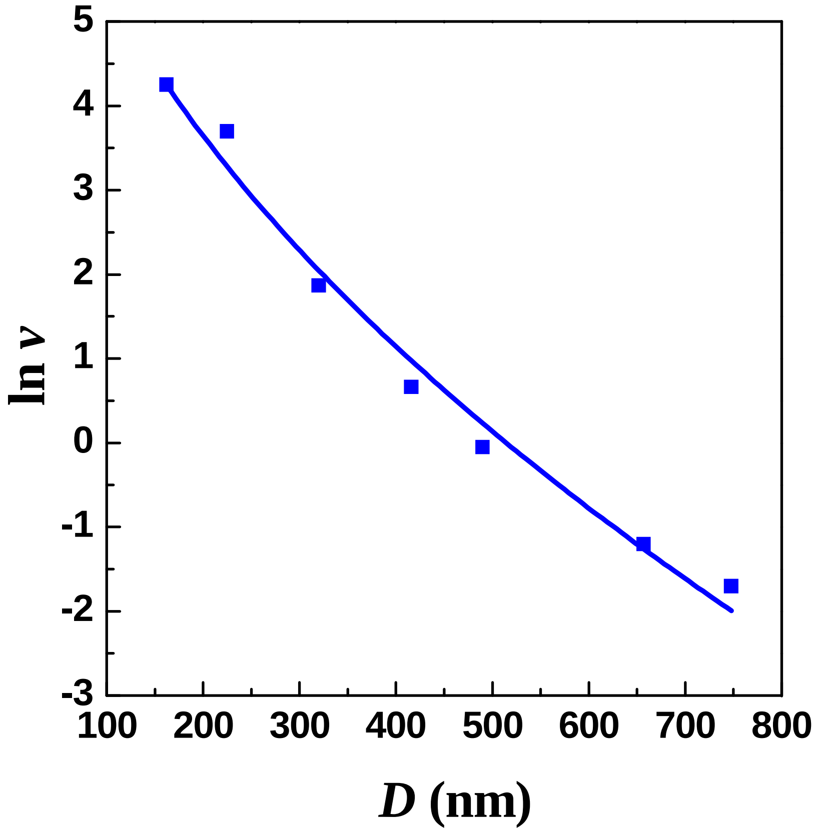

Fitting of the domain wall velocity gives:

$$\ln v = \ln v_\infty - \text{const} \cdot D^{1/2}$$

Thus:

$$v = v_\infty \exp\left[-\frac{U_a}{kT} \left(\frac{E_c}{E} \right)^\mu \right]$$

where U_a – activation energy,
E_c – critical electric field,
μ=0.5 for 2D wall for random bond disorder

■ **Random bond disorder slow down the domain wall growth, no depolarization energy evident (full screening of polarization charges)**

Pertsev et al, Nanotechnology **19** (2008)

Domain wall motion and roughness in PLZT ceramics

Domain wall motion: PLZT 9.5/65/35

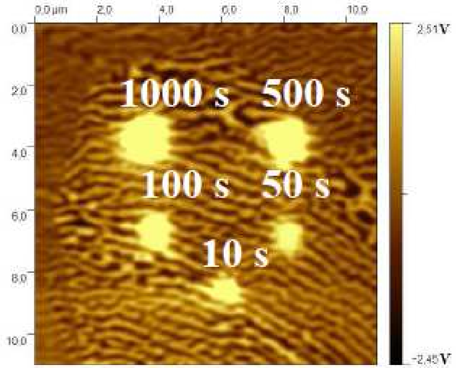

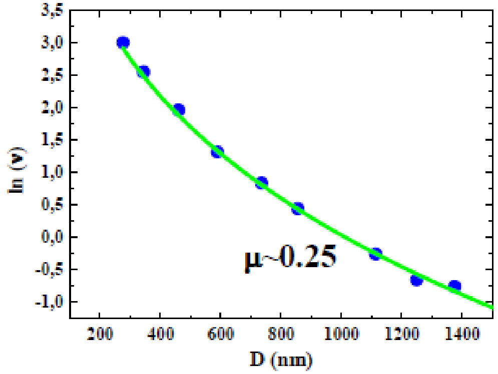

$$v = v_{\infty} \exp\left[-\frac{U_a}{kT}\left(\frac{E_c}{E}\right)^{\mu}\right]$$

Domain wall roughness: PLZT 9.5/65/35

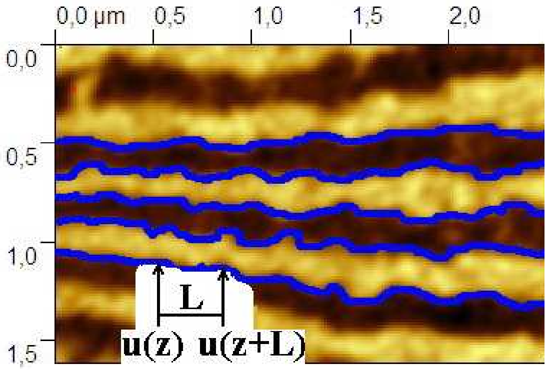

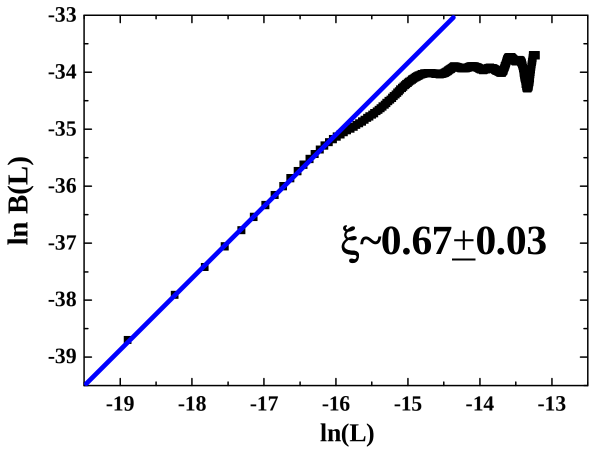

$$B(L) = \left\langle\left\langle [u(z+L) - u(z)]^2 \right\rangle\right\rangle \sim \left(\frac{L}{L_c}\right)^{2\varsigma}$$

$$\mu = \frac{d_{\text{eff}} - 2 + 2\zeta}{2 - \zeta}$$

1-D domain wall (?!)
random-bond disorder

Pertsev et al, J. Appl. Phys. (2011)

1-D walls and change of creep mechanism with La

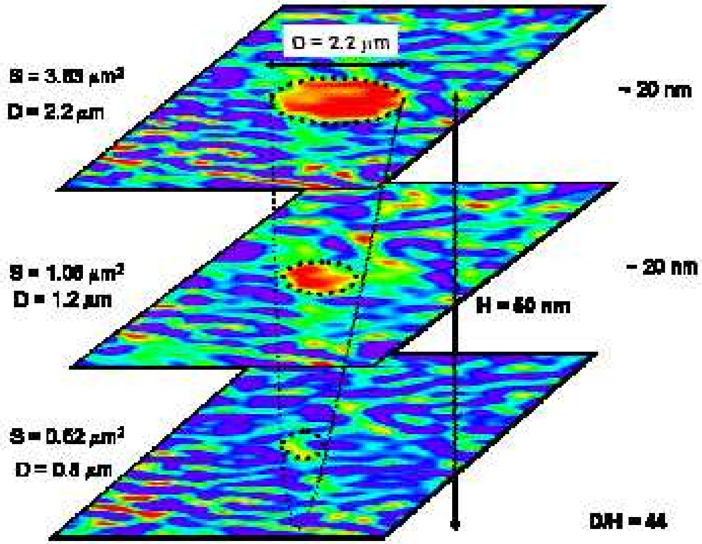

Polishing of ceramics
(D. Kiselev, PhD thesis, 2011)

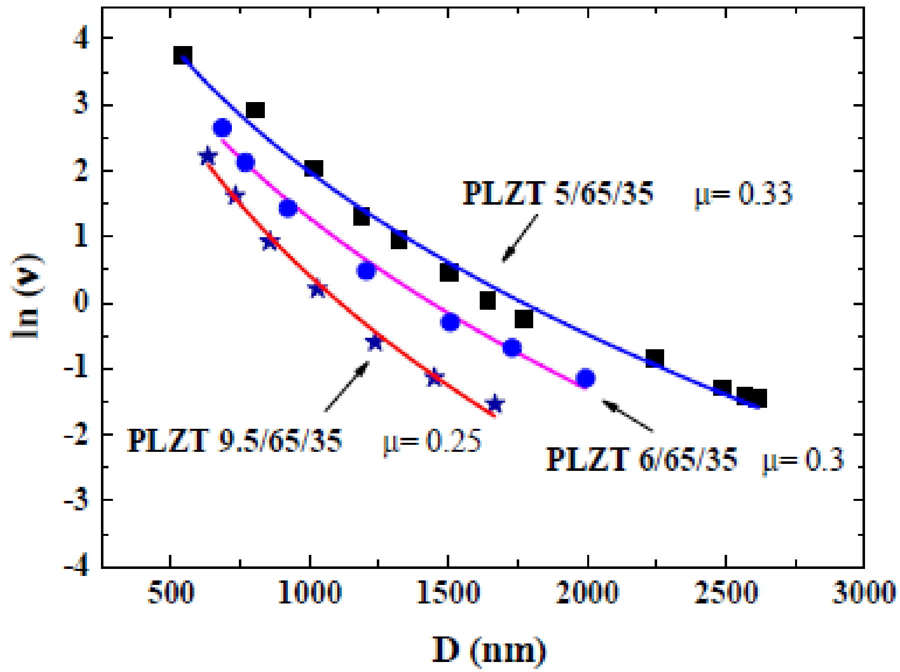

Encrease of creep exponent
with decreasing La content

Pertsev et al, J. Appl. Phys. (2011)

Mesoscopic disorder in relaxor ferroelectrics

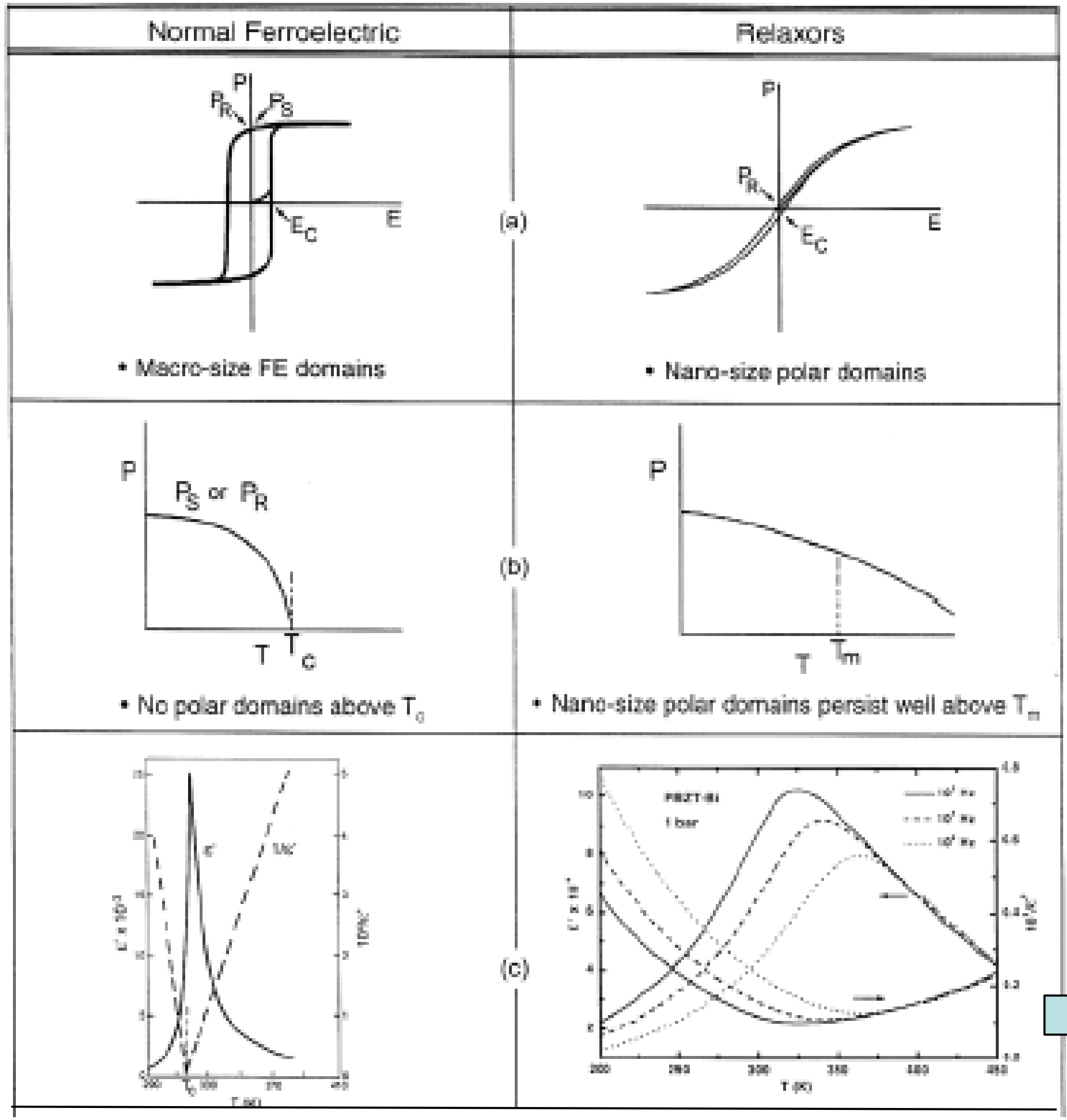

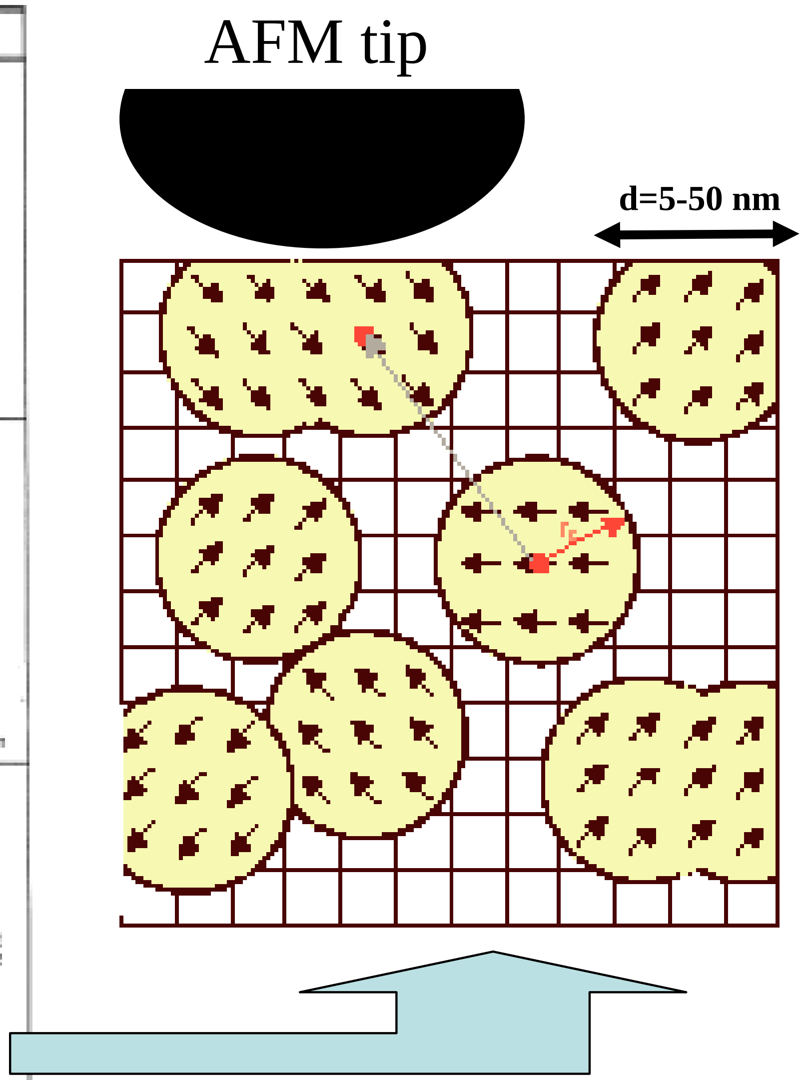

Solid solutions $Pb(Mg_{1/3}Nb_{2/3})O_3$-10%$PbTiO_3$

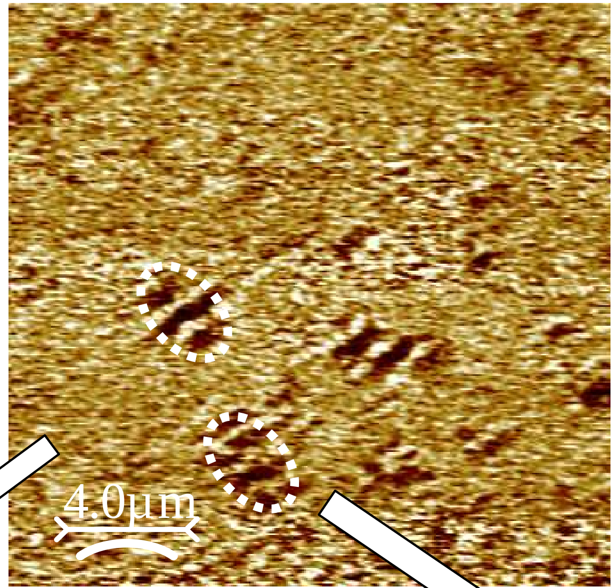

20 µm

Nanodomains (PNRs?)

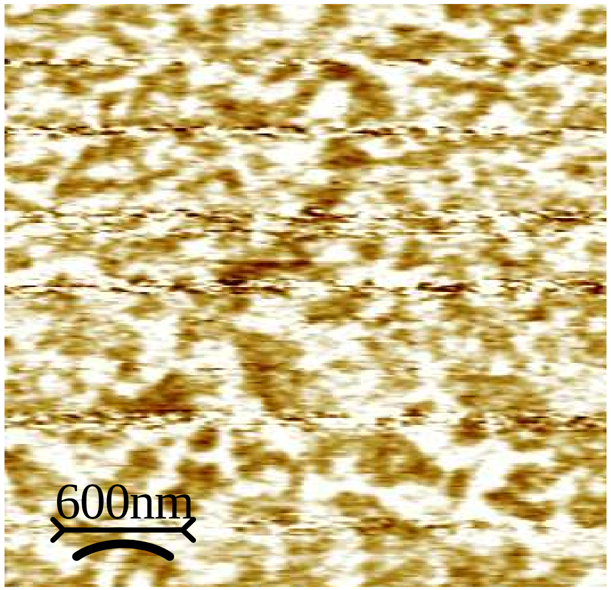

3 µm

Concentration of "ferroelectric" islands is 15-20% of total area

Properties intermediate between ferroelectrics and relaxors

ferroelectric domans

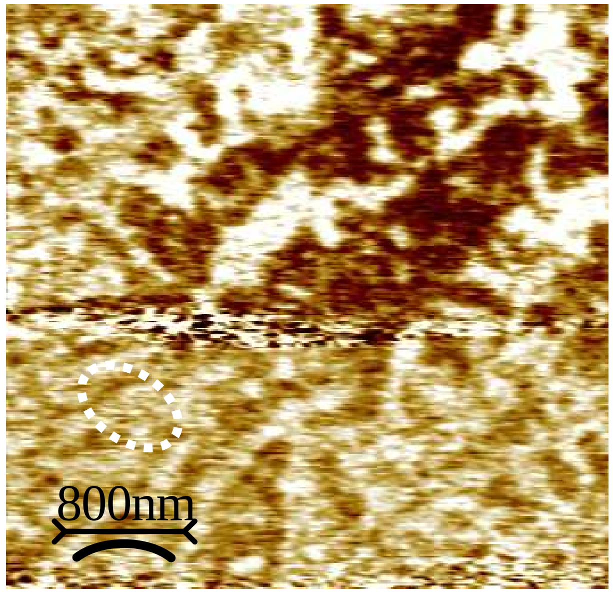

4 µm

PMN-10%PT: autocorrelation analysis

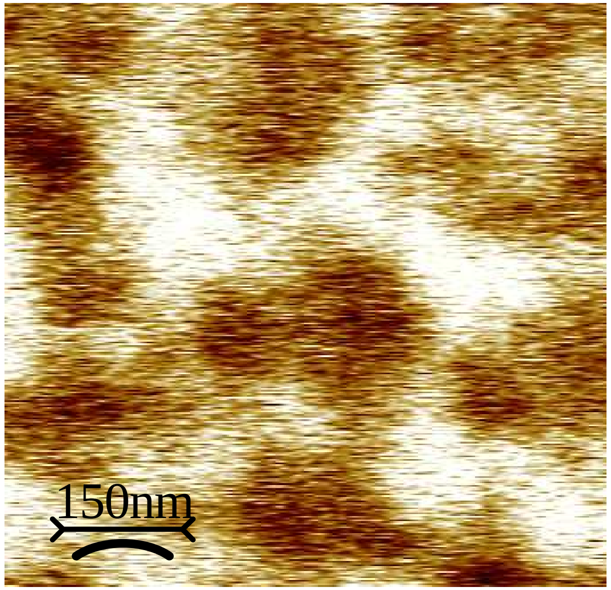

piezoresponse

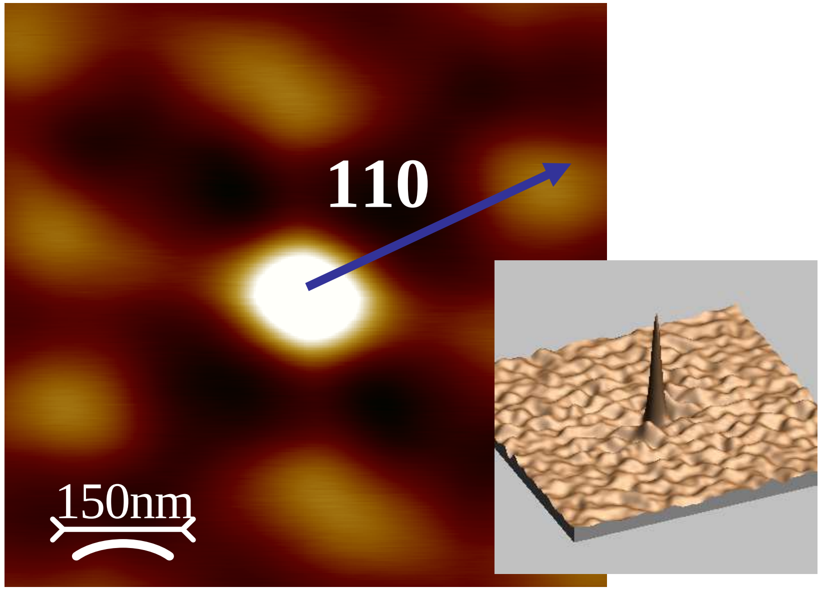

autocorrelation image of d_{33}

$$C(r_1, r_2) = \sum_{x,y} D(x,y)D(x+r_1, y+r_2)$$

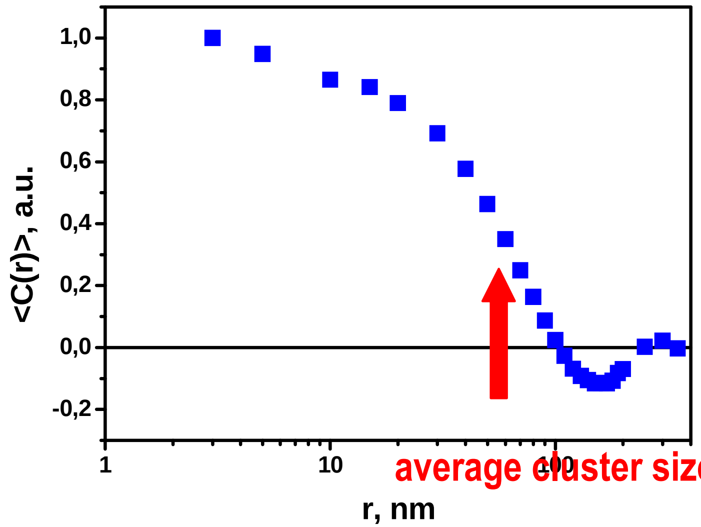

average cluster size = correlation length

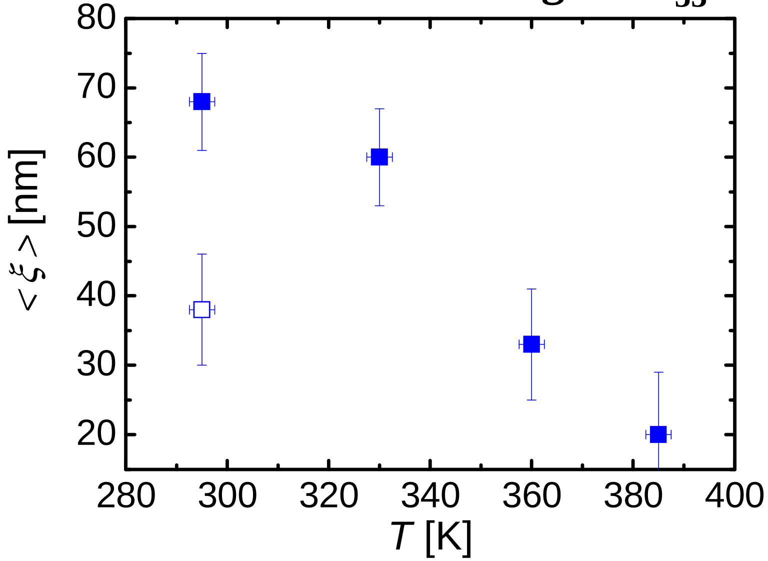

■ **Extracted correlation length gives a MEASURE OF DISORDER**

PMN-PT 80/20

Piezoresponse, D

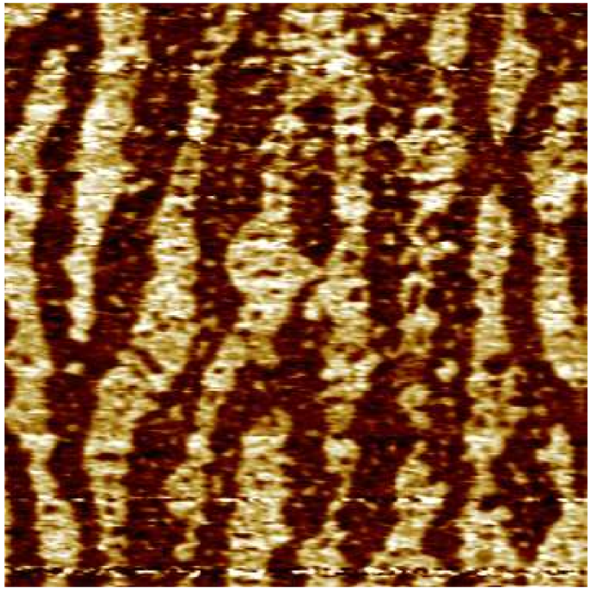

⊙ [001]

1.5 μm

Autocorrelation, C(x,y)

→ [110]

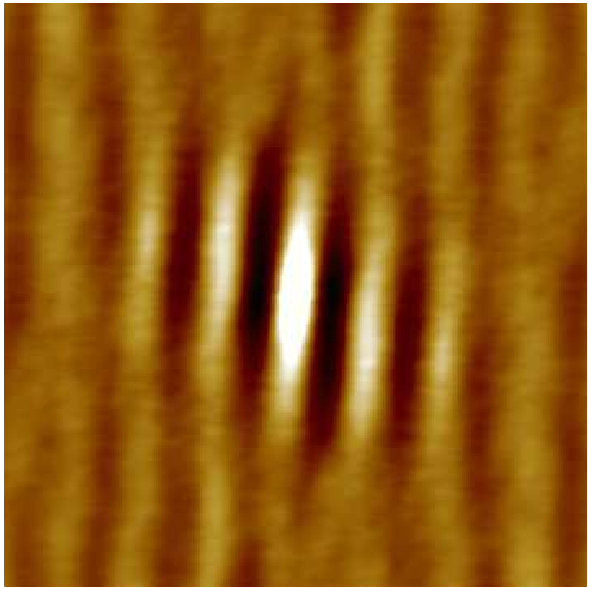

Cross-section of auocorrelation images along [110] direction

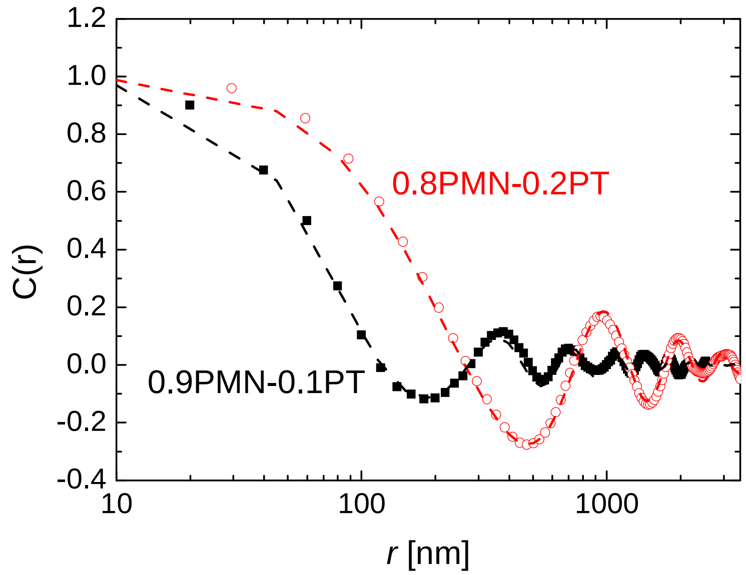

- Micron sized domains forming a quasi-regular structure and embedded nanodomains.
- Correlation along (110) direction is essentially stronger than in 0.9PMN-0.1PT

*Shvartsman & Kholkin PRB **69**, 014102 (2004)*

PMN-20%PT: temperature dependence

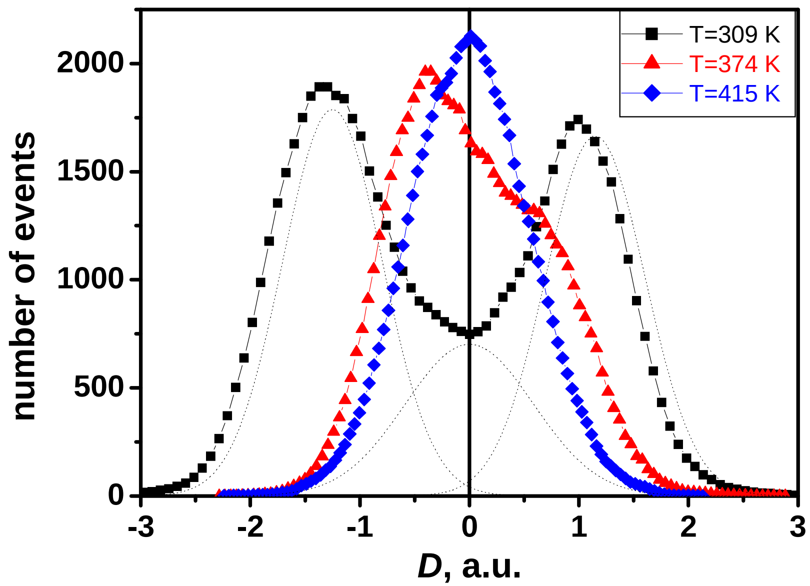

Domain histograms

Rhombohedral⇒cubic phase transition

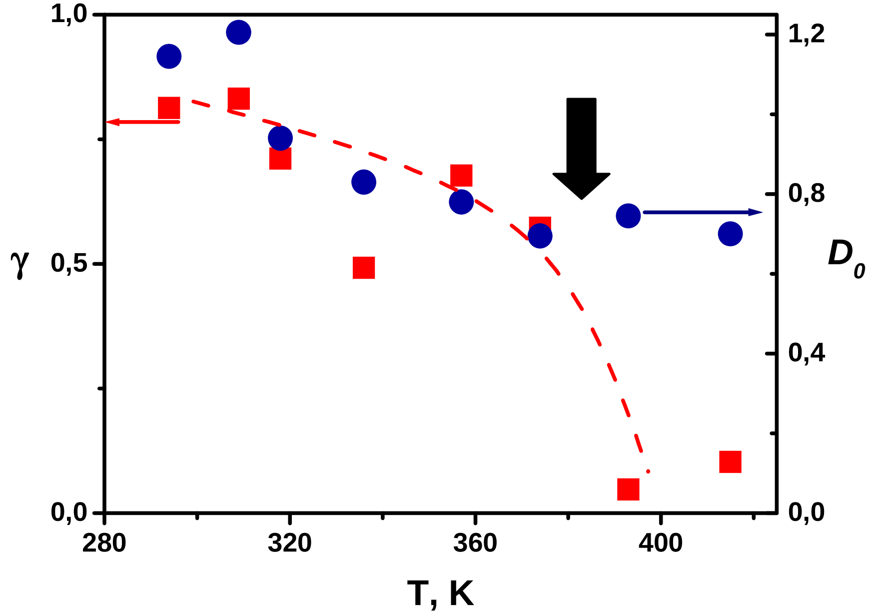

Contrast vs. temperature

- **Size of smallest domain is limited by the physical size of the tip (~8 nm)**
- **Nanodomains survive macroscopic phase transition but their number drops at $T_{c.}$**

*Shvartsman & Kholkin PRB **69**, 014102 (2004)*

Room-temperature domains ($T<T_c$)

grain boundaries

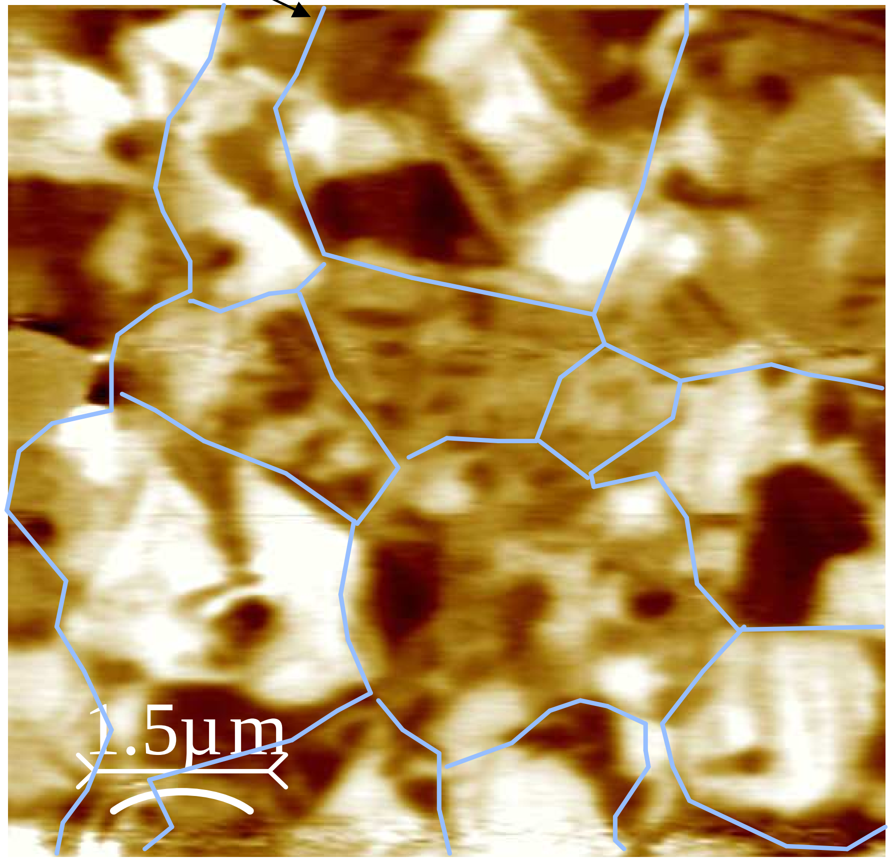

Piezoresponse histogram

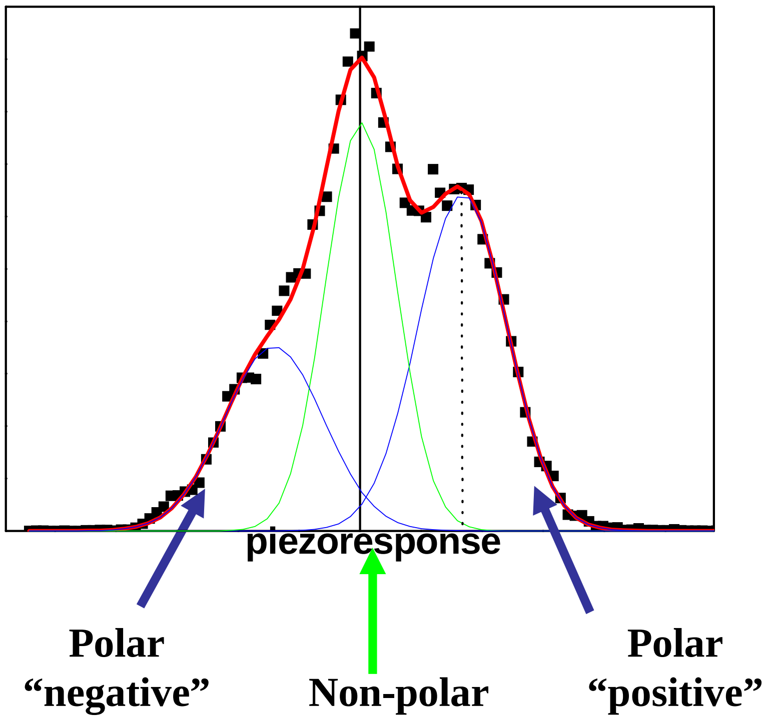

Typical piezoresponse image
at the room temperature

Shvartsman & Kholkin, J. Appl. Phys. (2010)

- **Piezoelectric histograms can be deconvoluted into simple Gaussian peaks corresponding to polar and non-polar phases**

As-grown domains vs. cooling (ZFC)

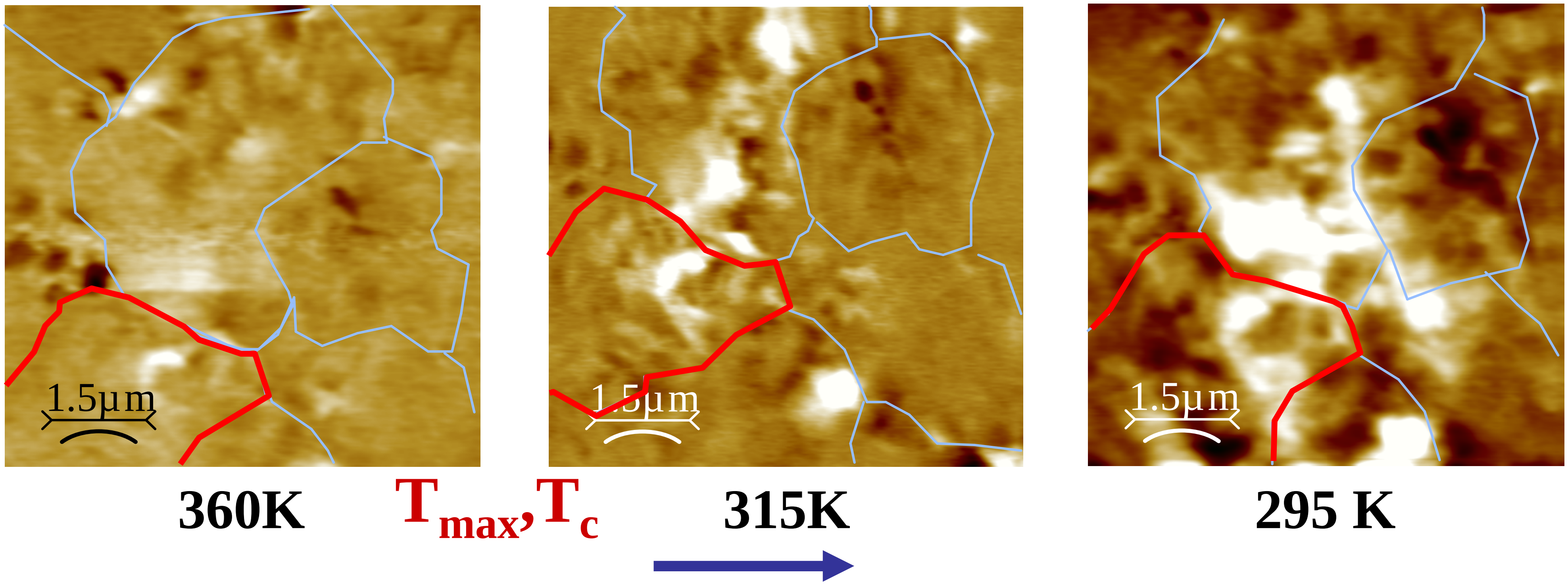

√ **Sample was annealed to 410 K *in situ***

√ **Small domains of size of several hundred nm above T_c and T_{max}**

√ **On cooling nanoscale domains grow and new domains nucleate**

√ **Preferential nucleation on a grain boundary**

Shvartsman & Kholkin, J. Appl. Phys. (2010)

Local temperature dependences

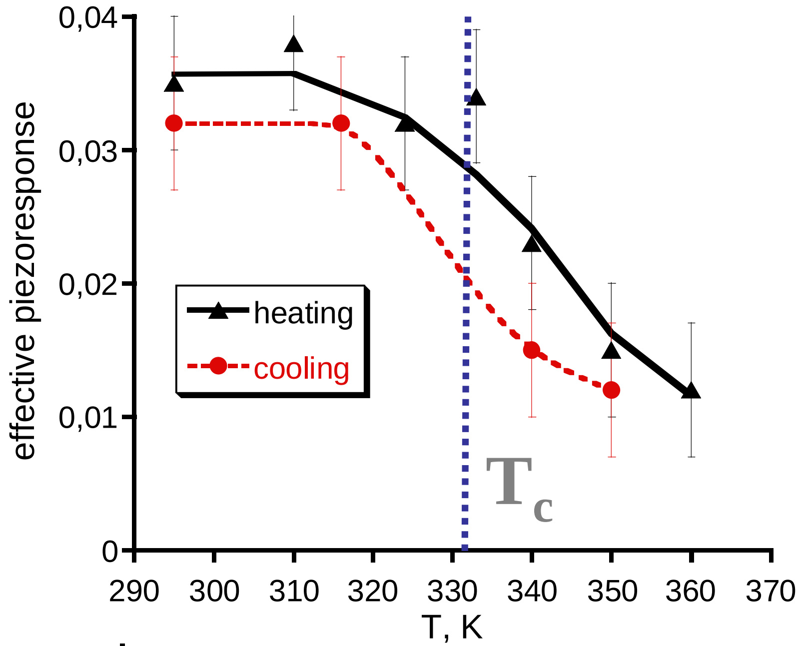

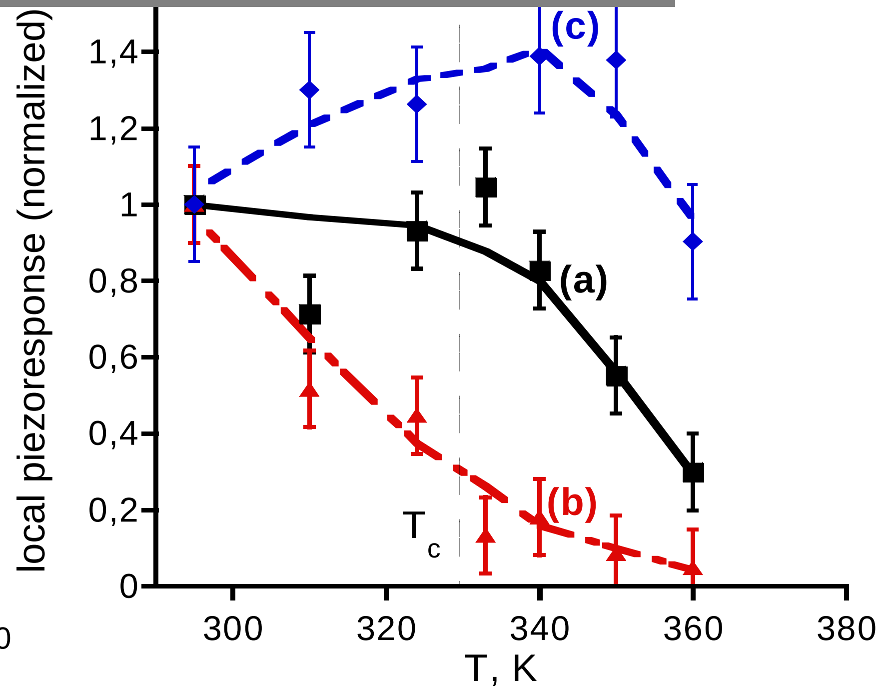

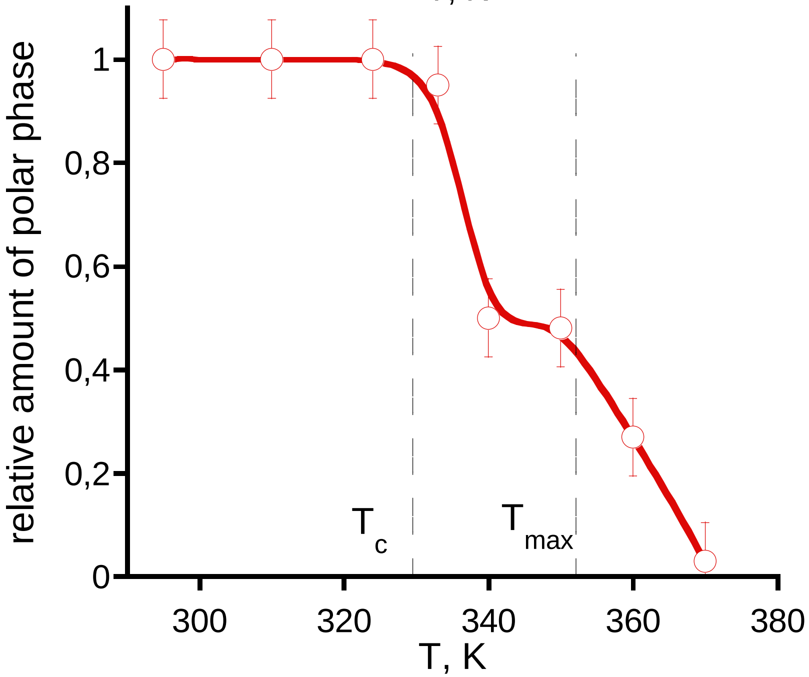

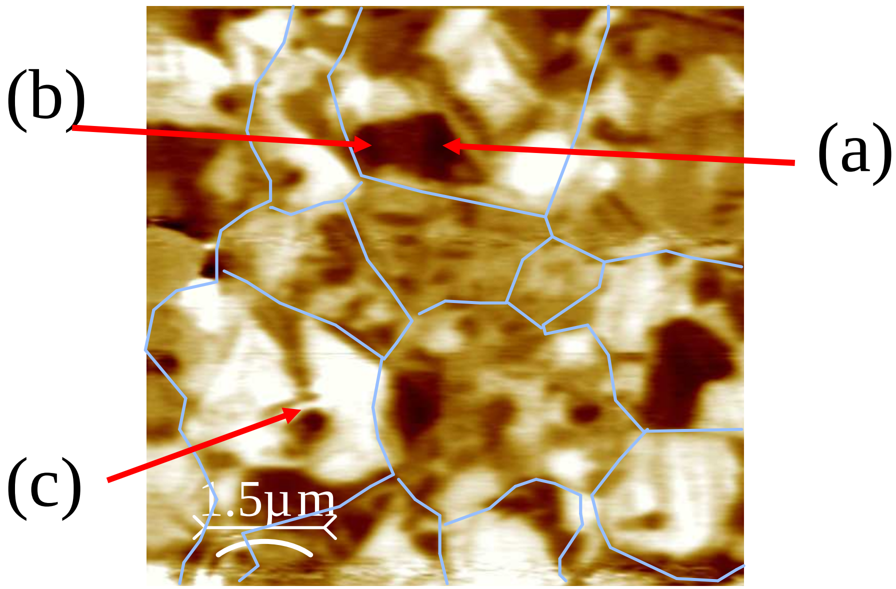

Shvartsman & Kholkin, J. Appl. Phys. (2010)

Mesoscale variations of correlation length

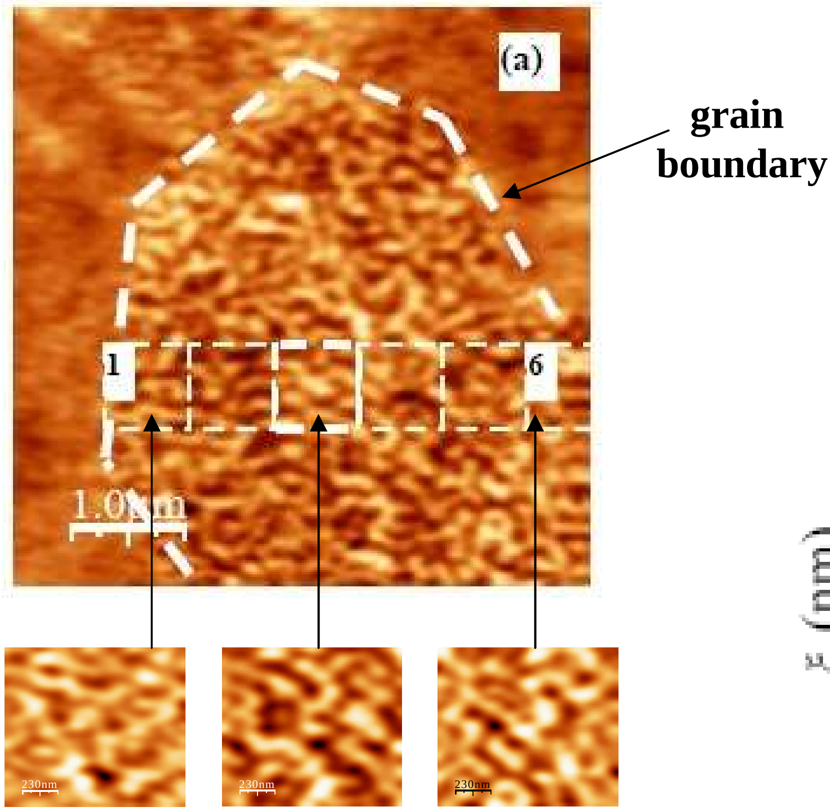

Autocorrelation function

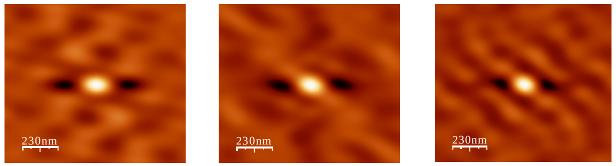

2D image of *C*(r) represents areas with correlated (parallel) polarization (bright contrast) and areas with antiparallel polarization (dark contrast)

$$< C(r) >= \sigma^2 \exp\left[-\left(\frac{r}{< \xi >} \right)^{2h} \right]$$

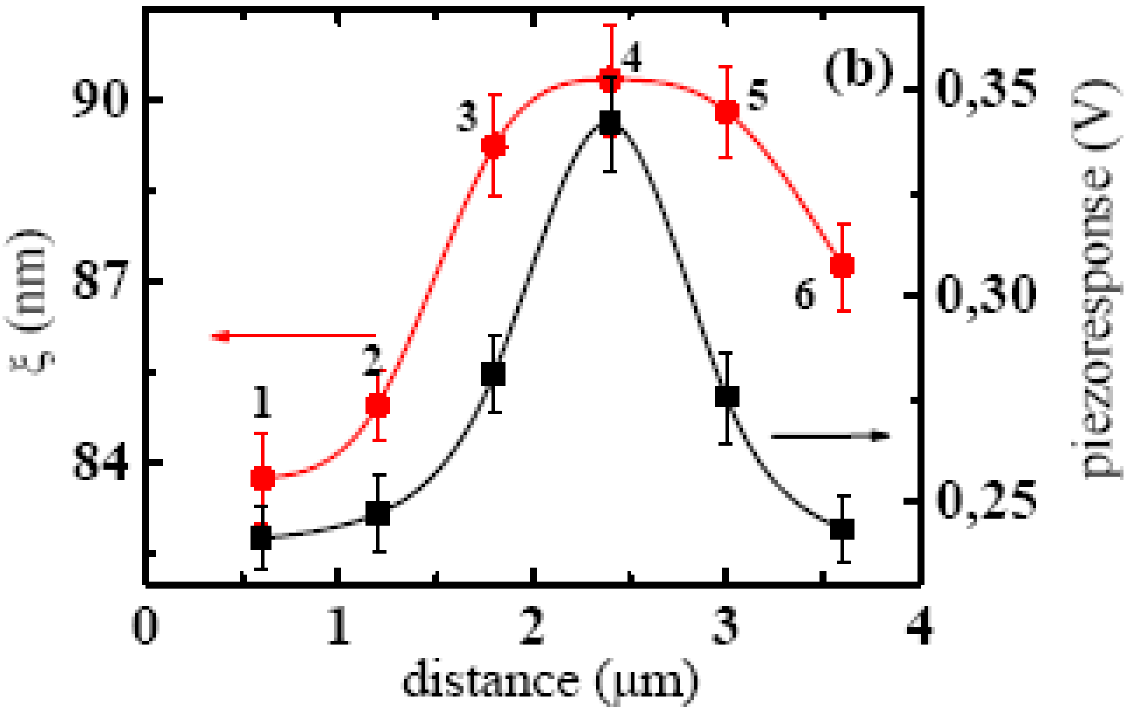

Kiselev et al, J. Phys. D 40 (2007)

Local FFT analysis: principle

Screenshot 1 – no ring

Total Image

Fit of cross-sections (vertical and lateral)

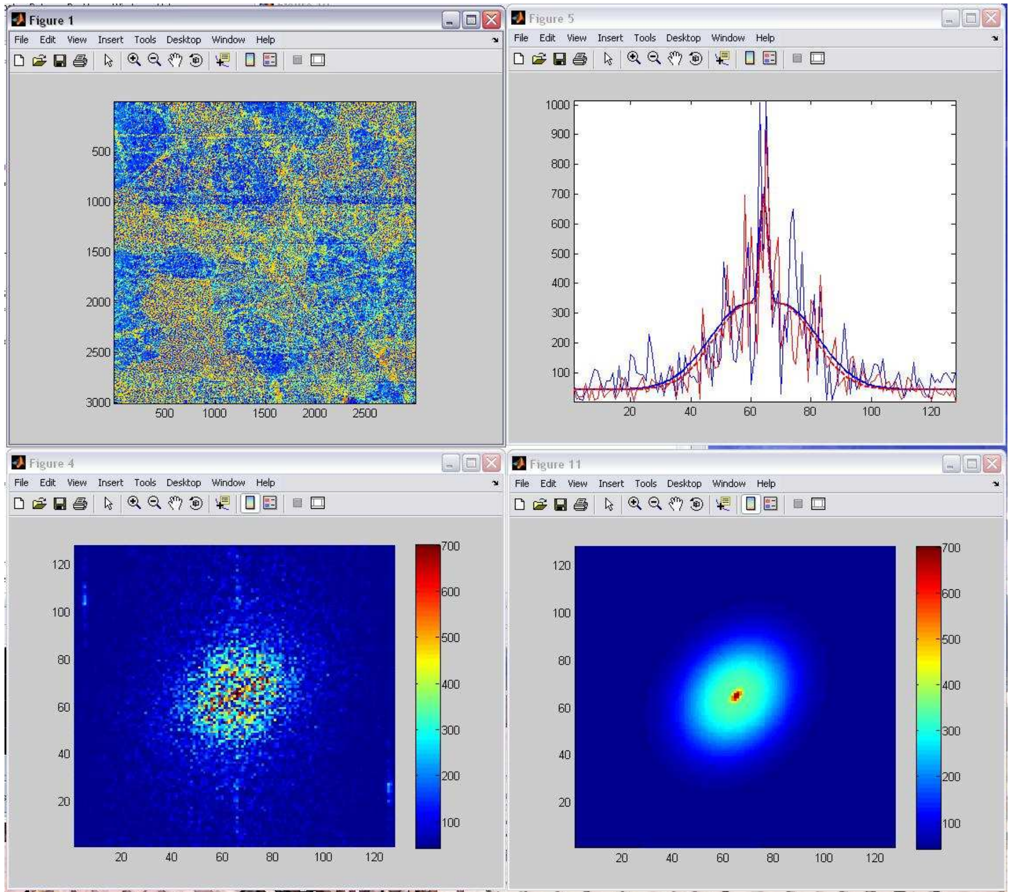

FFT of a selected small square

Fit of FFT

Screenshot 2 - ring

Total Image

Fit of cross-sections (vertical and lateral)

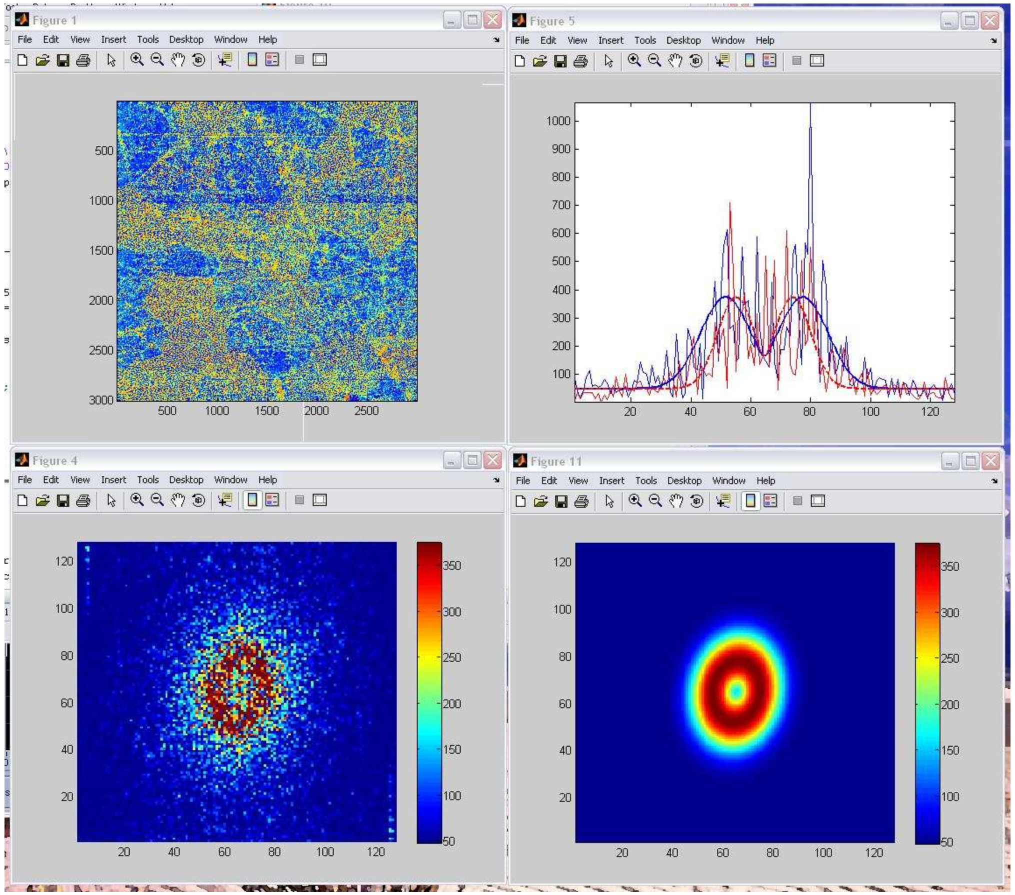

FFT of a selected small square

Fit of FFT

Kholkin et al, Materials (2010)

Local Fourier analysis in PLZT

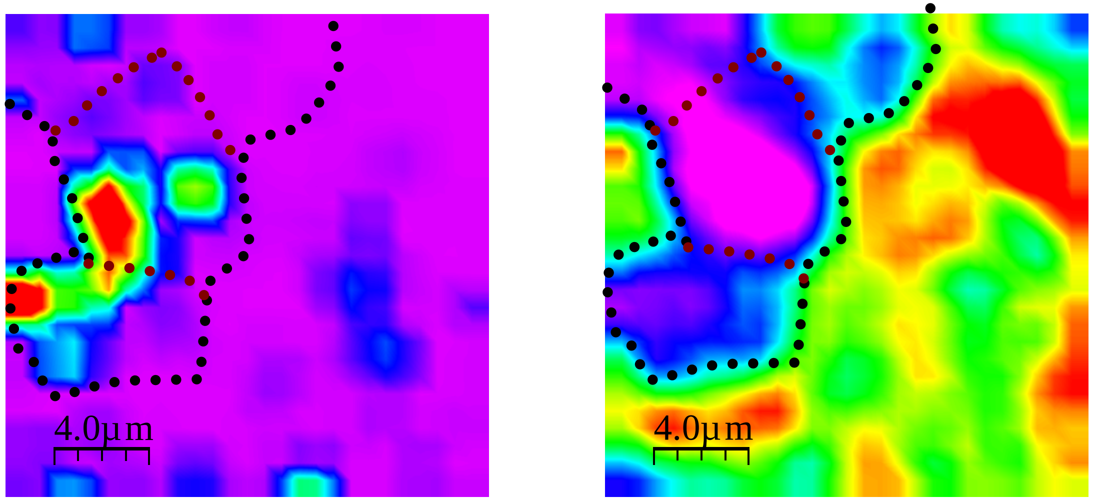

amplitude correlation length

rotation width

Kholkin et al, Materials (2010)

Macroscopic vs. local properties in PLZT

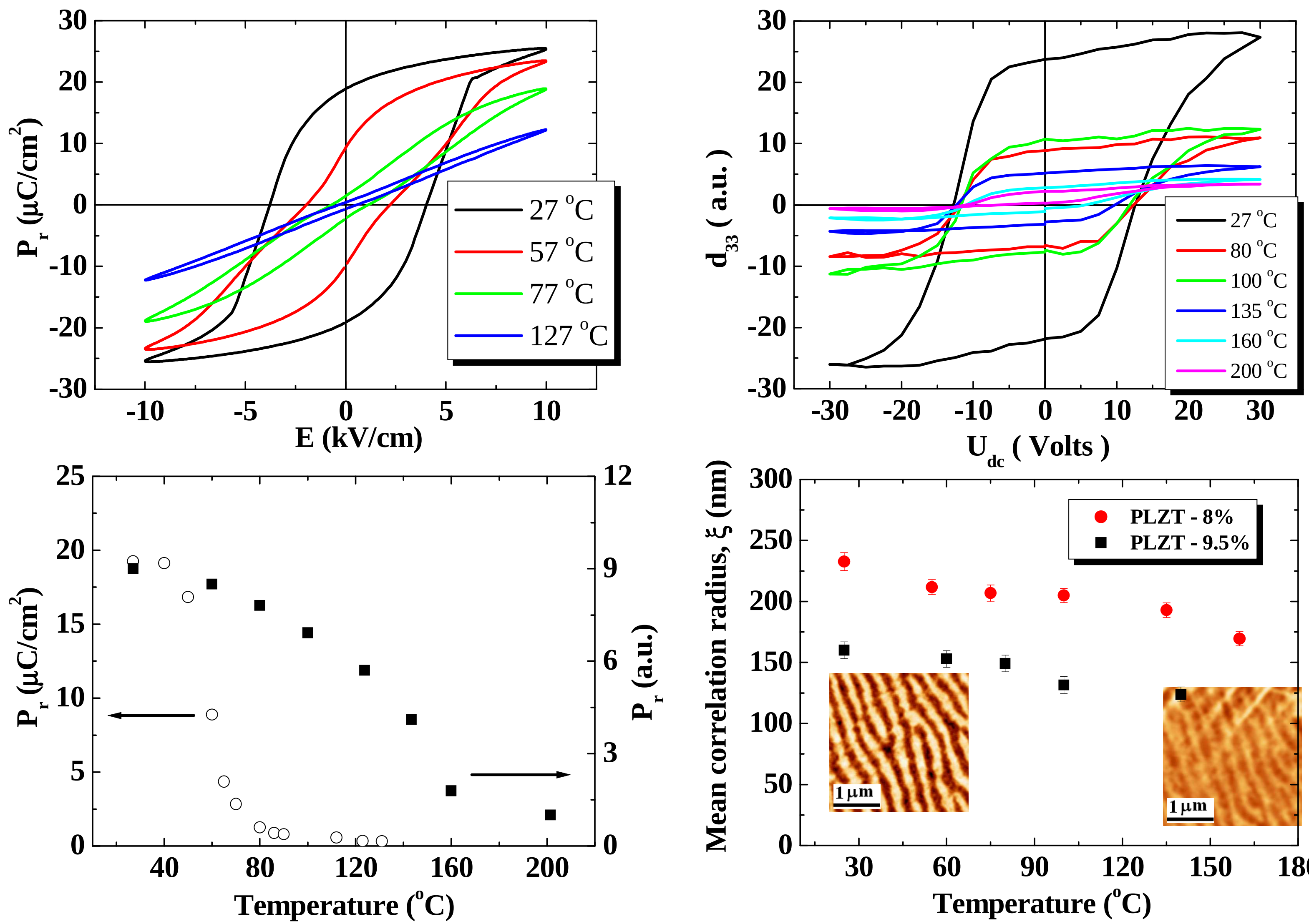

Kholkin et al, Adv. Func. Mat. (2011)

Surface phase transition and mesoscopic domains in relaxor ferroelectrics

Materials Views
www.MaterialsViews.com

ADVANCED FUNCTIONAL MATERIALS
www.afm-journal.de

Surface Domain Structures and Mesoscopic Phase Transition in Relaxor Ferroelectrics

Andrei Kholkin, Anna Morozovska, Dmitry Kiselev, Igor Bdikin, Brian Rodriguez, Pingping Wu, Alexei Bokov, Zuo-Guang Ye, Brahim Dkhil, Long-Qing Chen, Marija Kosec, and Sergei V. Kalinin**

Relaxor ferroelectrics are a prototypical example of ferroic systems in which interplay between atomic disorder and order parameters gives rise to emergence of unusual properties, including non-exponential relaxations, memory effects, polarization rotations, and broad spectrum of bias- and temperature-induced phase transitions. Despite more than 40 years of extensive research following the original discovery of ferroelectric relaxors by the Smolensky group, the most basic aspect of these materials – the existence and nature of order parameter – has not been understood thoroughly. Using extensive imaging and spectroscopic studies by variable-temperature and time resolved piezoresponse force microscopy, we find that the observed mesoscopic behavior is consistent with the presence of two effective order parameters describing dynamic and static parts of polarization, respectively. The static component gives rise to rich spatially ordered systems on the ~100 nm length scales, and are only weakly responsive to electric field. The surface of relaxors undergoes a mesoscopic symmetry breaking leading to the freezing of polarization fluctuations and shift of corresponding transition temperature.

glasses,[3] ferroelectric relaxors,[4] structural glasses,[5] as well as more exotic matter such as vortex lattices in superconductors[6] have remained a focus of extensive theoretical and experimental effort over the last 5 decades. This interest is precipitated by the unique properties emerging as a result of disorder interaction with order parameter field, including high magnetic and electromechanical coupling constants, tunability of dielectric and magnetic responses, as well as unique memory effects. By now, many of the theoretical concepts formulated on the quest to understand the physics of disordered systems, such as Edwards–Anderson models for spin glasses[1] and spherical random bond-random field model for relaxors,[7] have become the bedrock of statistical physics.

PFM in macroscopically nonpolar materials

$SrTiO_3$

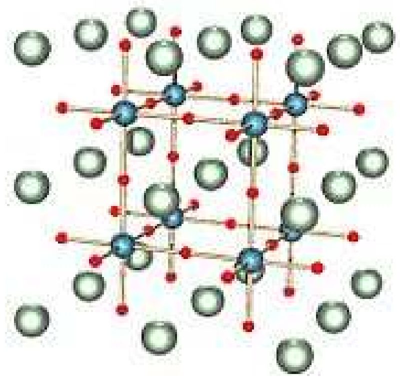

O_h cubic symmetry at room temperature,
no macroscopic piezoelectricity and pyroelectricity
highly non-linear dielectric material used in tunable microwave filters, varactors, cell phones, antennas, etc

Flexoelectricity is single crystals

Strain-Gradient-Induced Polarization in $SrTiO_3$ Single Crystals

P. Zubko,* G. Catalan,† A. Buckley, P. R. L. Welche, and J. F. Scott

Centre for Ferroics, Department of Earth Sciences, University of Cambridge, Cambridge CB2 3EQ, United Kingdom

(Received 26 July 2007; published 19 October 2007)

PRL (2007)

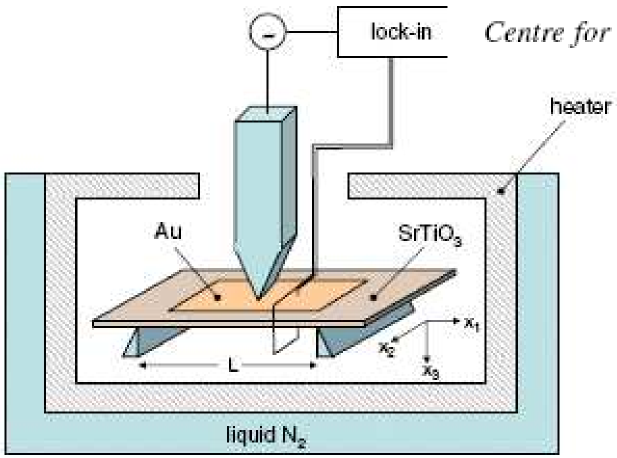

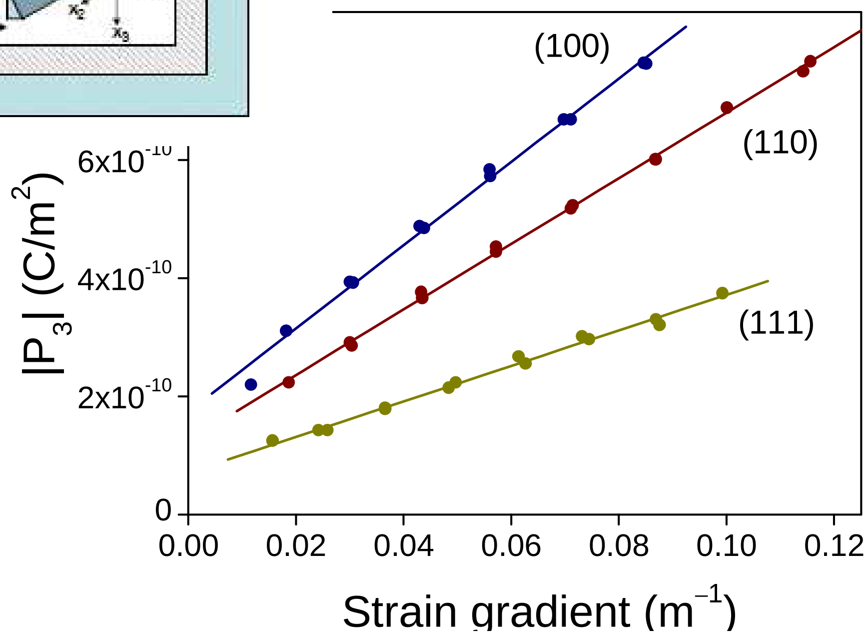

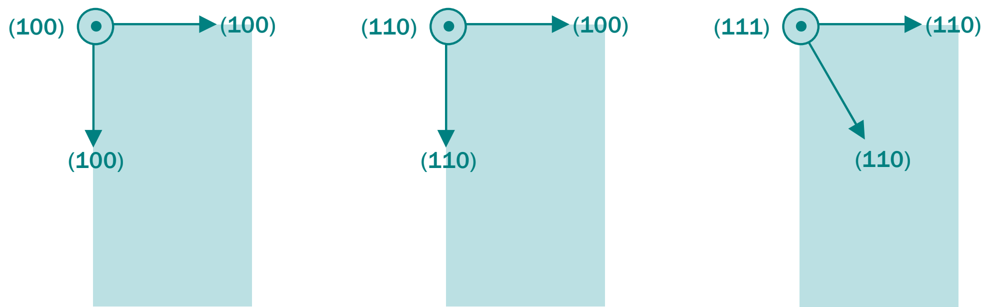

$$\mu_{001} = +6.1\text{nC/m}$$
$$\mu_{101} = -5.1\text{nC/m}$$
$$\mu_{111} = -2.4\text{nC/m}$$

These are considerably smaller than measured for ferroelectric ceramics (~μC/m)

Strain gradients in thin films

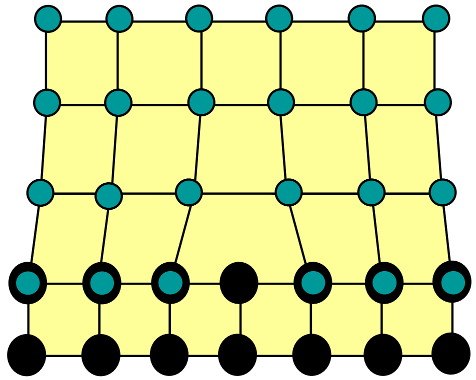

inhomogeneous strain around misfit dislocation

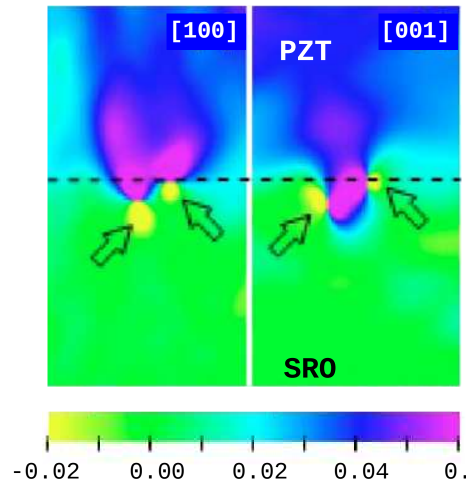

Nagarajan *et al.* APL (2005)

- Mismatch strain relaxes with thickness: is relaxation homogeneous or inhomogeneous?

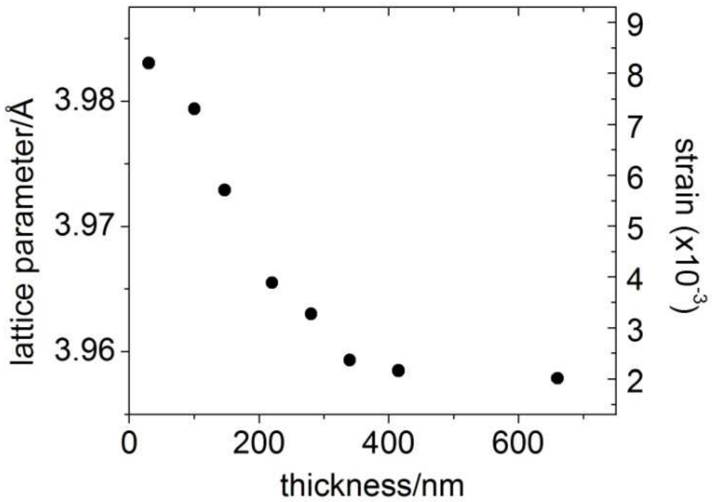

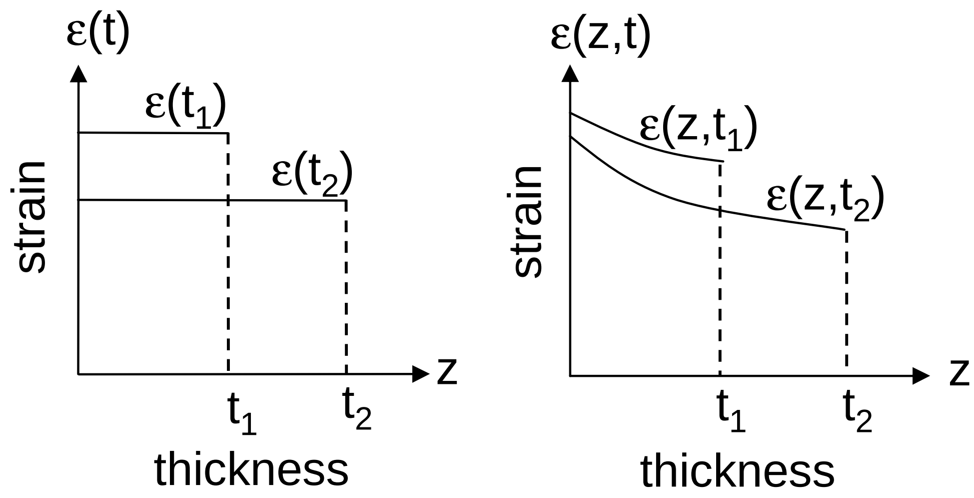

Courtesy Gustau Catalan (University of Barcelona)

Pure $SrTiO_3$ ceramics | Sol-gel PZT film

Topography

Lateral PFM

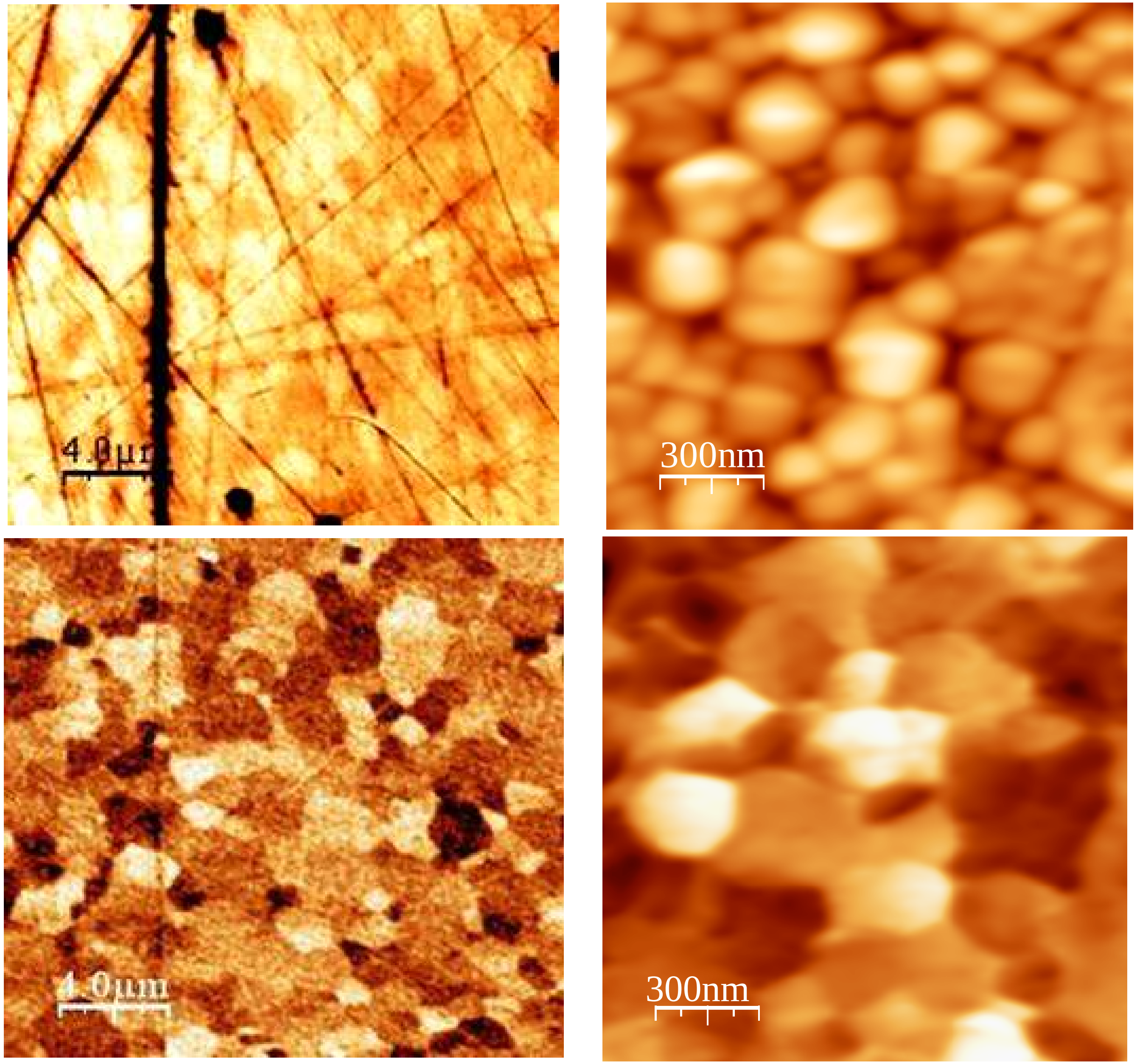

Collaboration with J. Petzelt (Institute of Physics, Prague)

Collaboration with S.-H. Kim (Inostek, Korea)

Proof of the piezoelectric nature

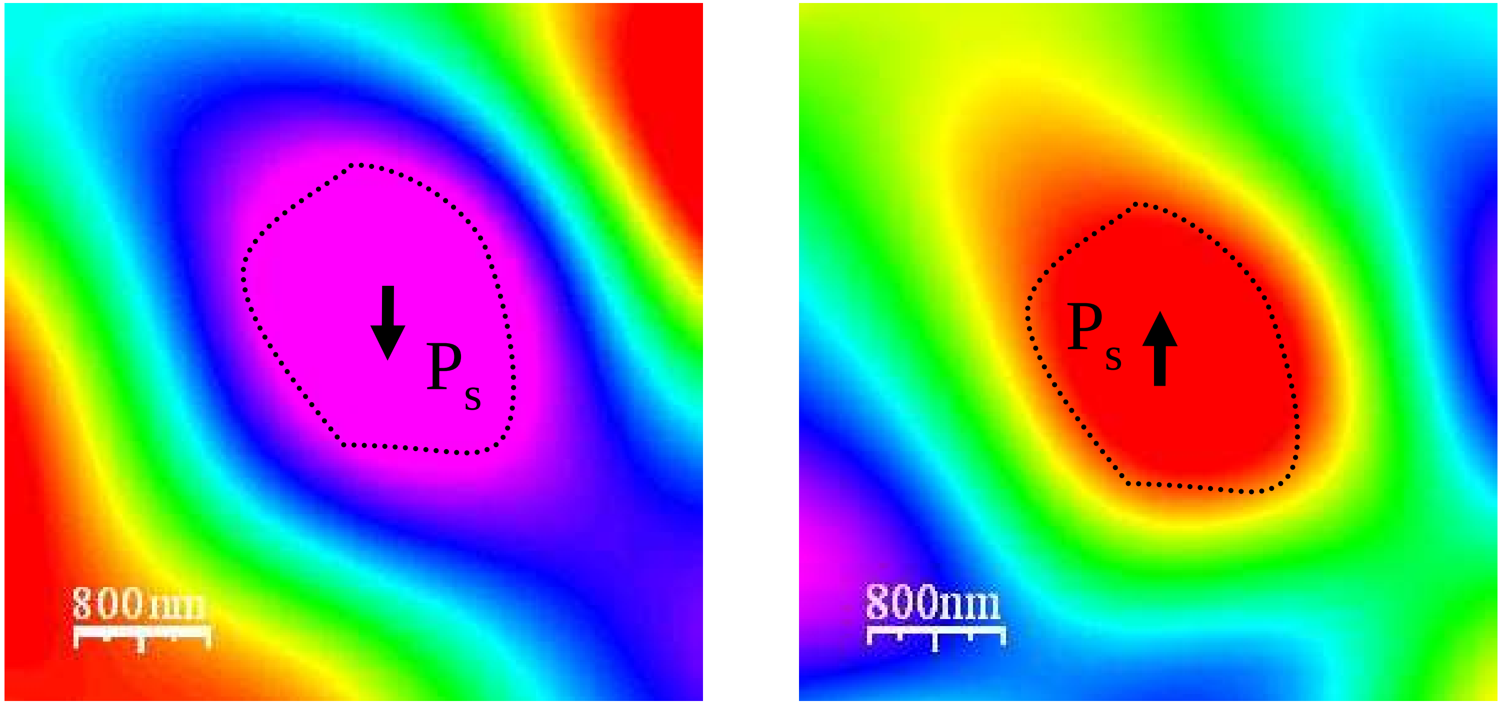

Original lateral PFM | After rotation at 180º

- **Observed in both annealed and as-polished sample**
- **No effect of bleaching after chemical etching**
- **d_{33} values of the order of quartz (1-3 pm/V)**

Kholkin et al, Appl. Phys. Lett. (2008)

Piezoresponse distribution

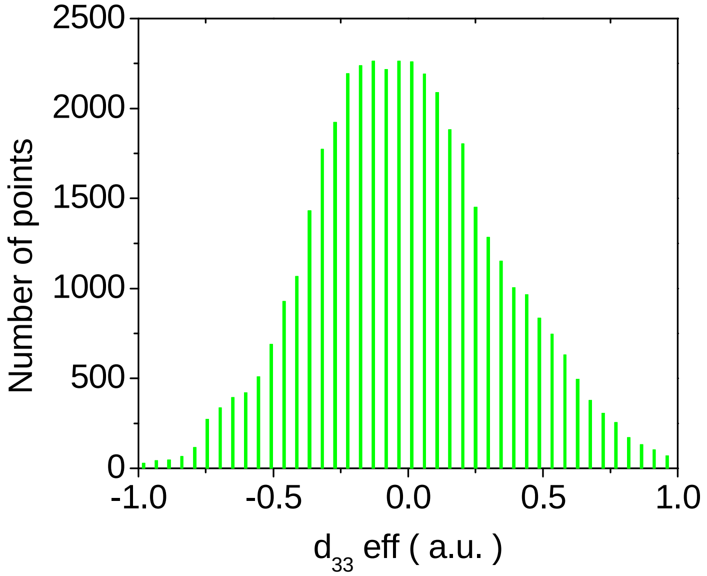

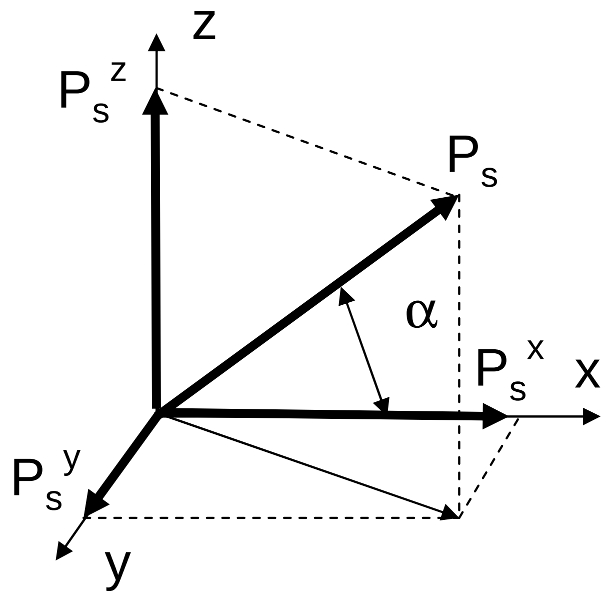

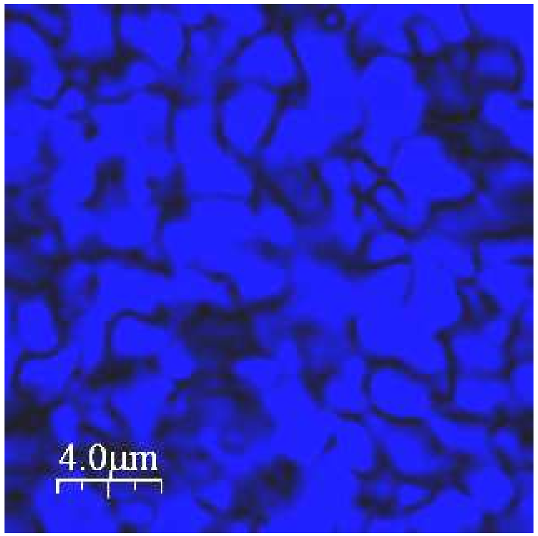

$$\sqrt{X(d_{15})^2 + Y(d_{15})^2}$$

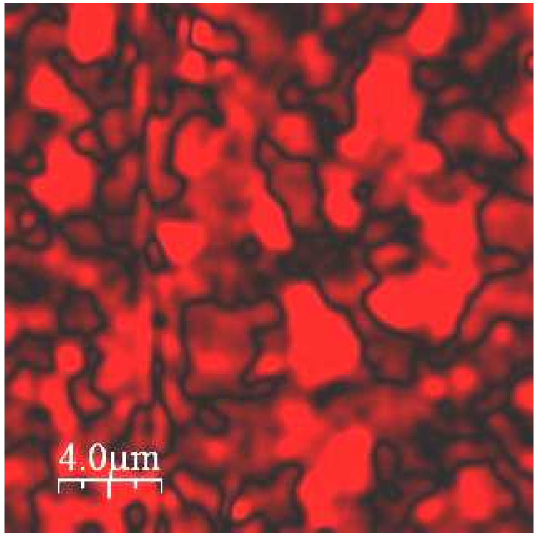

$$\left|Z(d_{33})\right|$$

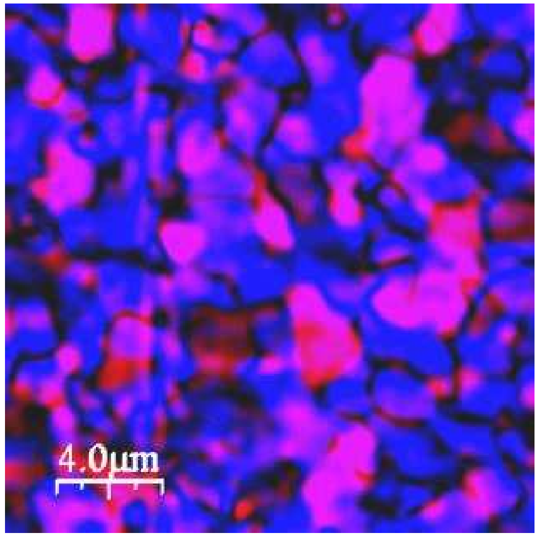

$$\frac{\sqrt{X(d_{15})^2 + Y(d_{15})^2}}{\left|Z(d_{33})\right|}$$

Enhancement of the lateral response across grain boundary

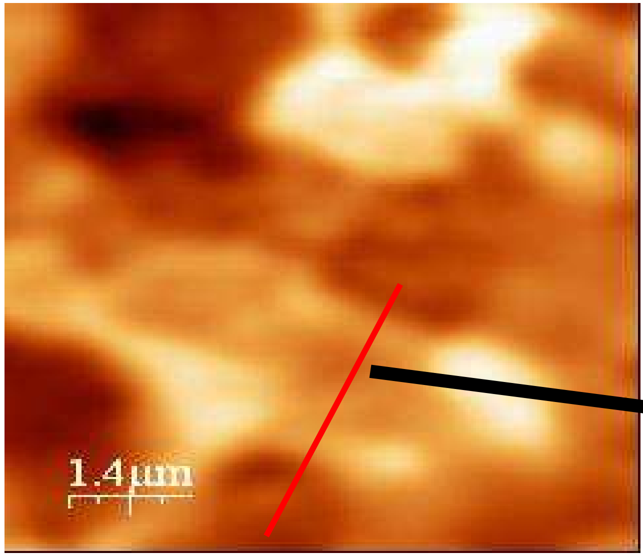

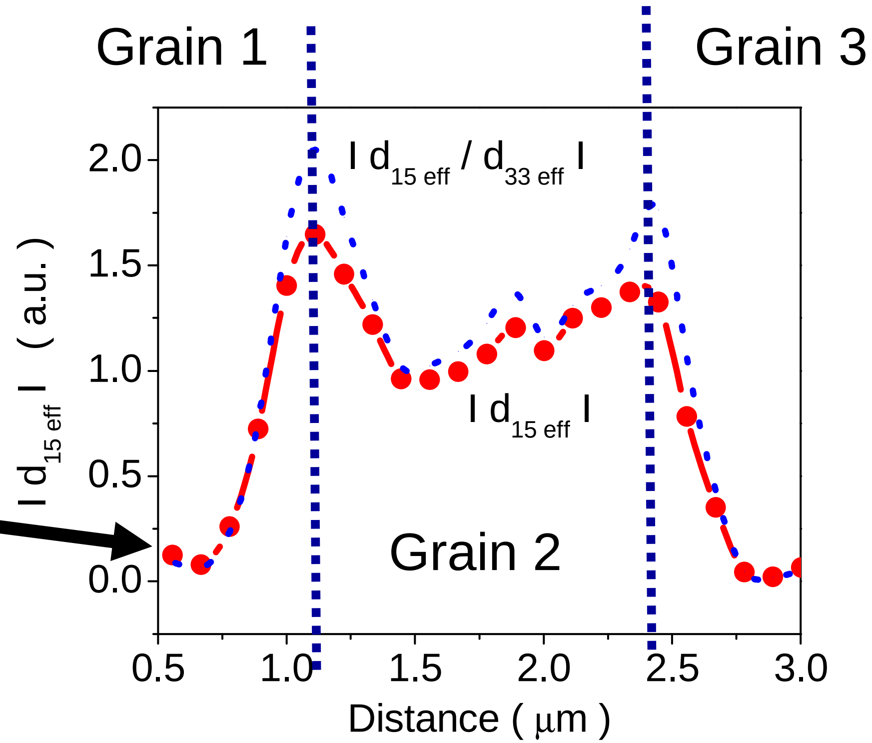

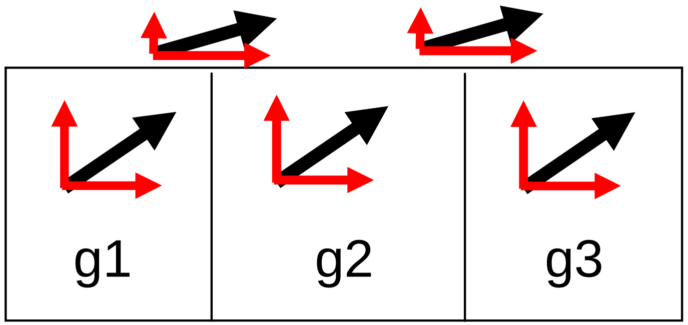

Kholkin et al, Appl. Phys. Lett. (2008)

Polar grain boundaries in $SrTiO_3$ ceramics

The disordered grain boundary (*GB*) contains ***charged oxygen vacancies.***

Distorted polyhedra near GB, leading to tetragonal axis perpendicular to GB.

The polar vector is therefore perpendicular to the grain boundary and is coupled to the oxygen vacancies.

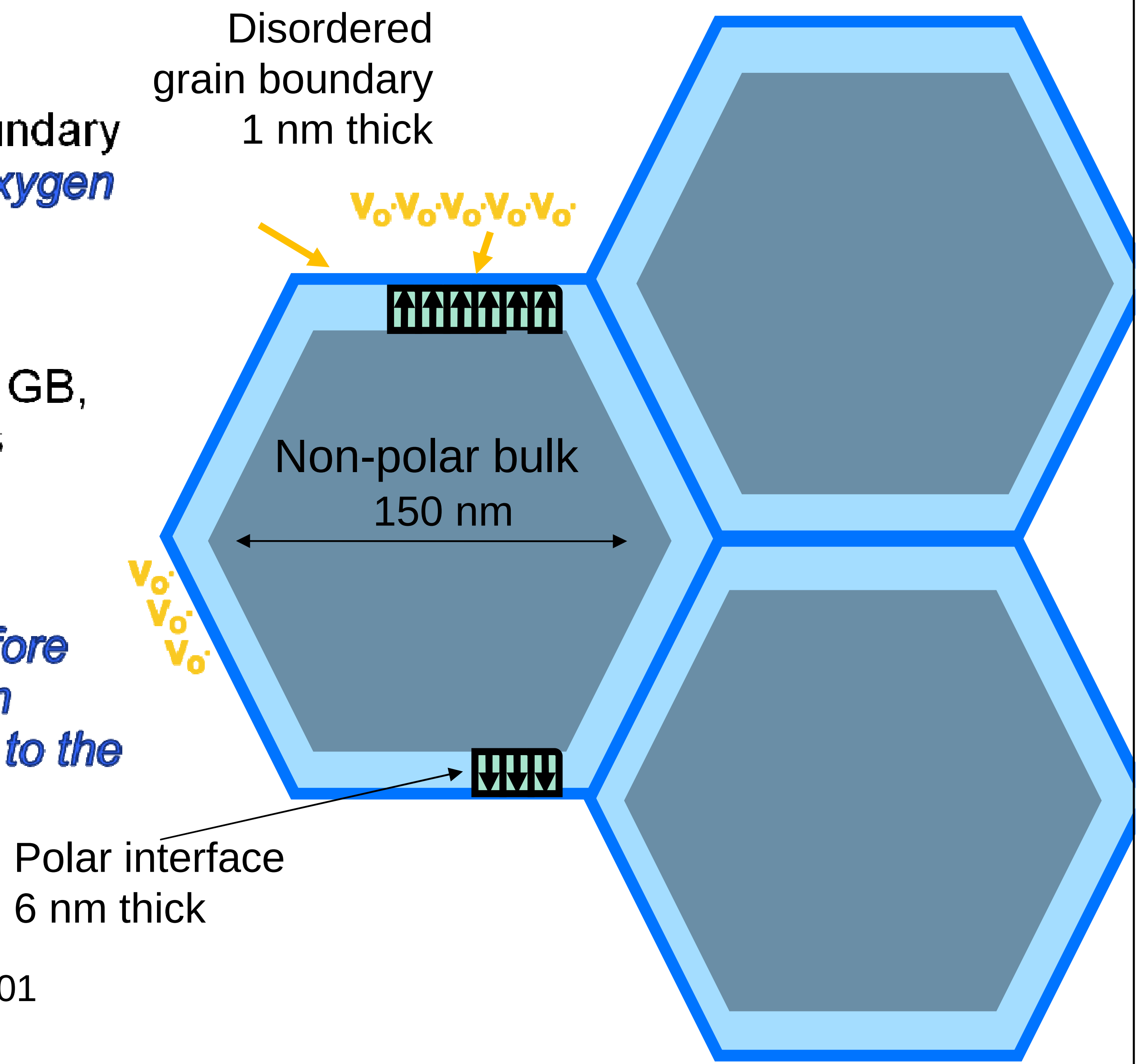

Petzelt, Waser et al. PRB 2001
Petzelt et al. JPhysCM 2007

Origin of the contrast inside the grains

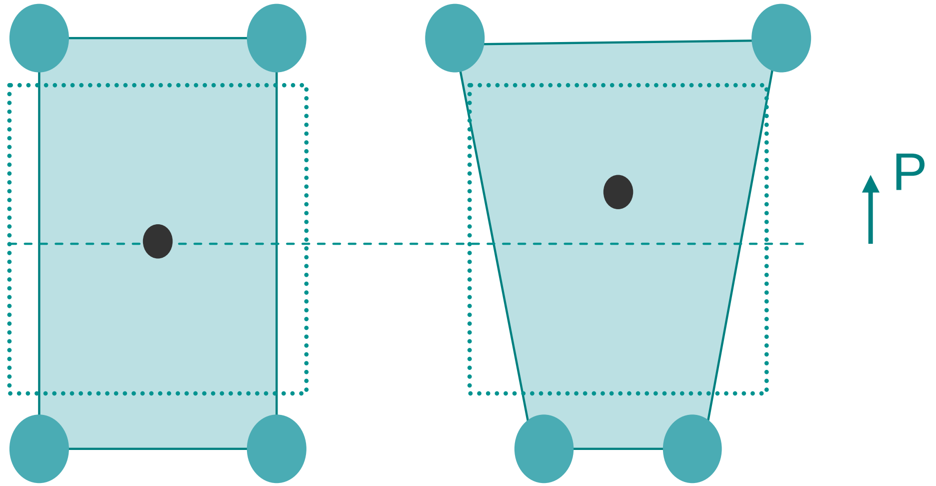

$$P_i = f_{ijkl} \frac{\partial \varepsilon_{kl}}{\partial x_j}$$

$$f \sim \frac{e}{a} *$$ dielectric constant

Flexoelectricity proportional to strain gradient and dielectric constant.

Kogan, Soviet Phys. Solid State (1964)

Tagantsev, Phys. Rev. B (1986)

Tagantsev, Phase Transitions (1991)

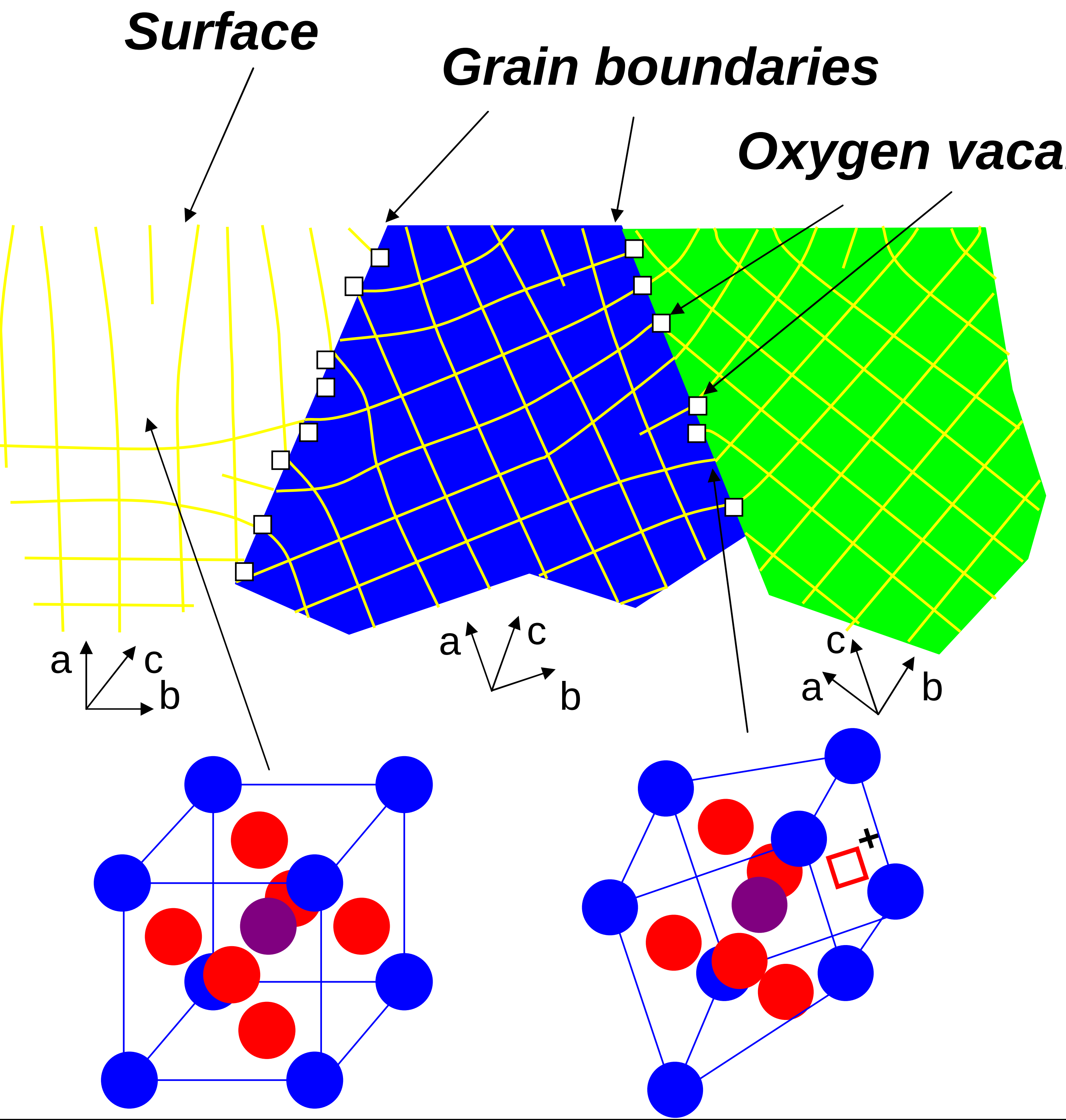

$$P_i = f_{ijkl}\frac{\delta\varepsilon_{kl}}{\delta x_j}$$

$$P_i \cong 0.7\mu C / cm^2$$

$$f_{ijkl} \cong 0.1nC / m$$

$$d_{33} \propto 2Q\varepsilon_o\varepsilon P_i \propto \varepsilon^2$$

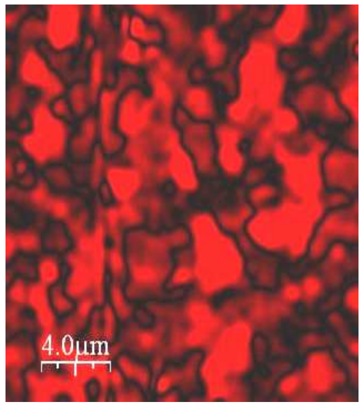

$CaCu_3Ti_4O_{12}$: material with giant dielectric constant

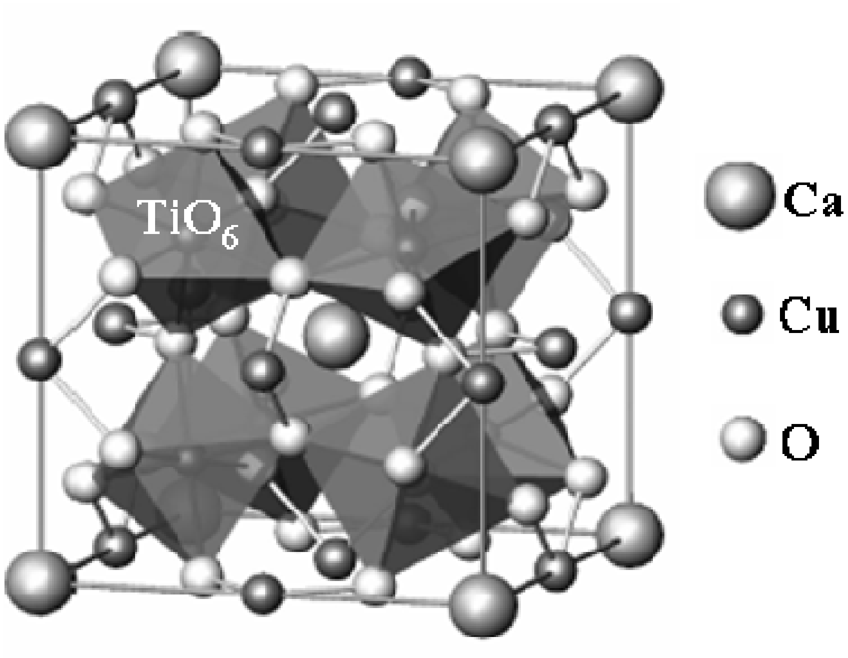

- Cubic structure *Im3* space group
- Giant K up to 100,000 even in single crystals
- Ferroelectric displacements suppressed by Cu^{2+} ions and associated tilt of oxygen octahedra
- Important material for capacitor and energy storage applications

Combined VPFM-LPFM on CCTO ceramics

Topography

VPFM

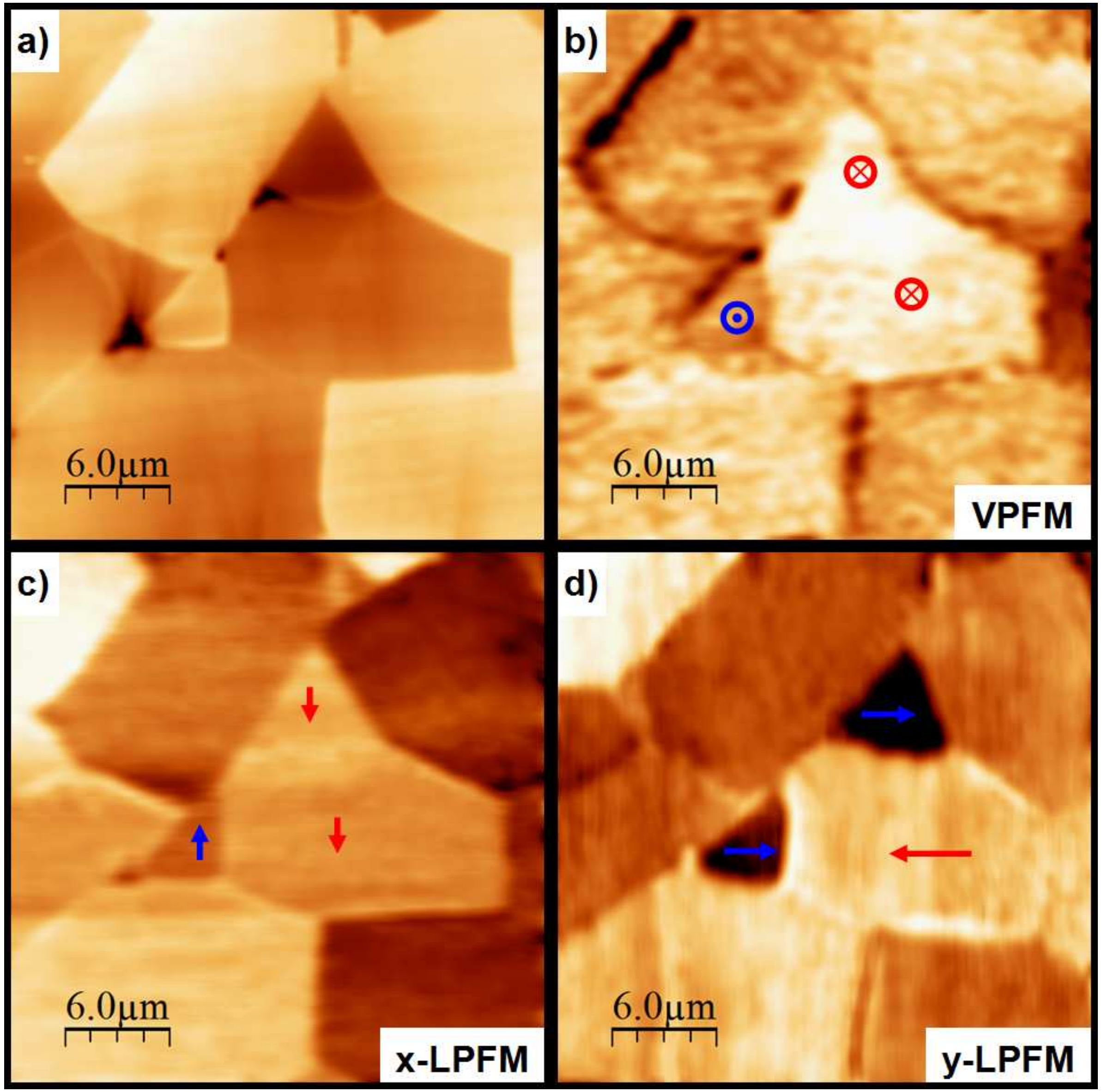

X-LPFM

y-LPFM

Tararam et al, J. Appl. Phys. (2011)

Proof of piezoelectric nature of the signal

180º rotation of LPFM (no electrostatic contribution)

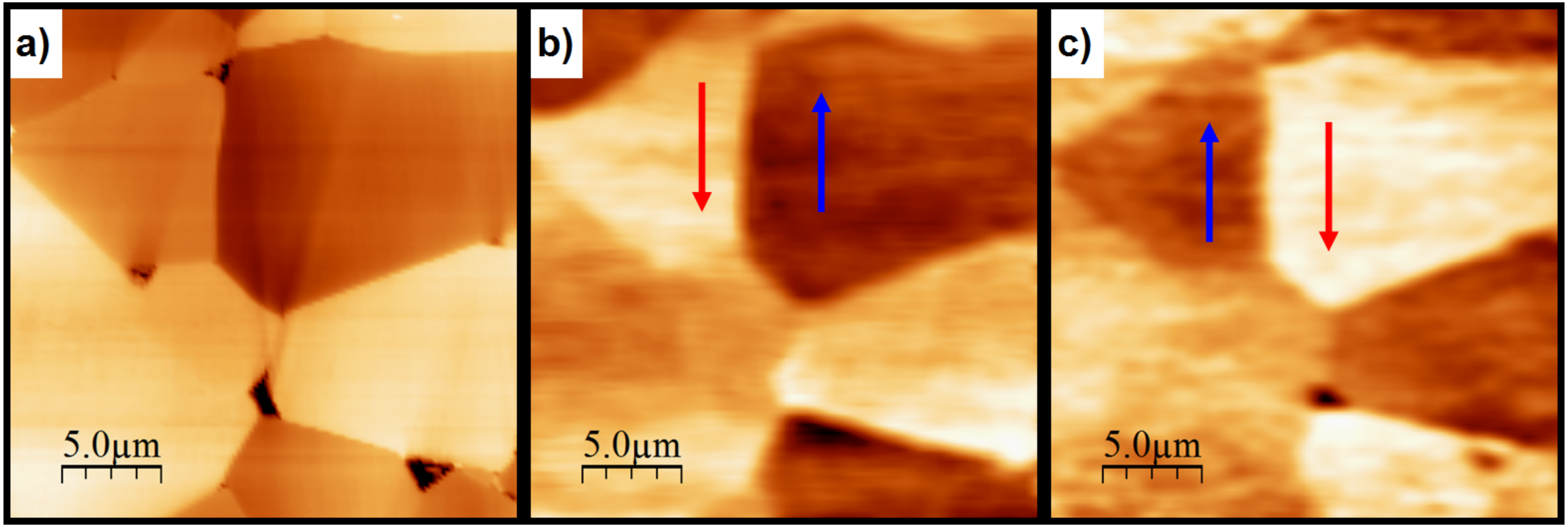

Topography **LPFM** **LPFM after rotation**

Tararam et al, J. Appl. Phys. (2011)

Local poling and signal relaxation

Local piezoresponse hysteresis loops

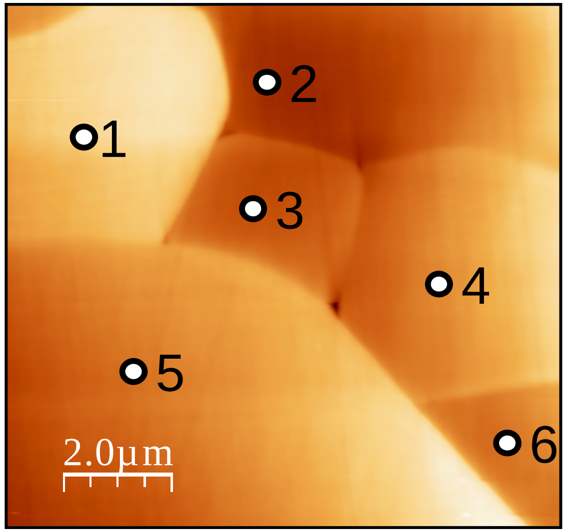

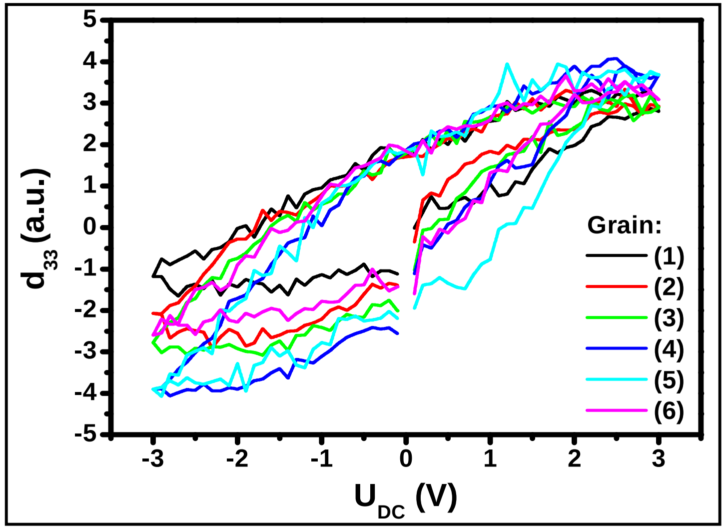

Local poling and relaxation

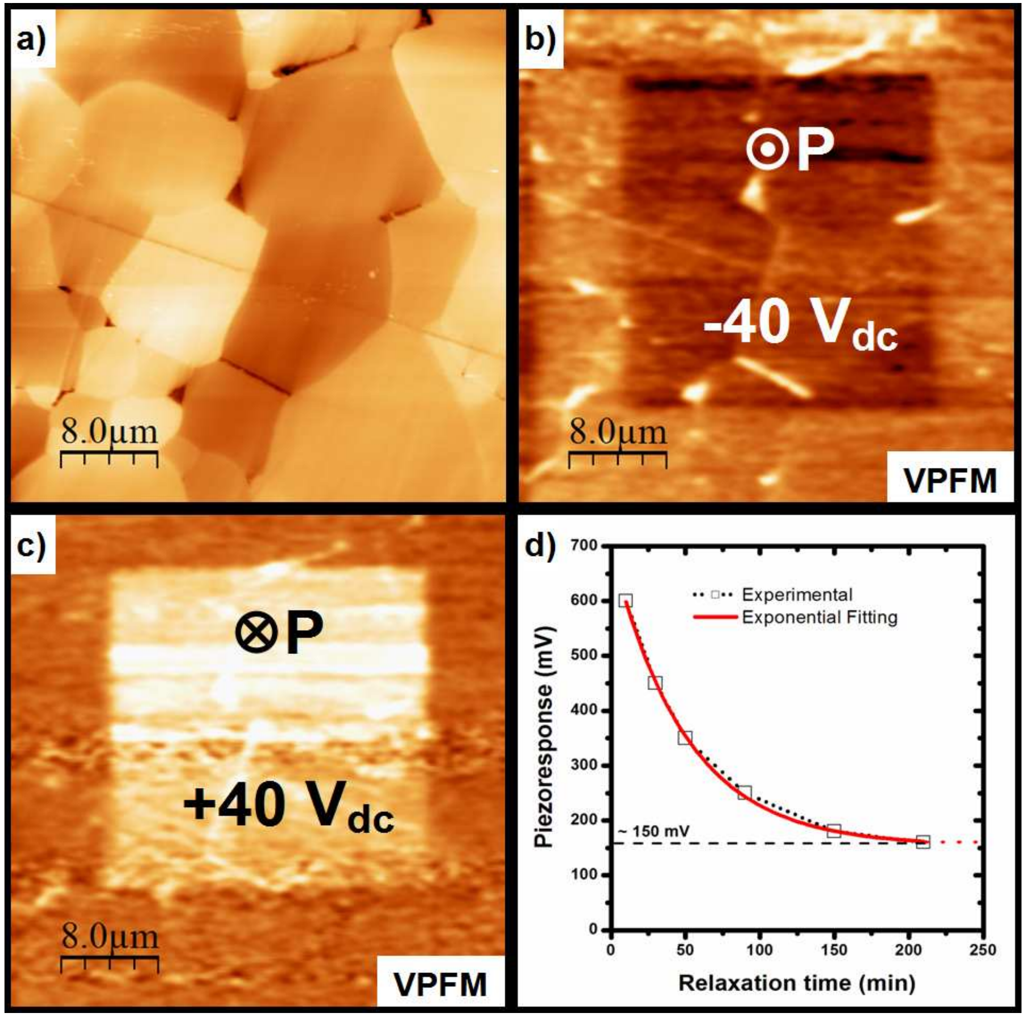

Tararam et al, J. Appl. Phys. (2011)

Self-assembling peptide nanotubes

Biological proteins and peptides have the intrinsic ability to self-assemble into elongated solid nanofibrils[1–7], which may give rise to amyloid diseases[8–11] or inspire applications ranging from tissue engineering to nanoelectronics[12–16]. Proteinaceous fibrils are extensively studied and well understood, to the extent that detailed theoretical models have been proposed that explain and predict their behavior[17,18]. Another intriguing state of protein-like self-assembly is that of nanotubes (NTs), defined here as an elongated nano-object with a definite inner hole. In contrast to proteinaceous fibrils, nanotubes are much less frequently observed and far less well understood. However, they have attracted research interest internationally as key components for nanotechnology.

Shane Scanlon and Amalia Aggeli*
Centre for Self-Organizing Molecular Systems (SOMS), School of Chemistry, University of Leeds, Leeds, LS2 9JT, UK
*E-mail: a.aggeli@leeds.ac.uk

Nano Today (2008)

Short aromatic dipeptides from solution

The core recognition motif of Aβ peptide (Alzheimer's disease), the diphenylalanine.
dipeptide NH2-Phe-Phe-COOH (FF) is self assembled into ordered peptide nanotubes

Bio-inspired crystalline peptide nanotubes (PNTs)

Fast evaporation from aqueous solution

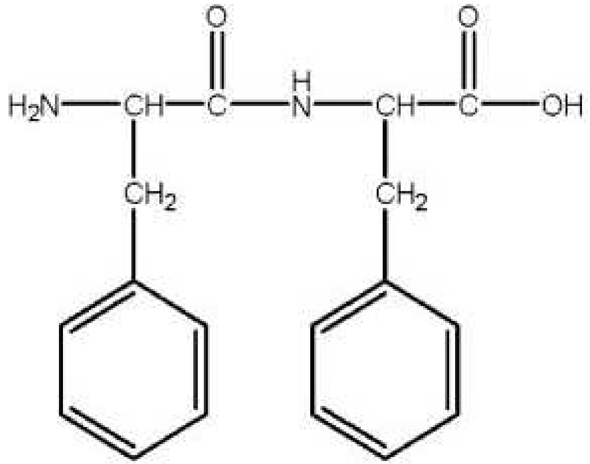

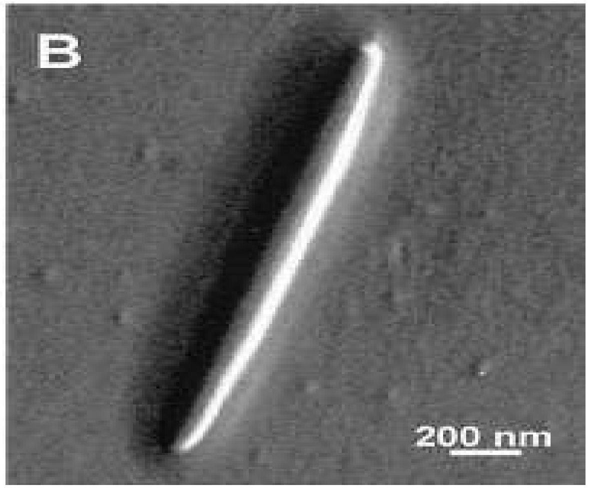

Fast evaporation from organic solution

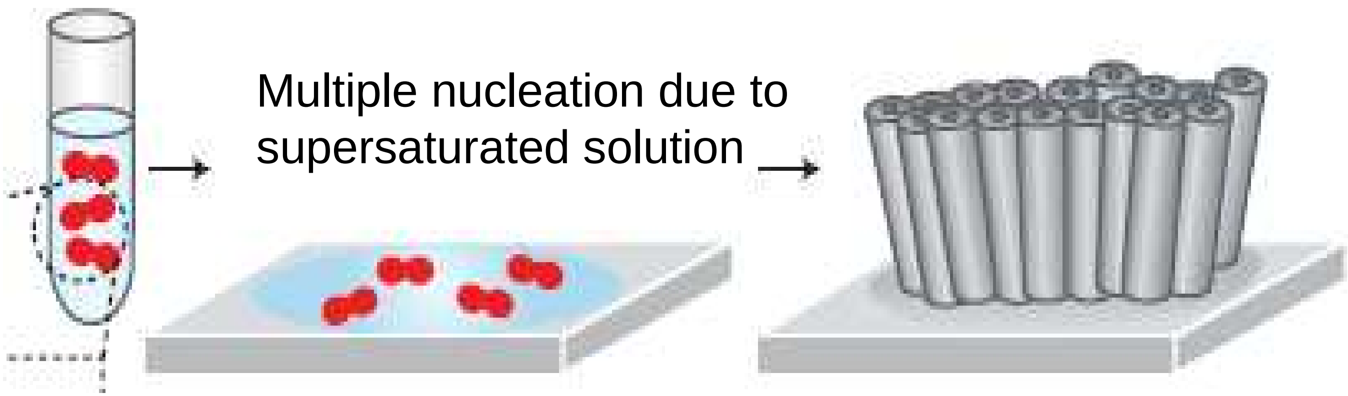

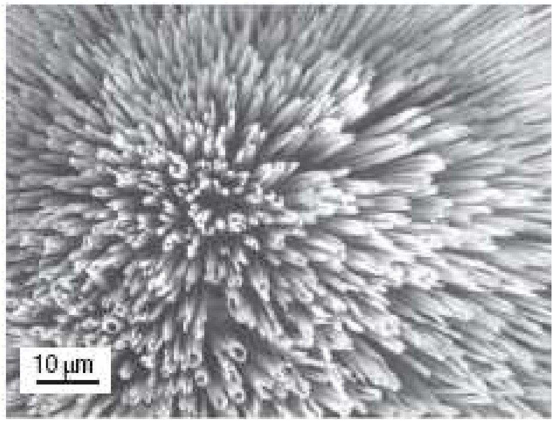

M. Reches, E. Gazit, Nature Nanotechnology, 2006

Unidirectional growth

Vertical and horizontal tubes prepared from the solution

FAST TRACK COMMUNICATION

Temperature-driven phase transformation in self-assembled diphenylalanine peptide nanotubes

A Heredia[1], I Bdikin[2], S Kopyl[2], E Mishina[3], S Semin[3], A Sigov[3], K German[4], V Bystrov[1,5], J Gracio[2] and A L Kholkin[1]

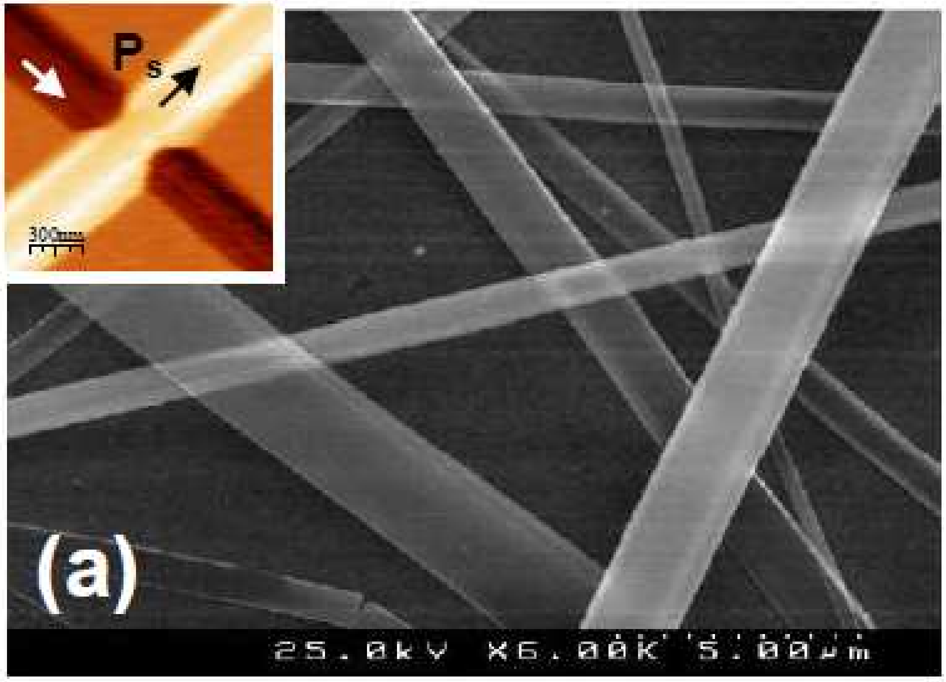

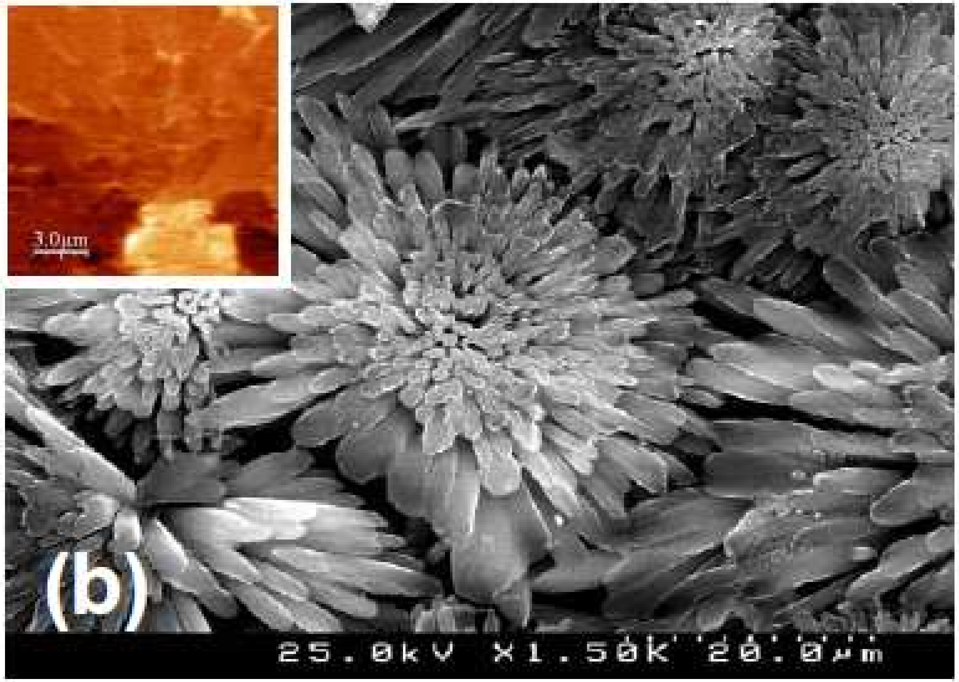

Inset: Lateral PFM

Inset: Vertical PFM

A. Heredia et al, J. Phys. D (2010)

Testing nanoscale piezoelectricity in peptides

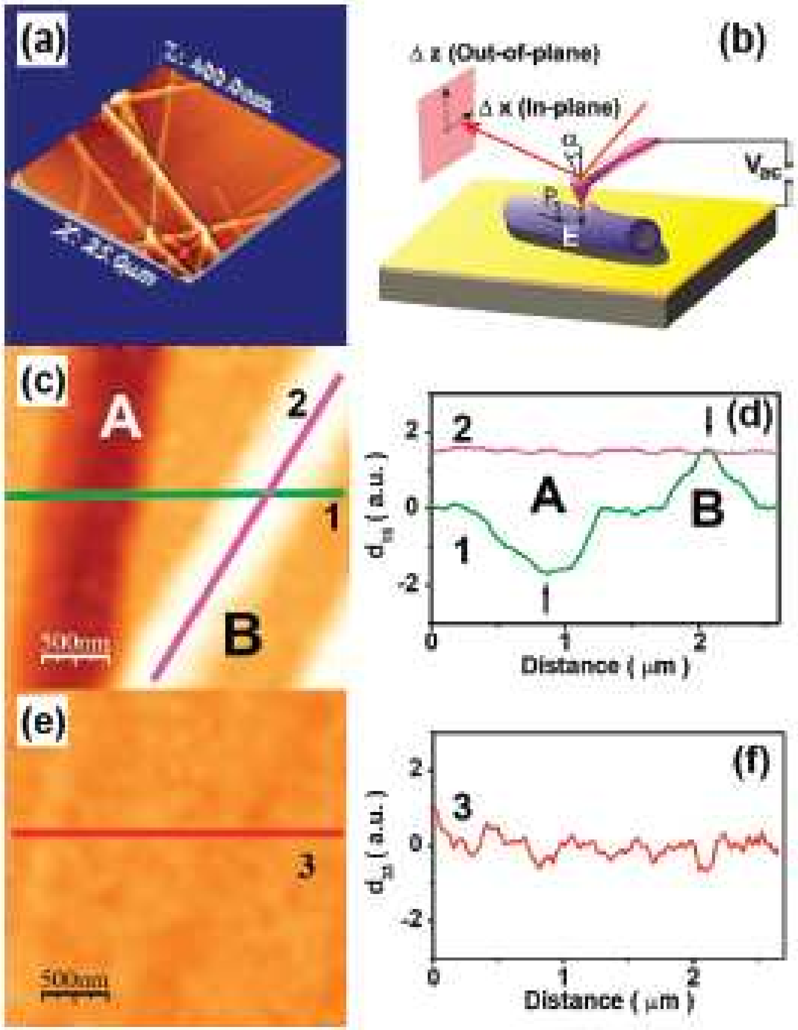

→ LPFM

→ VPFM

Driving field dependence

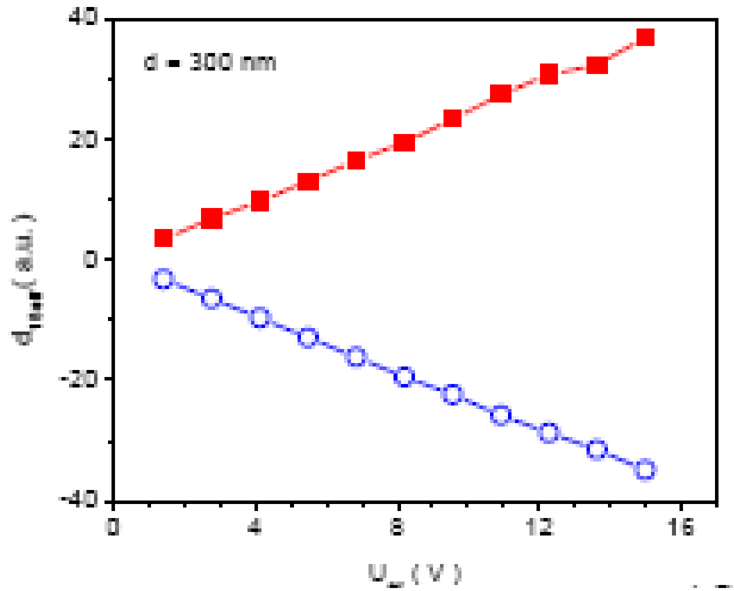

Piezoelectric coefficients:

Peptide Nanotubes:

d_{15} ~ 70 pm/V d_{33} ~ 15 pm/V

Lithium Niobate:

d_{15} ~ 74 pm/V d_{33} ~ 16 pm/V

Kholkin et al, ACS Nano (2010)

Testing nanoscale piezoelectricity in peptides

Thick vs. Thin walls

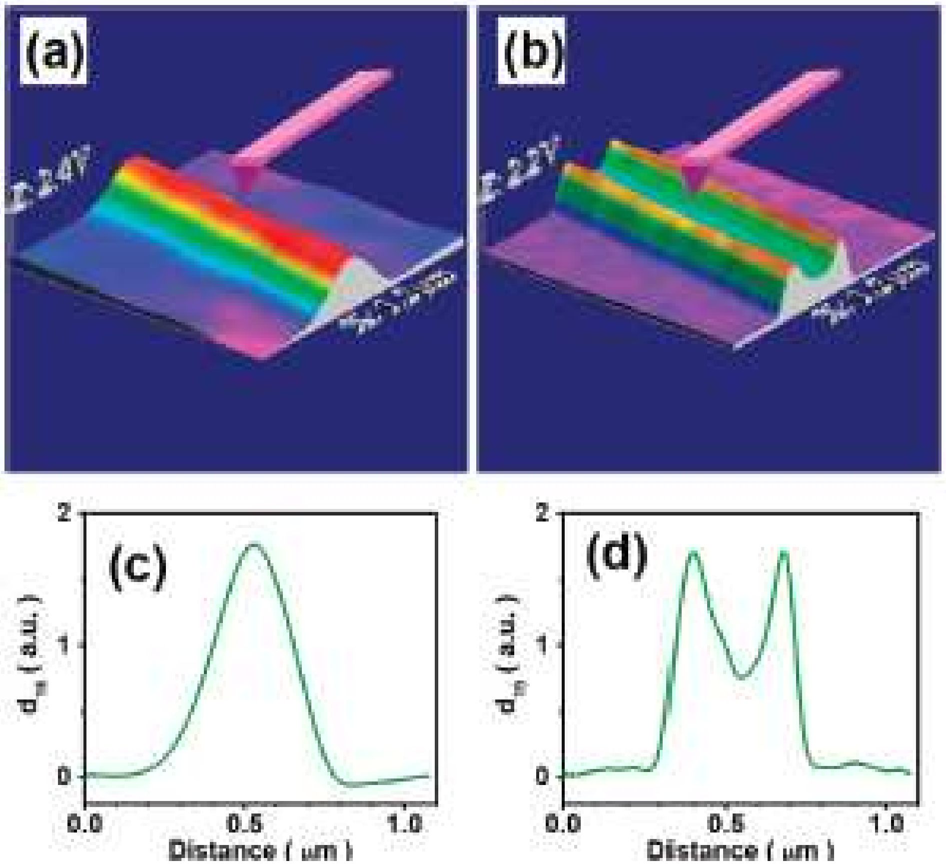

PFM angle dependence

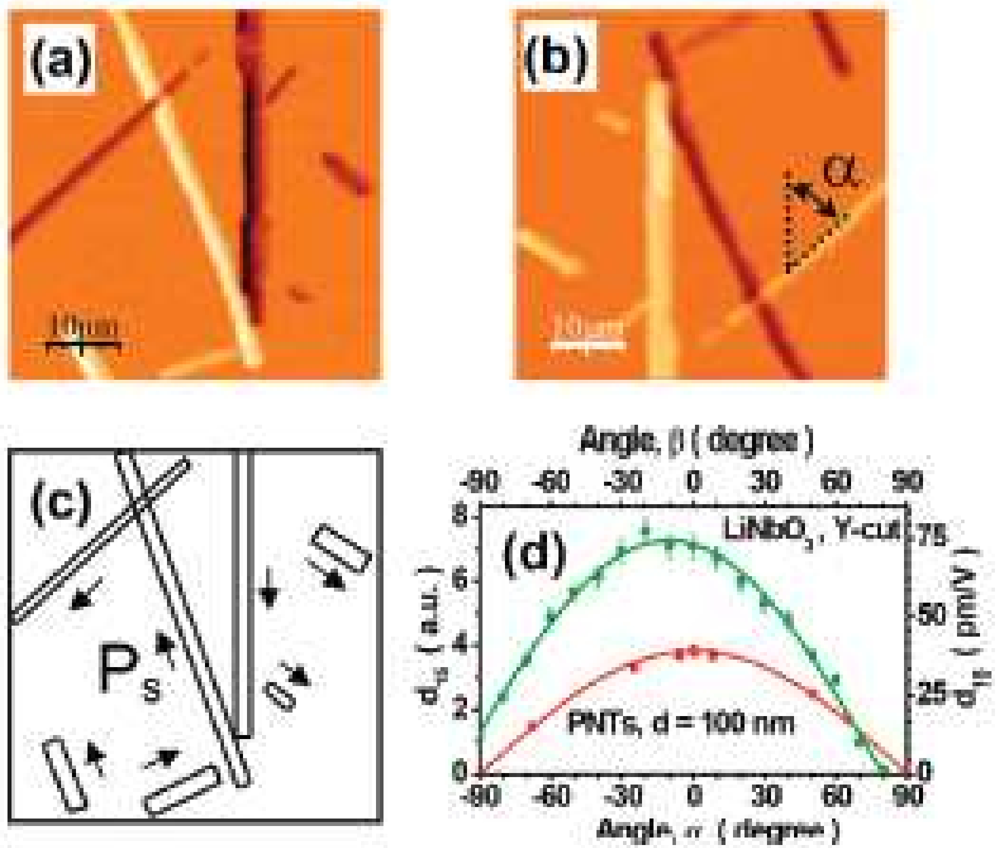

Kholkin et al, ACS Nano (2010)

PFM on bundles of vertical nanotubes

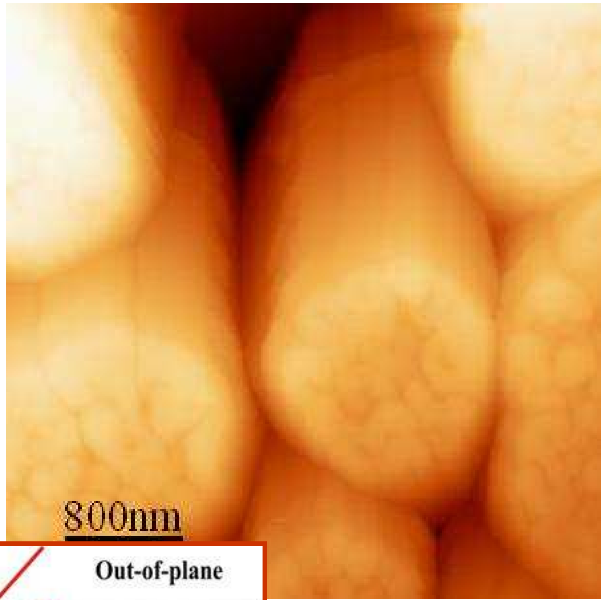

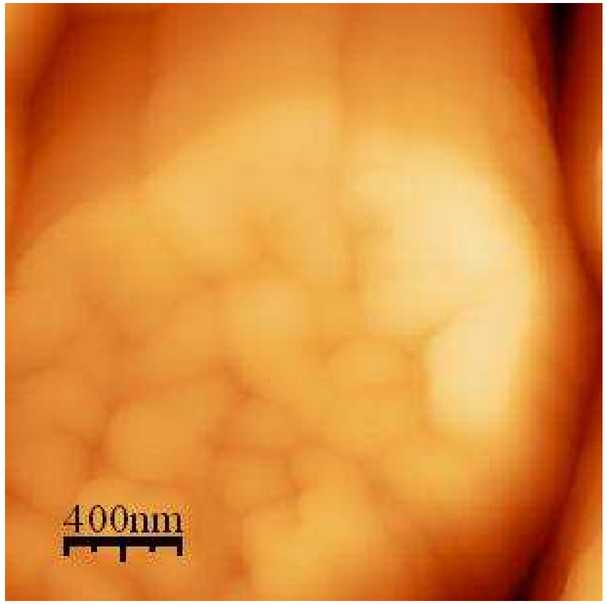

Topography

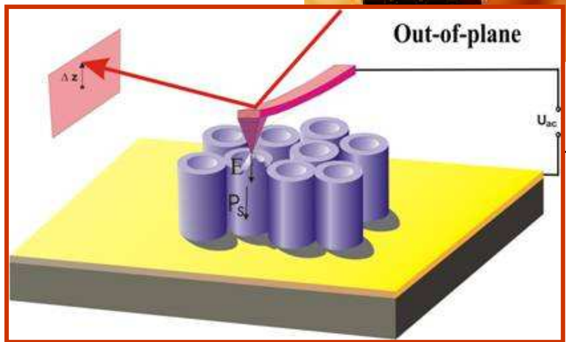

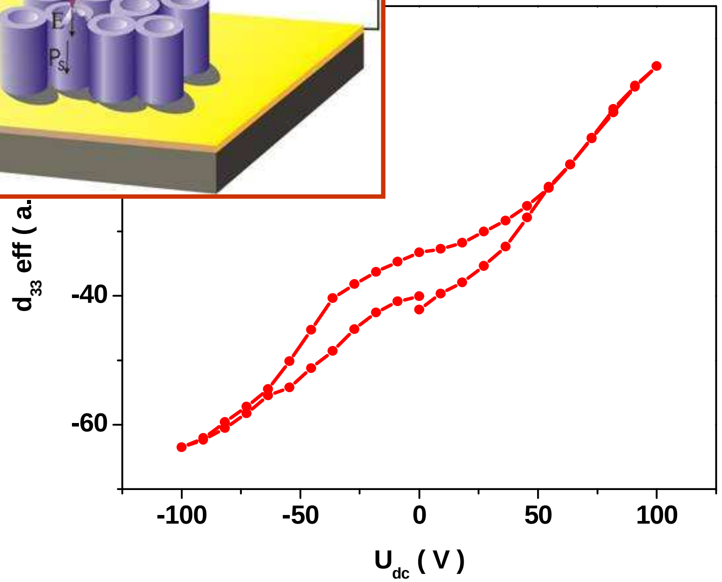

Piezohysteresis

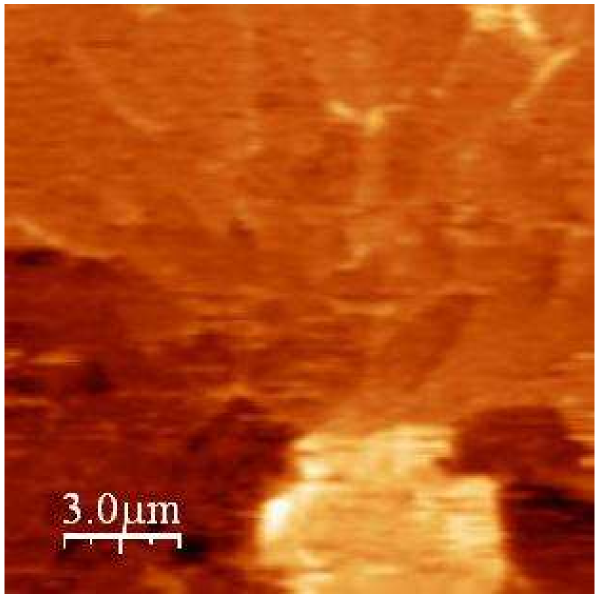

Piezocontrast

Irreversible phase transition into centrosymmetric phase

Second Harmonic Generation

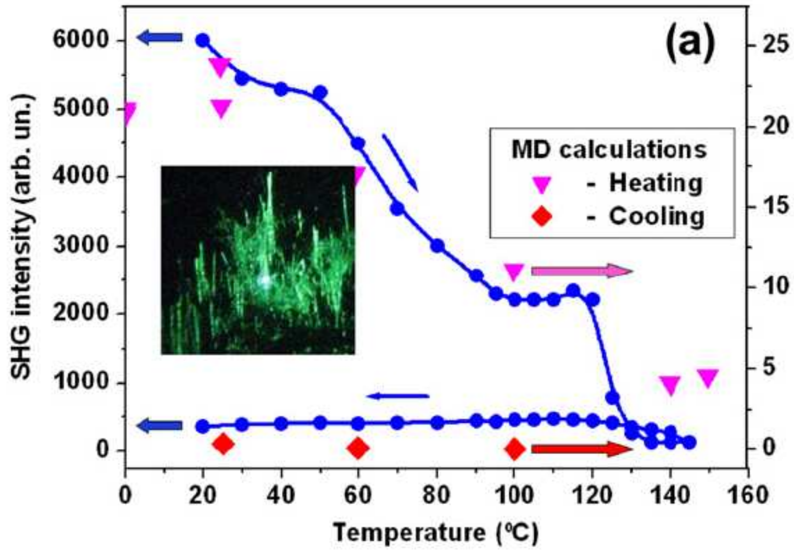

Piezoresponse Force Microscopy

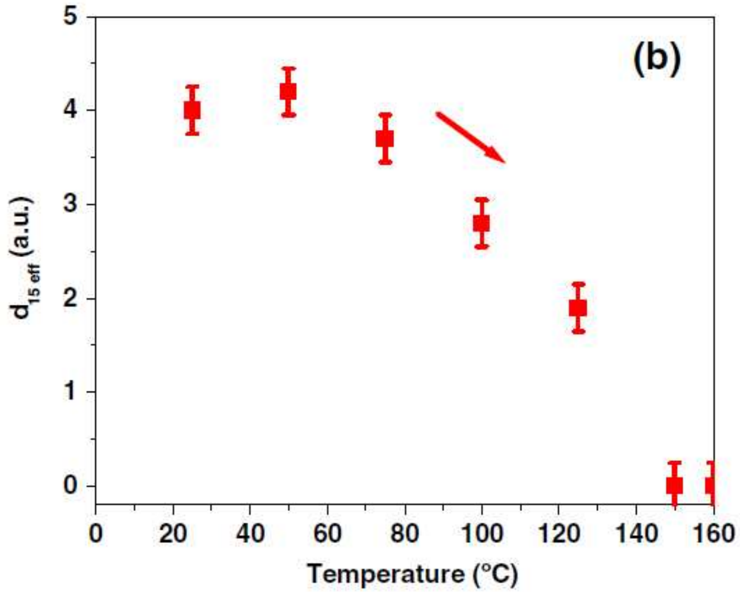

P*6$_1$ ⇒ *Pmmm

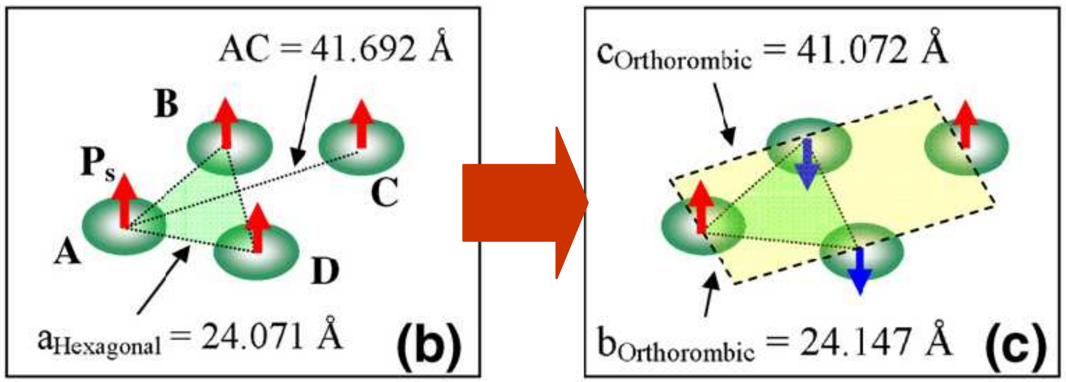

Heredia et al, J. Phys. D: Fast Track (2010)

PFM characterization of TGS/PEO fibers

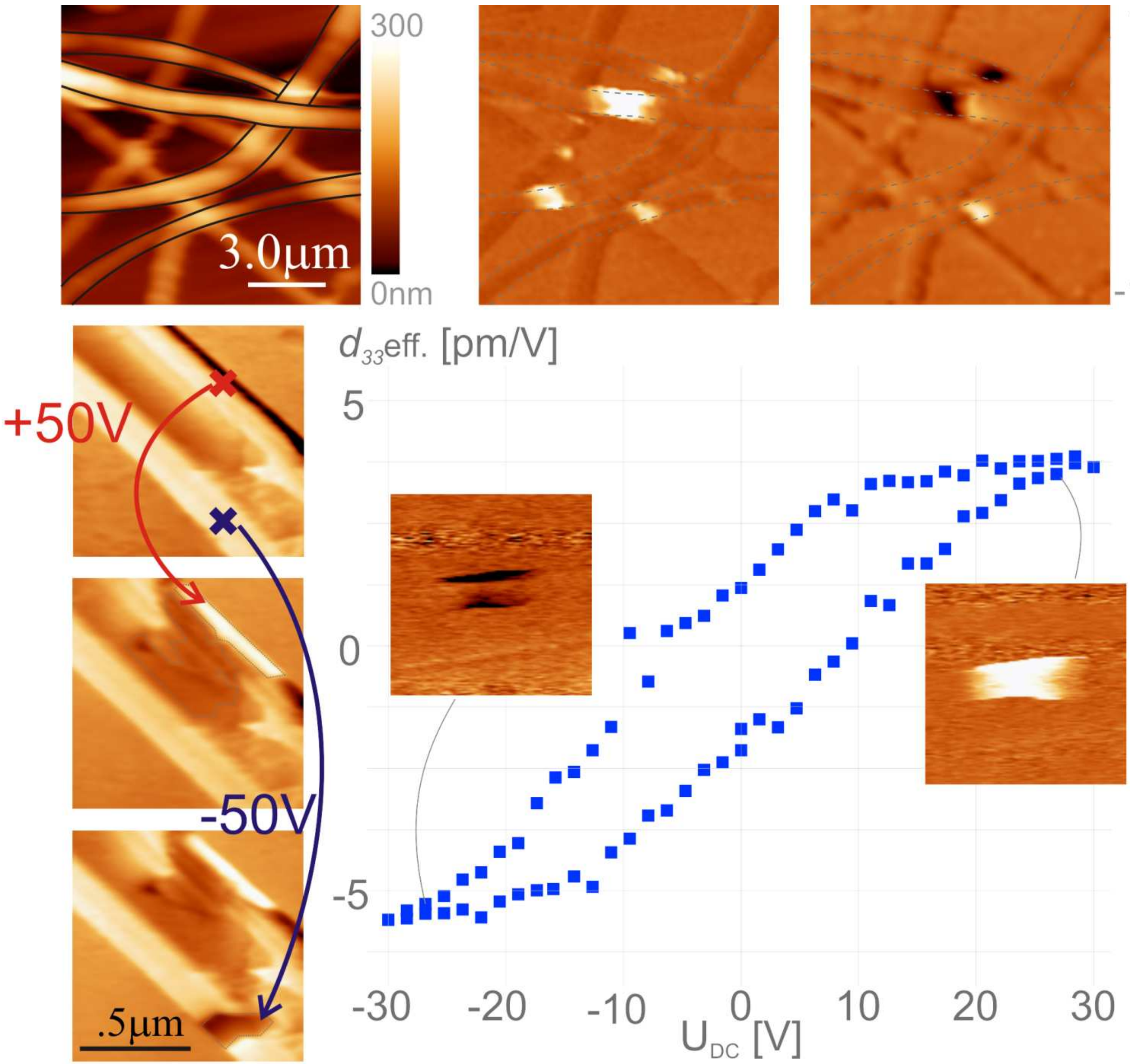

Courtesy Dmitry Isakov (Uni Minho)

Isakov et al., J. Appl. Phys. **108**, 042011 (2010)

TGS microcrystal distribution by PFM

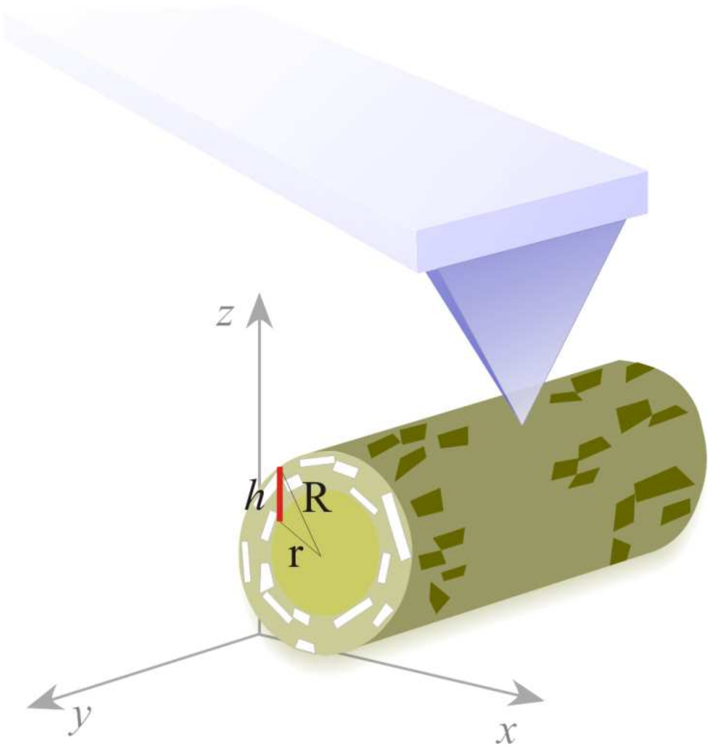

The cross-sectional distribution of the piezoresponse across and along the TGS fibers representing the TGS/PEO distribution.

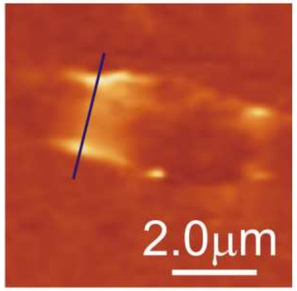

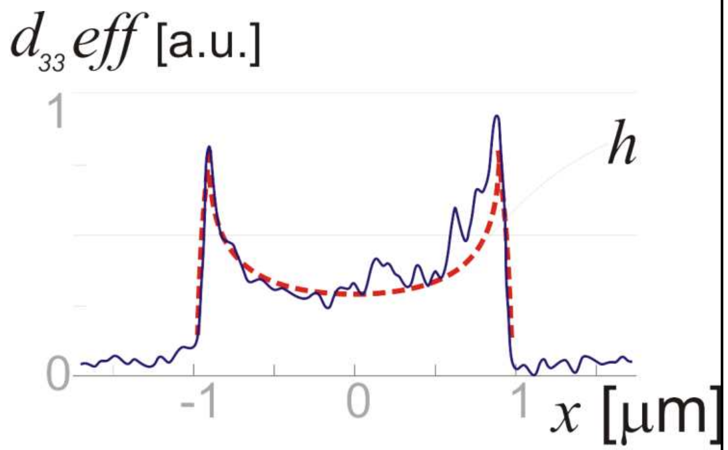

$$h(x) = \sqrt{R^2 - x^2} - \sqrt{r^2 - x^2}\,\Theta(r^2 - x^2) + \sqrt{R^2 - x^2}\,\Theta(x^2 - r^2)$$

- **h represents the effective thickness of TGS volume fraction that contributes to piezoresponse**

- **Volume fraction of the piezoelectric phase can be thus calculated**

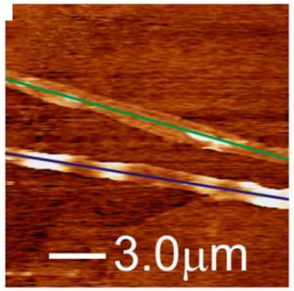

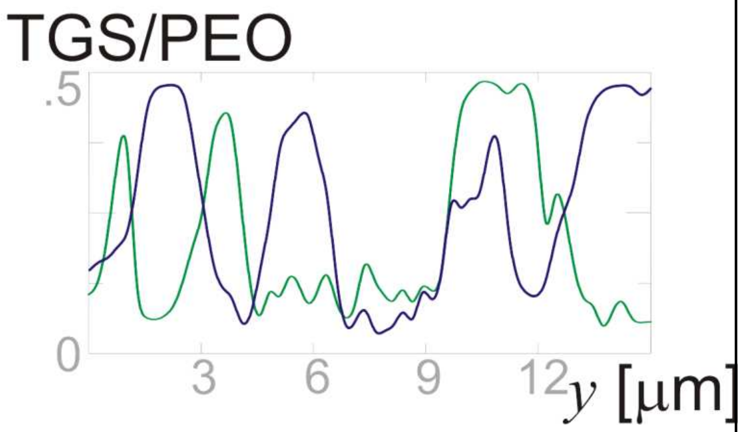

Courtesy Dmitry Isakov (Uni Minho)

Isakov et al., J. Appl. Phys. **108**, 042011 (2010)

PZT single crystals via flux growth

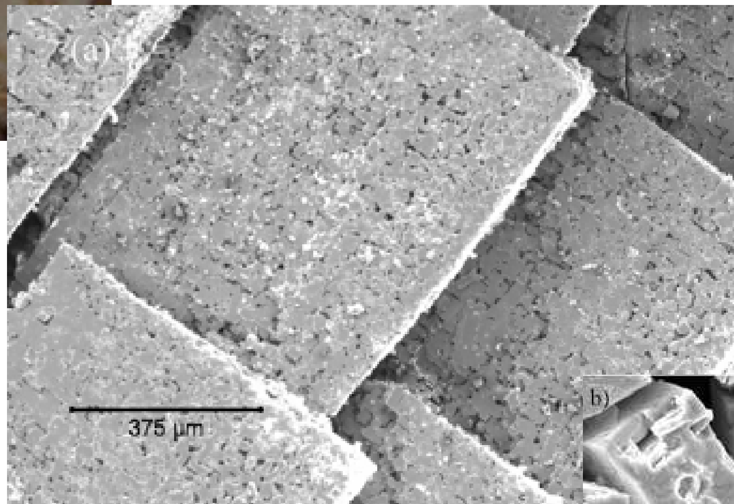

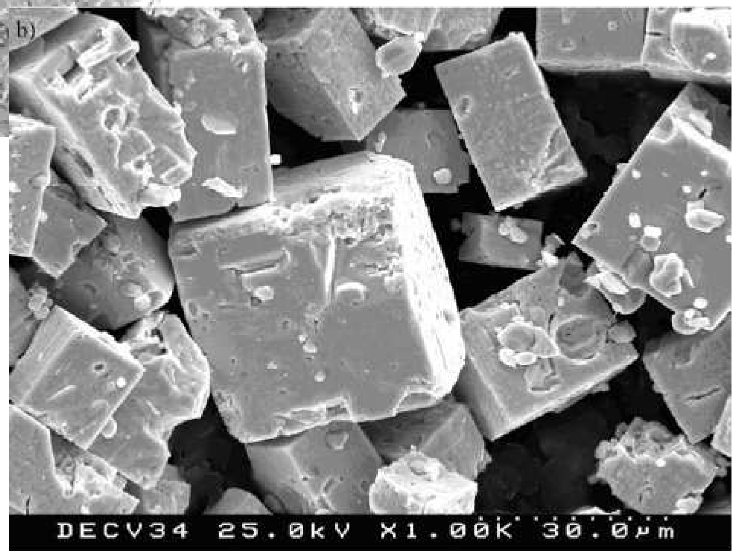

PZT (40/60) crystals at the nanoscale

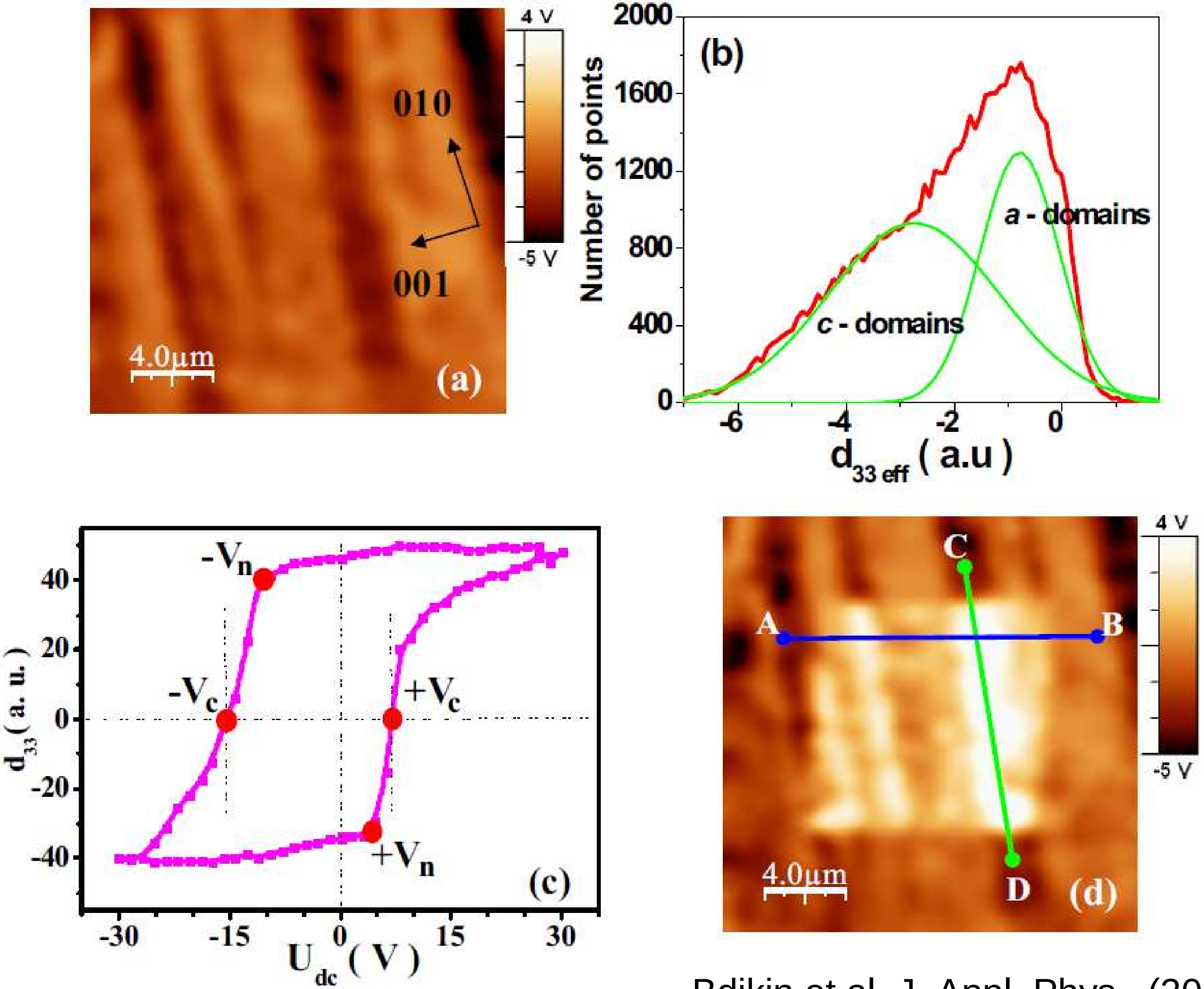

Bdikin et al, J. Appl. Phys. (2011)

Apparent 90º domain wall broadening in PZT

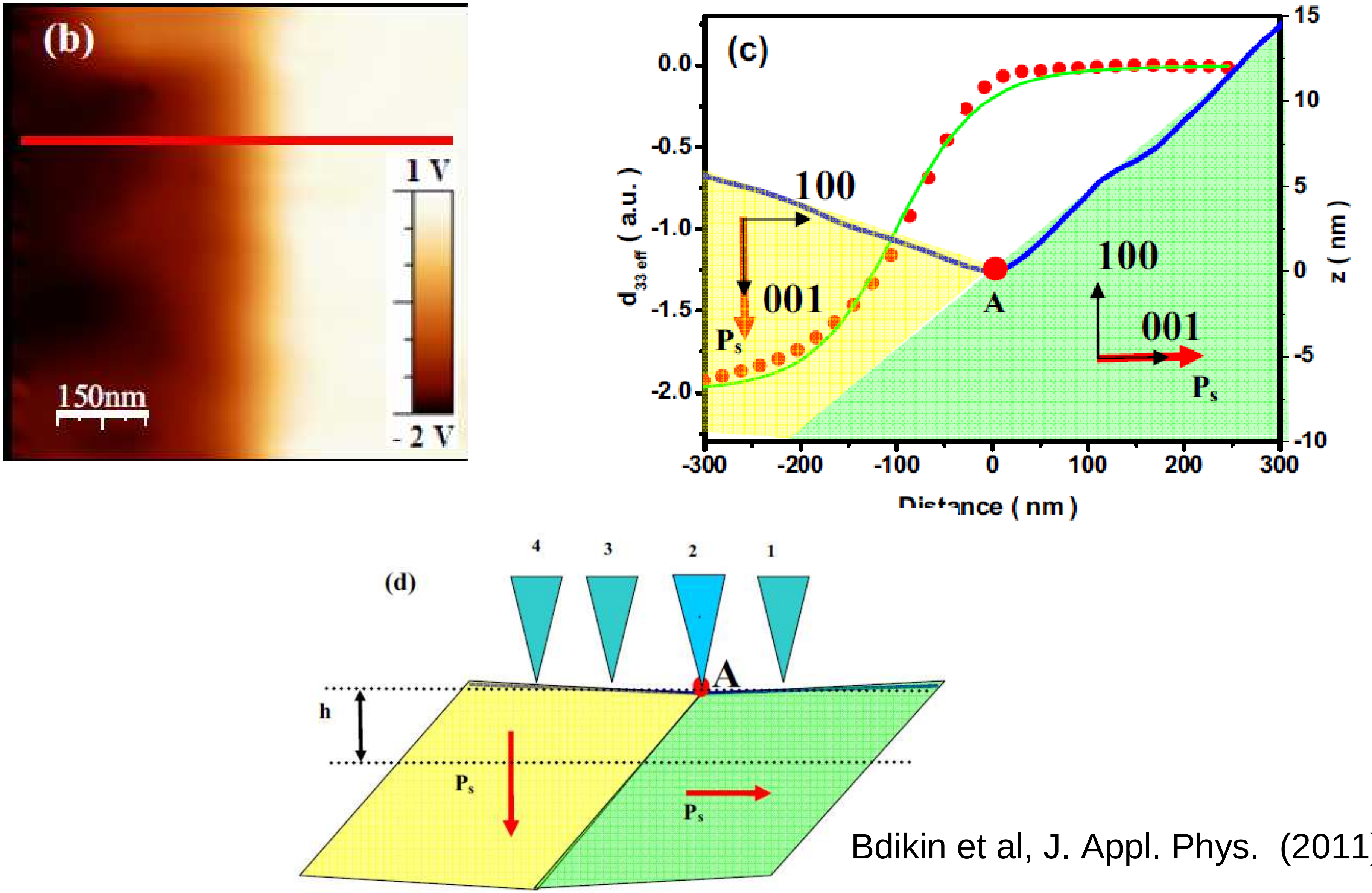

Bdikin et al, J. Appl. Phys. (2011)

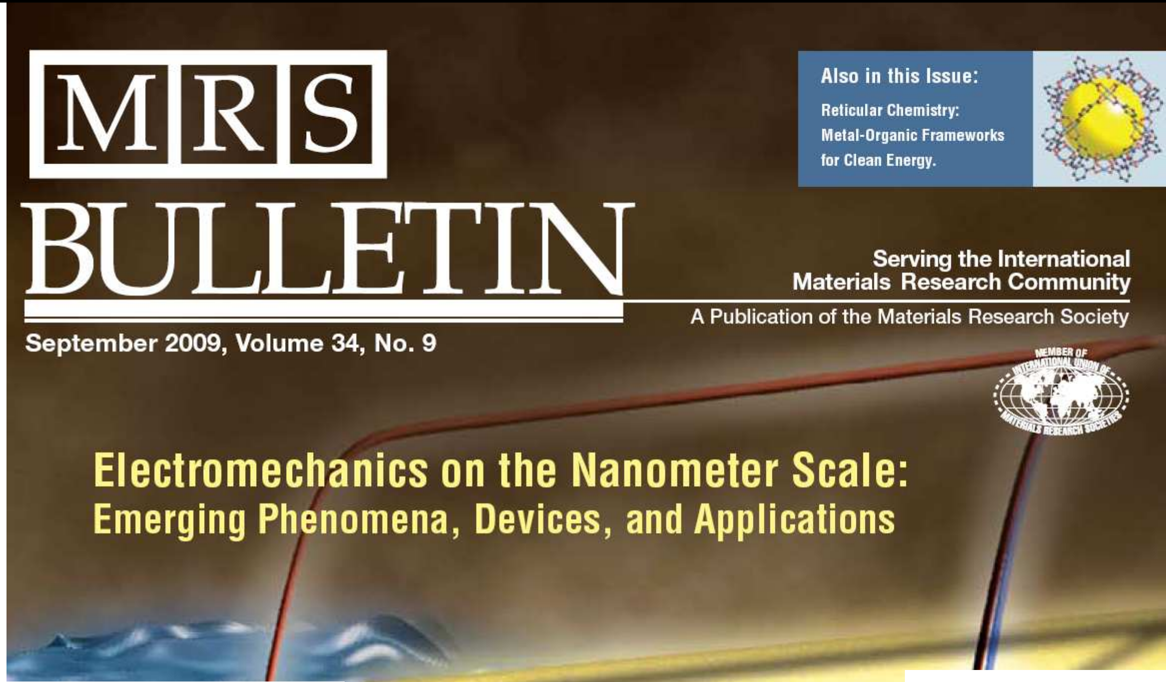

Electromechanics on the Nanometer Scale: Emerging Phenomena, Devices, and Applications

Sergei V. Kalinin, Nava Setter, and Andrei Kholkin

Abstract

Coupling between mechanical and electrical phenomena is ubiquitous at the nano- and molecular scales, with examples ranging from piezoelectricity and flexoelectricity in perovskites to complex molecular transformations in redox active molecules and ion channels. This article delineates the field of nanoelectromechanics enabled by recent advances in scanning probe, indentation, and interferometric techniques and provides a unified outlook at a number of related topics, including membrane and surface flexoelectricity, local piezoelectricity in ferroelectrics and associated devices, and electromechanical molecular machines. It also summarizes experimental and theoretical challenges on the pathway to visualize, control, and manipulate electromechanical activity on the nanoscale and molecular levels.

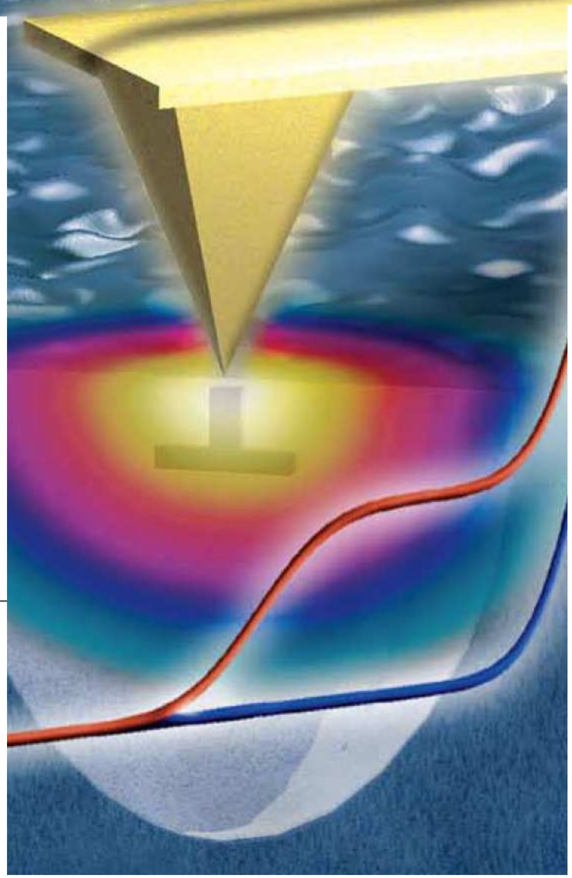

Piezoresponse Force Microscopy: A Window into Electromechanical Behavior at the Nanoscale

D.A. Bonnell, S.V. Kalinin, A.L. Kholkin, and A. Gruverman

Abstract

Piezoresponse force microscopy (PFM) is a powerful method widely used for nanoscale studies of the electromechanical coupling effect in various materials systems. Here, we review recent progress in this field that demonstrates great potential of PFM for the investigation of static and dynamic properties of ferroelectric domains, nanofabrication and lithography, local functional control, and structural imaging in a variety of inorganic and organic materials, including piezoelectrics, semiconductors, polymers, biomolecules, and biological systems. Future pathways for PFM application in high-density data storage, nanofabrication, and spectroscopy are discussed.

Joint International Conference

ISAF – PFM – 2011

July 24 – 27, Vancouver, Canada

The 20th International Symposium on the Application of Ferroelectrics (ISAF)

The International Symposium on Piezoresponse Force Microscopy & Nanoscale Phenomena in Polar Materials (PFM)

Co-chairs: Zuo-Guang Ye

&

Andrei Kholkin

FP7 Initial Training Network

"Nanomotion" (budget 3.3 M€, 1.08.2011-1.08.2015)

Principal Partners:

- University of Aveiro (Portugal) - coordinator
- University of Duisburg-Essen (Germany) – multiferroics, simulations
- Bosch (Germany) – battery materials, ionic conductors
- Tyndall Institute (Ireland) – lead-free, high-T piezoelectrics
- University College Dublin (Ireland) - biomaterials
- University of Leeds (UK) – multiferroics, lead-free
- National Physical Laboratory (UK) – instrumentation, multiferroics
- Nanotec (Spain) – instrumentation, nanostructured materials

Associate Partners:

NT-MDT (Russia) , Nanoforce (UK), Ecole Centrale Paris (France), Materials Institute of Madrid (Spain)

OPENING

of 12 PhD and 1 Post-Doctoral Positions
with competitive salaries

- **Lead-free piezoelectrics (2 positions)**
- **Nanostructured ferroelectrics (1 position)**
- **Calculations and modelling (2 positions)**
- **Magnetoelectric and multiferroic materials (3 positions)**
- **Piezoelectric biomaterials and nanostructures (3 positions)**
- **Li-ion battery materials for energy storage (2 positions)**